Master's thesis

NTNU
Norwegian University of Science and Technology
Faculty of Engineering
Department of Geoscience and Petroleum

Helene Markhus Brekke

The northern Vøring outer ridges complex: new structural and sedimentary constraints

Master's thesis in Petroleum Geoscience and Engineering
Supervisor: Gwenn Peron-Pinvidic
June 2023

NTNU
Norwegian University of
Science and Technology

Helene Markhus Brekke

The northern Vøring outer ridges complex: new structural and sedimentary constraints

Master's thesis in Petroleum Geoscience and Engineering
Supervisor: Gwenn Peron-Pinvidic
June 2023

Norwegian University of Science and Technology
Faculty of Engineering
Department of Geoscience and Petroleum

NTNU
Norwegian University of
Science and Technology

Abstract

This study focuses on finding new structural and sedimentary constraints for the geometry of the Nyk High, located in the distal parts of the Vøring Basin; a segment of the Mid-Norwegian rifted margin. During this study, a 3D seismic block has been studied in Petrel to investigate different structures and stratigraphic sequences. The focus was set on interpreting geometries that could improve the understanding of the development of the Nyk High. Interpretations show a rather complex and challenging area, with rotated extensional fault blocks, local folding, several large and high-angle normal faults, magmatic sills, and sedimentary sequences. To further analyse the fault system, two throw profiles were created. These show variations in the throw, and both faults are interpreted as possibly created by the hybrid fault growth model presented by Rotevatn et al. (2018). The results are compared to published literature to develop a discussion. The distal and outer domains in the Vøring Basin have been studied for decades and significant knowledge has been well-established. However, the understanding and evolution of the distal and outer domains of the Mid-Norwegian rift are still debated, and remain ambiguous, mainly because of great depths and thus imagery issues. Based on the findings in this study, I propose that the Nyk High structural evolution can be summarized by the development of two main rotated fault blocks, with the top Cretaceous and intra Mid-Campanian sedimentary horizons as main capping envelopes, indicating that at least two rift periods were crucial for the formation of Nyk High.

Sammendrag

Denne masteroppgaven fokuserer på å finne nye strukturelle og sedimentære avgrensninger for geometrien til Nykhøyden som ligger i den ytre delen av Vøringbassenget; en del av den midtnorske riftmarginen. Gjennom dette studiet har en seismisk 3D-blokk blitt tolket i Petrel for å studere ulike strukturer og stratigrafiske sekvenser. Fokuset var på å tolke geometrier som kan forbedre forståelsen av Nykhøydens utvikling. Tolkninger viser et ganske komplekst og utfordrende område, med roterte ekstensjonsforkastningsblokker, lokal folding, flere store og høy-vinkel normalforkastninger, horisontale magmatiske intrusjoner og sedimentære sekvenser. For å videre analysere forkastningssystemet har to profiler som viser vertikal forskyvning blitt laget. Disse forskyvningsprofilene viser variasjonene i den vertikale forskyvningen, og utviklingen av begge forkastningene kan muligens beskrives av hybrid-modellen presentert av Rotevatn et al. (2018). Resultatene er sammenlignet med publisert litteratur for å utvikle en diskusjon. De distale og ytre domenene i Vøringbassenget har blitt forsket på i tiår, og viktig kunnskap om disse er veletablert. Imidlertid er forståelsen og evolusjonen av det distale og ytre domenet i den midtnorske riften fortsatt debattert og tvetydig, hovedsakelig på grunn av store dybder som fører til dårlig kvalitet på seismiske bilder. Basert på funnene i denne masteroppgaven foreslår jeg at den strukturelle evolusjonen av Nykhøyden kan bli oppsummert av to hoved-rotasjonsforkastningsblokker, med de sedimentære horisontene topp-Kritt og intra midt-Campanian som hovedhorisonter, hvilket indikerer at minst to riftperioder var avgjørende for dannelsen av Nykhøyden.

Acknowledgement

This master's thesis finalizes five years of studying Petroleum Geoscience and Engineering here at the Norwegian University of Science and Technology (NTNU) in Trondheim. This thesis is written under the Department of Geoscience and Petroleum, with a specialisation in Petroleum Geology. During these past years, I have participated in many exciting courses, and I have especially enjoyed the diversity of geology courses. This thesis is written with a time limit of 20 weeks.

I would like to thank my supervisor, Gwenn Peron-Pinvidic, for her guidance and motivation throughout this master's thesis, in addition to the previous semester where I wrote my specialisation project. I have been able to work on a challenging and exciting project where I have learned a lot and improved my technical skills, especially in Petrel. Thank you for your valuable feedback, rapid e-mail replies and helpful discussions.

Furthermore, I would like to thank my friends and the people I have gotten to know during this five-year study. Thank you for all the memories we have created together. Thank you to my family for supporting me and motivating me throughout this experience. A special thank you to those who have helped and encouraged me during this past year.

NTNU-NPD-SCHLUMBERGER PETREL READY Database is acknowledged for providing the seismic dataset used in this study.

Trondheim, June 2023

Helene Markhus Brekke

Contents

Figures

Abbreviations

2D	Two-dimensional
3D	Three-dimensional
aka	Also known as
E	East
e.g.	For example
Fw	Footwall
Hw	Hanging wall
m	Meter(s)
Ma	Million years ago
ms	Millisecond(s)
Myr	Million years
N	North
NTNU	Norwegian University of Science and Technology
s	Second(s)
S	South
s-twtt	Seconds to-way travel time
S1	Segment one
S2	Segment two
SDR	Seward dipping reflector
W	West

Symbols

β	Stretching factor
l_0	Pre-rift length
ΔL	Change in length (extension)
t_0	Original thickness
t_1	Final thickness

1 Introduction

This chapter gives insights into the background of this study, what information and research exists and why the chosen topic is pertinent and necessary to investigate further. An introduction to the focus and methods of this study is also stated. Lastly, the structure of the thesis is presented.

1.1 Background

Extension within the crust eventually leads to the formation of conjugate margins. Rifted margins have been studied thoroughly, especially during the last couple of decades (Peron-Pinvidic et al., 2019). Research has suggested that rifted margins are created through several phases of extension and deformation, leading to five structural domains: the proximal, necking, distal, outer, and oceanic domains (e.g., Peron-Pinvidic et al. (2013)).

Figure 1 illustrates the evolution of rifted margins' understanding, starting with a relatively simple illustration in the '70s and '80s, evolving into a much more complex and detailed illustration in the 2000s to 2010s. Improved seismic imaging, analytical methods, and sampling of deep wells at distal offshore settings have during the past three decades brought new observations, leading to an amendment of the primary used models. This advancement led to the two archetypal margins: the Iberia margin as a non-volcanic margin and the Norwegian-Greenland Sea margins as a volcanic margin (Peron-Pinvidic et al., 2013). Later studies proposed that the division was too simple, and Müntener et al. (2010) showed that strict non-volcanic margins probably do not exist. More correct terms were furthermore determined to "magma-rich" and "magma-poor" margins, with a range of margins in between those two end members (e.g., Franke (2013)). Studies contributed to further development, and terms referring to morphology, domains and geological processes changed and developed as newer and higher resolution geophysical datasets were used together with data from borehole drillings. Despite this consensus, the distal and outer domains of rifted margins are still hot topics for debate and a subject for greater research, mainly because of great depths in the distal and outer domains, which is limiting the accessibility of good core samples and making the knowledge of the outer domains greatly based on used datasets and individual interpretations (Peron-Pinvidic and Osmundsen, 2016, Brekke, 2022).

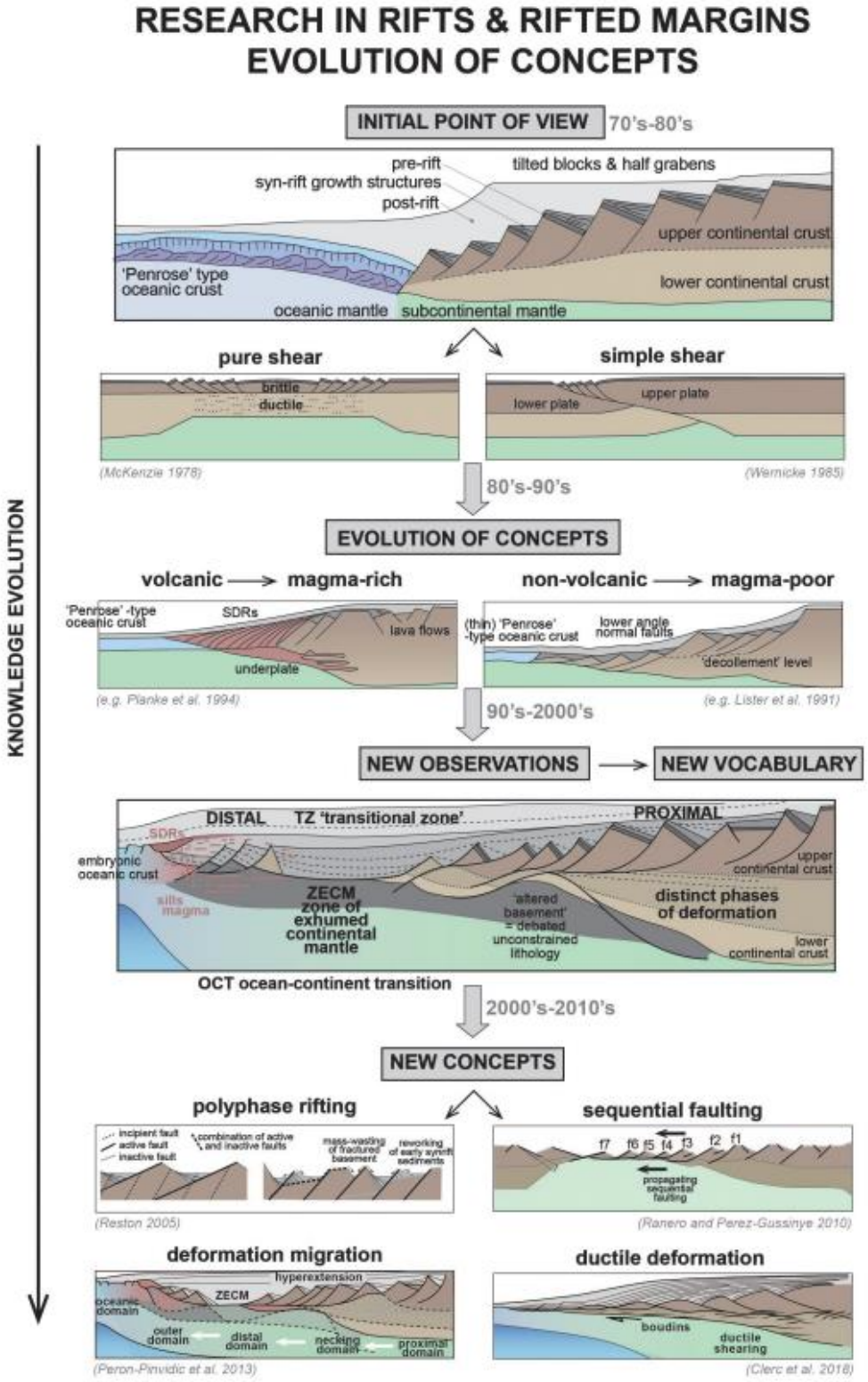

Figure 1 The evolution of the rifted margin concept is illustrated here. It started with a simplistic approach in the '70s and '80s, gradually becoming more detailed and evolved as new observations led to new concepts (Peron-Pinvidic et al., 2019).

The magma-rich Mid-Norwegian – NE Greenland conjugate rift system was created through several rift periods, interfered by periods of quiescence over a time of ~ 300 Myr (Peron-Pinvidic and Osmundsen, 2018, Peron-Pinvidic and Osmundsen, 2016). The exceptional long rift period has affected the architecture of the rift and led to complex geological structures and architecture. The observed geometries obviously mostly relate to the extensional setting of the rift, including normal faults, rotated fault blocks and basins, however some local folds are also observed. Several authors, including Larsen and Skarpnes (1984), Blystad et al. (1995) and Omosanya (2020) have argued for some events of compressional regimes in the Vøring Basin, such as fault inversion, folding and reverse faults. On the other hand, Gowers and Lunde (1984) argued that the folds observed in the area are mostly related to extensional regimes affected by sinistral strike-slip faulting and flexuring.

During the fall semester of 2022, I wrote a specialisation project focusing on new sedimentary and structural constraints in the Vøring Basin on a regional scale, the project is referred to as Brekke (2022).

Brekke (2022) presents interpretations of 16 different 2D seismic profiles, all located in the Vøring Basin, one of which is presented in chapter 2.2.3. A shallow core interpretation was also executed. Several of the profiles allowed for interpretations along the whole rifted margin. The focus of that study was to map the main horizons, such as the top basement, the seabed and possibly the Moho, in addition to large normal faults, to better constrain the study area on a regional scale. Results mainly showed mapping of the top basement at shallow depths in the proximal and outer domain, and an increase in depth towards the necking domain. This observation corresponds well with extreme thinning of the crust towards the outer and oceanic domains, as illustrated in the lower left of Figure 1. A significant increase in magmatic additions was observed and interpreted towards the distal and outer domains, including SDRs (seaward dipping reflectors). Further, Brekke (2022) argues for the presence of a significant wedge-shaped normal fault in her study, indicating syn-sedimentary deposition. The presence of such structures is also suggested by different authors (e.g., Færseth and Lien (2002)).

Nyk High is a structure, interpreted as a rotated fault block, and located in the distal parts of the Vøring Basin in the Mid-Norwegian – NE Greenland rift. It is elongated in the NE-SW direction (Blystad et al., 1995). The structure is dominated by extension and normal faults; however, signs of possible reverse faults and strike-slip components are observed (Blystad et al., 1995, Ren et al., 2003). Because of Nyk High's location in the distal Vøring margin, it is highly affected by the evolution of the margin, other surrounding structures, as well as magmatic activity and complex geology.

This study focuses on the Nyk High in the distal Vøring margin, where the approach was two-fold with first a specialisation project (Brekke, 2022). During this present master's thesis, interpretation of a 3D-seismic block in Petrel is used to better constrain the structural and sedimentary architecture of the high. Focus is set on the tectonic evolution, and the structural constraining is therefore more represented than the sedimentary constraining. Further, the results from this study will be compared to published research and to the specialisation project by Brekke (2022).

The findings in this study will give a better understanding of the geometries of the Nyk High and can be used for further research. Since rifted margins are important to several professions, such as hydrocarbon exploration and in the understanding of climate changes (Peron-Pinvidic et al., 2019), a further constraining of the study area is considered to be important to several different disciplines.

1.2 Structure of the report

The structure of the report is as follows:

- **Chapter 2** presents the theory relevant for this thesis.
- **Chapter 3** describes methods used during this research.
- **Chapter 4** presents the results.
- **Chapter 5** discusses the main findings.
- **Chapter 6** presents the conclusions.
- **Chapter 7** suggests possibilities for further work.

2 Theory

This chapter describes the theory relevant for this thesis. Parts of the definitions and concepts summarized in this chapter are issued from my specialisation project Brekke (2022). New topics have been added, and the subchapters are edited and modified to be relevant for this present thesis.

2.1 Definitions and assumptions

- "Magmatic additions" refer to magmatic structures such as either intrusions, sills, lavas or SDRs (seaward dipping reflectors), when not specified.
- Given the 3D dataset used in this study, the top basement is not visible, and thus impossible to interpret. The top basement was studied on the regional seismic (Brekke, 2022), where it was interpreted at the boundary between the base of sedimentary layers and the top of the crystalline bodies.
- Dip directions of faults are interpreted by studying the actual fault in at least two different directions, usually inline and crossline. Further analysis of selected faults is presented in throw profiles.
- Inline refers to the seismic line that is parallel to the direction of the data that was obtained, and is oriented N-S.
- Crossline refers to the seismic line that is perpendicular to the direction the data was obtained, and is oriented E-W.
- The study area is defined within the outlined red square which is first presented in chapter 2.2. When referring to this area, words as "3D seismic cube", "3D seismic block" and "cube" are used.
- "Increment" refers to the distance used when moving from profile to profile in the 3D seismic cube in Petrel.
- The erosional surfaces that are interpreted (especially horizon 6) do not necessarily follow a specific seismic reflector, as the aim was to interpret the actual erosional surfaces.
- The seabed is defined as peak.

2.2 Geological setting

Important geological setting, especially with focus on the Mid-Norwegian – NE Greenland rift and the Nyk High is described here. Additionally, information on the well 6707/10-1 is presented.

An overview of the study area is presented in Figure 2, where a) shows segments of the Vøring margin, including an outline of the location of the 3D seismic, in addition to two drilled wells. The figure in b) presents the location of the 2D lines that were interpreted in

Brekke (2022). The legend displayed in a) is representative for all figures that visualize the location map (both the overview and the zoomed-in maps) in this thesis.

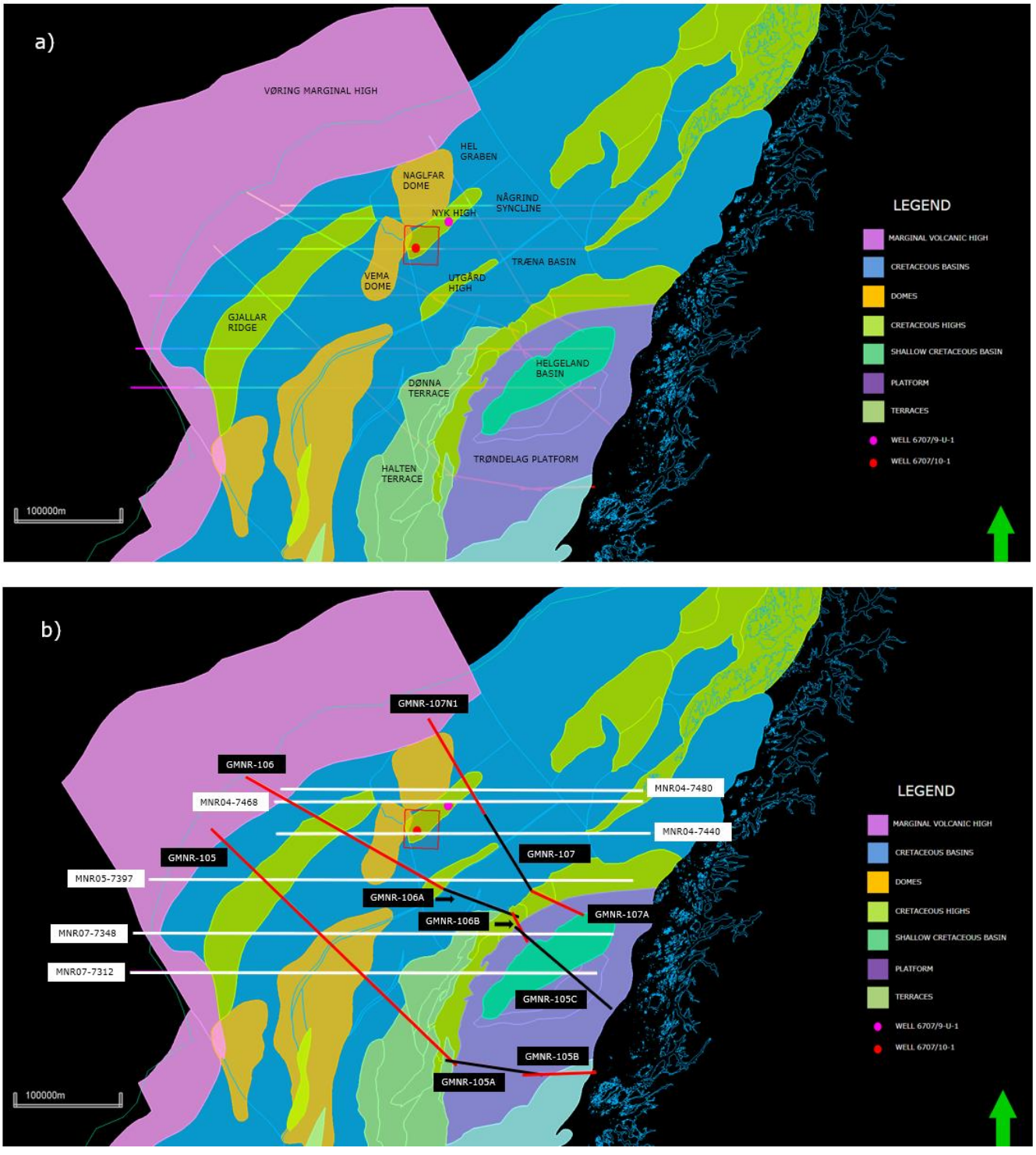

Figure 2 a) is showing the study area (outlined by the red square) and the surrounding regions in the Norwegian Sea. b) is showing the 2D seismic lines that were interpreted in Brekke (2022).

2.2.1 Extensional sedimentary basins

This subchapter is modified from Brekke (2022).

Extensional basins form because of thinning and stretching within the lithosphere, leading to subsidence in the crust and basin formation (Newman et al., 1999, Allen and Allen, 2013, Brekke, 2022). Such basins are formed in environments that are highly dominated by extensional forces (Sclater and Célérier, 1987). The stretching factor, the β-factor, is important in the understanding of extensional basins and its formation. As explained below, this factor relates the original thickness of a basin to its final thickness. It is also explained by the relation between the pre-rift length and the post-rift length (Allen and Allen, 2013, Brekke, 2022). The relation between the pre-rift length and the post-rift length is explained by adding the pre-rift length with the extension (post-rift length), and dividing it by the pre-rift length:

$$\beta = \frac{l_0 + \Delta L}{l_0}$$

where l_0 is the pre-rift length and ΔL is the extension. The relation between the original thickness and the final thickness is described as follows:

$$\beta = \frac{t_0}{t_1}$$

where t_0 is the original thickness, and t_1 is the final thickness. Both formulas have their strengths and weaknesses, but they both have in common to describe how much an object is stretched (Brekke, 2022). The greater the β-factor, the more extension has been applied to the area.

Two important models that are used to explain rifts are the following two (see Figure 1 for illustrations):

- The pure shear McKenzie model from 1978
- The simple shear Wernicke model from 1985 (Allen and Allen, 2013)

There are different assumptions for both models, and the McKenzie model (Osmundsen, 2022, Allen and Allen, 2013, McKenzie, 1978) assumes a vertical heat transfer, airy isostasy, instantaneous rifting, and a symmetric extension. These factors cause an initial subsidence that occur after the extension and a post-rift subsidence. For the Wernicke model (Wernicke, 1985), the assumptions are an asymmetric stretching, and that the area of maximal thermal subsidence and the area of maximal crustal thinning are at a distance from each other (Allen and Allen, 2013, Osmundsen, 2022, Brekke, 2022). Further, the Wernicke model is created based on field observations. Both models are relatively simplified compared to the reality, which can lead to some misinterpretations in certain situations. One example is that observations of simple shear in the lithosphere where extensional detachment faulting occurs contradicts the assumption of pure shear that is needed for the McKenzie model (Allen and Allen, 2013, Osmundsen, 2022, Brekke, 2022). Followingly, the Wernicke model has been challenging to use in rifts and rifted margins at places where the area of maximal crustal thinning and maximal thermal subsidence is observed above each other (Allen and Allen, 2013, Osmundsen, 2022, Brekke, 2022).

Also, the McKenzie and Wernicke models are primarily created for proximal domains. By using high-resolution geophysical data together with deep-sea drilling and onshore analogue studies, it is shown that the outer and distal domains are quite different from the proximal domains (Peron-Pinvidic et al., 2013, Brekke, 2022). The finding of hyperextended continental crust and exhumed subcontinental mantle are examples of this difference because they appear as unexpected structural settings (Peron-Pinvidic et al., 2013, Brekke, 2022).

2.2.2 Rifted margins

This subchapter is modified from Brekke (2022).

Plate tectonics and the opening and closing of oceanic basins can be explained by the "Wilson Cycle", which is often divided into six stages. These stages are the formation of an *orogeny*, followed by a *collapse*, then *rifting* when the plates move in opposite directions, *breakup* followed by *drifting*, and *convergence and subduction*, then back to the formation of an orogeny (Wilson, 1966). The cycle, presented in Figure 3, has been important in the understanding of, and further evolution of plate tectonics (Wilson et al., 2019), including the evolved understanding of rifted margins.

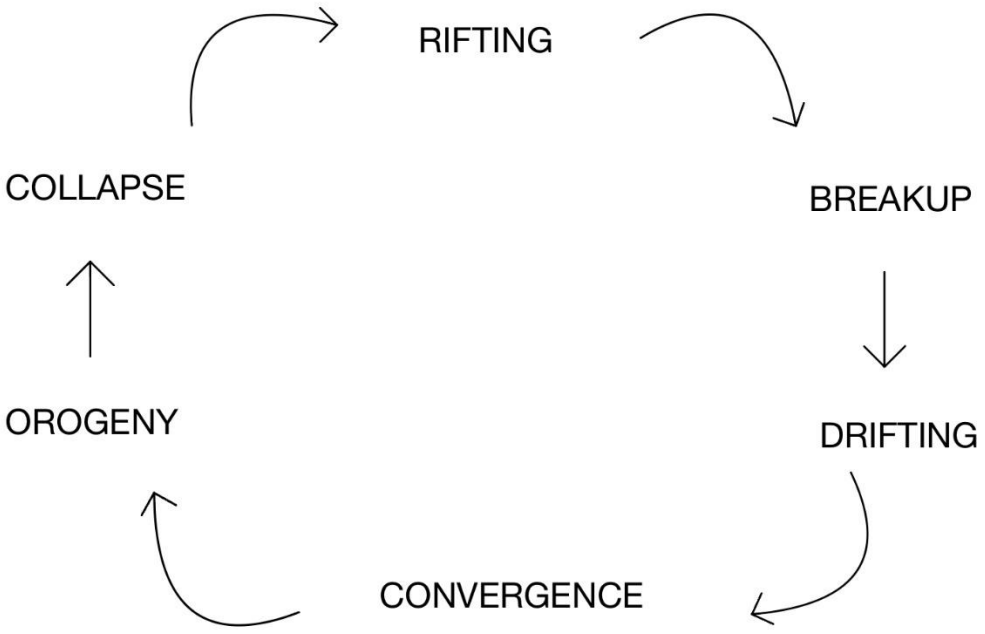

Figure 3 Illustration of the Wilson cycle, first presented by Wilson (1966).

Rifted margins mark the breakup, as a result of extensive rifting and extension within the lithosphere (Peron-Pinvidic et al., 2019, Brekke, 2022). Over the past couple of decades, immense research regarding rifted margins is published. This research has led to an explanation where the rifts are divided into different domains based on characteristic architecture along the margin (Peron-Pinvidic et al., 2013, Brekke, 2022). Rifted margins consist of an upper plate margin, a lower plate margin and an H-block. Since the research area of this thesis pertain within the lower plate margin, neither the upper plate, nor the H-block will be elaborated further.

Rifted margins are sectioned into these five domains: the proximal, necking, distal, outer, and oceanic. All these stages are created during different phases of deformation, and they portray distinct characteristics and processes (e.g., Peron-Pinvidic et al. (2013), Brekke (2022)). The domains are illustrated in Figure 4.

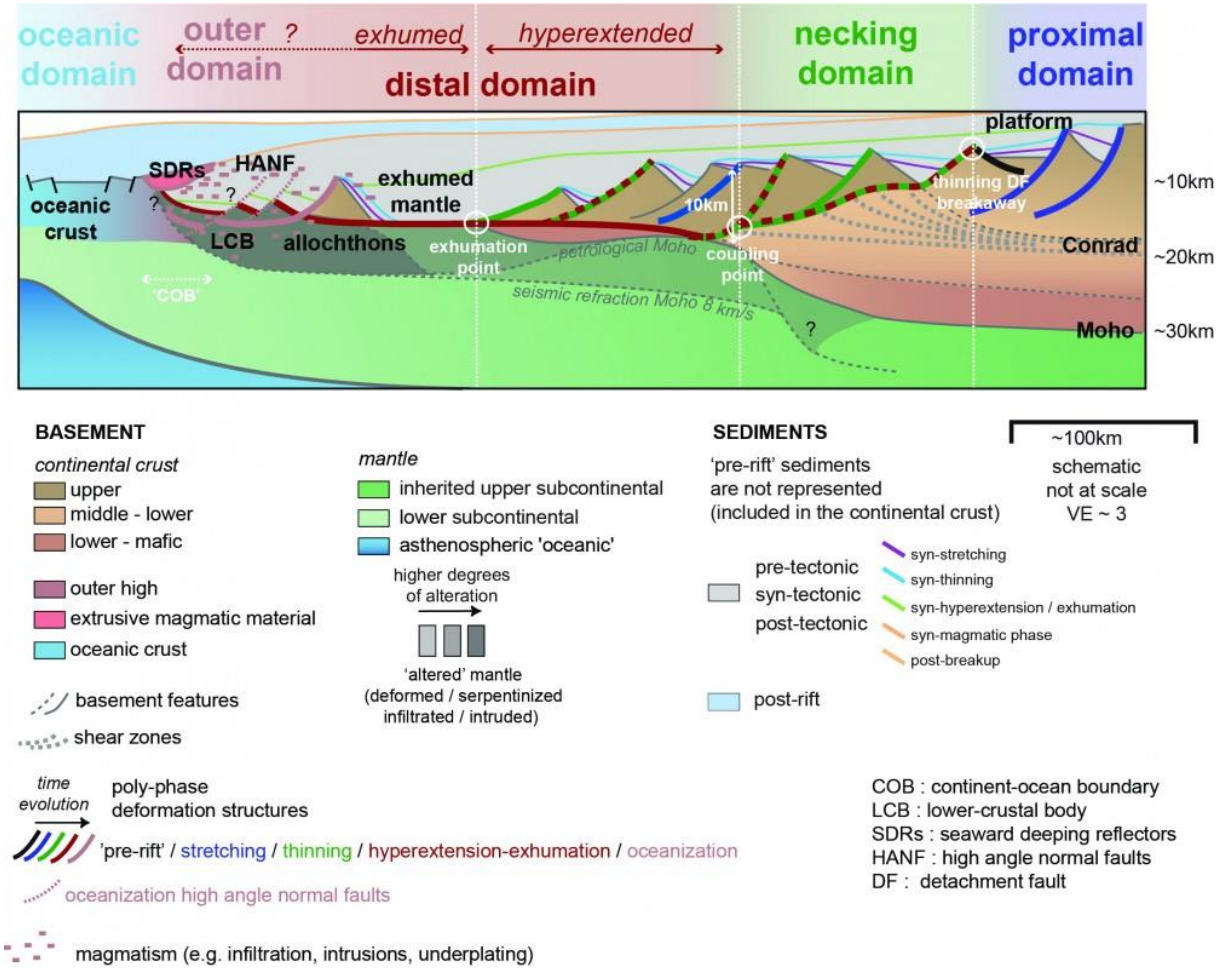

Figure 4 This figure displays the dividing of the five domains of the lower plate margin together with important characteristics for each domain. The illustration is modified from Peron-Pinvidic et al. (2013).

The following division of the five domains is inspired by Peron-Pinvidic et al. (2013). These domains are illustrated in the Mid-Norwegian rift portrayed in Figure 5.

The proximal domain

The proximal domain is the domain closest to the platform. Characteristics of this domain which is dominated by a stretching deformation process, are half graben basins, wedge-shaped sedimentary strata and high-angle normal faults (Brekke, 2022).

The necking domain

Succeeding is the necking domain, where thinning and crustal deformation coupling occurs. This domain is recognized by a rise in Moho, extreme thinning of the crust, and wedge-shaped structures (Brekke, 2022).

The distal domain

Further out towards the ocean, the distal domain appears. There, the architecture is defined by sag-type basins, possible exhumation of the mantle and low angle detachment faults. Hyperextension is also characteristic for this domain, which is a process that can lead to an embrittlement of the upper and lower crust, causing penetration of major faults into the mantle. An even weaker and more deformed crust can occur if the exhumed mantle causes serpentinization, which can happen in the distal domain (Brekke, 2022).

The outer domain

The outer domain is also characterized by exhumation and serpentinized mantle. Further, it also has a significant increase in magmatic activity, creating magmatic intrusions, sills and SDRs. The final lithospheric breakup and the mechanisms in the outer domain help to trigger the final lithospheric breakup and seafloor spreading (Cannat et al., 2009, Bronner et al., 2011). The outer domain is also prominent in defining whether a rift is magma-rich or magma-poor (Peron-Pinvidic et al., 2013, Brekke, 2022).

The oceanic domain

The last domain is the oceanic domain, marking the changeover between the continental and the oceanic crust. Compared to the other domains, the crust is at its thinnest in this domain. Further, the basement is here often observed at shallow depths, a statement supported by findings from e.g., Brekke (2022)’s specialisation project.

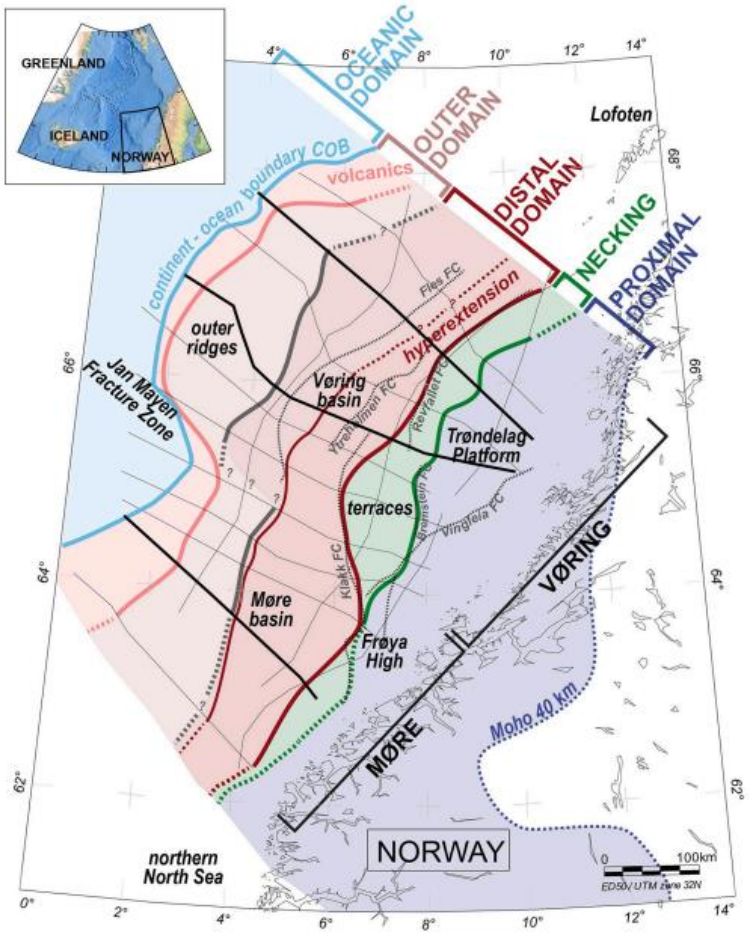

Figure 5 Map of the lower plate margin in the Norwegian Sea, with all the domains outlined. Thin, grey dashed lines represent the main fault complexes. Please disregard the thick black lines. Figure from Peron-Pinvidic et al. (2022).

The study of rifted margins has historically been mostly important to the petroleum industry, with focus on hydrocarbon exploration. However, they are also proven to give significant information within other disciplines as well (Peron-Pinvidic et al., 2019). A broader knowledge about rapid climate changes, greater CO_2-production caused by rifting and breakup, and the understanding of the sediment supply within the distal basins are some examples of why a better understanding of rifted margins is important (Peron-Pinvidic et al., 2019, Brekke, 2022). This project focuses on the distal parts of the Mid-Norwegian Vøring margin.

2.2.3 Mid-Norwegian – NE Greenland conjugate rift

This subchapter is modified from Brekke (2022).

The information provided in this subchapter is based on the references Blystad et al. (1995), Brekke (2000), Faleide et al. (2008), and Peron-Pinvidic and Osmundsen (2018) except when mentioned otherwise (Brekke, 2022).

The Mid-Norwegian – NE Greenland rift system has an extraordinary long rifting period. The collapse of the Caledonian Orogeny in Devonian time, about 400-410 Ma, is interpreted as the first episode related to the formation of this margin. The final breakup occurred about 54 Ma, in the Early Tertiary (Paleogene) (Talwani and Eldholm, 1977, Brekke, 2022). However, it can be argued that the first event related to rifting is in fact not the collapse of the orogeny, but rather occurred during the Early Carboniferous. Thus, it comes down to the definition of what rifting is. Anyhow, the rifting period is estimated to at least 300 Myr (Brekke, 2022).

Instead of treating the rift as one large and long-lasting rift period, a more reasonable scenario of the evolution is that the margin was created during a longer period of alternation between multiple rift changes and quiescence (Doré et al., 1999, Brekke, 2022). According to Peron-Pinvidic and Osmundsen (2018), the evolution of the rift can be divided into four major geological events. The two first events include the *formation* of an orogeny and its *collapse,* which occurred in respectively Silurian and Devonian-Carboniferous. Followingly, two successful *rifting phases* occurred. The first during the Carboniferous, Permian and Middle Jurassic times, and the second in Middle and Late Jurassic to Early/Mid Cretaceous times (Brekke, 2022).

Basins found in the proximal settings, for example on the Trøndelag Platform, were created during the first rifting period in Carboniferous, Permian and Middle Jurassic times. During the second rifting phase, the Vøring Basin was formed. A final rifting episode had great impact on the outer ridges complexes between Late Cretaceous and Paleocene, and Eurasia and Greenland finally separated in early Eocene, about 54 Ma (Talwani and Eldholm, 1977, Brekke, 2022). The outer domain was significantly influenced by massive volcanic activity of around 61 Ma (Skogseid and Eldholm (1987), Saunders et al. (1997), Peron-Pinvidic and Osmundsen (2018)).

According to Blystad et al. (1995), the regional stress regimes were greatly affected by the continental breakup, the Caledonian orogeny and the two major rifting events. Before the Late Devonian, the lithospheric plates were in a compressional stress regime. Followingly, the stress regime altered to an extensional stress regime between the Late Devonian and the Eocene, and during the ensuing seafloor spreading in Tertiary, the stress regime changed to slightly compressional (Brekke, 2022). Zastrozhnov et al. (2018) highlights different inversion structures from Mid-Cenozoic as indications of compressional stress, probably caused by a ridge push (Vågnes et al., 1998, Doré et al., 2008). This is also discussed by several authors, for instance those mentioned in chapter 1.1.

The migration of fault activity in the NW-NNW direction, and a change in the maximum elongation trend from WSW-ENE in Devonian time to NW-SE orientation during the last phases of the Paleocene rifting are important observations because they indicate a large change in the orientation regional stress regime in the Mid-Norwegian rift. (Mosar et al., 2002, Peron-Pinvidic and Osmundsen, 2016, Brekke, 2022). Moreover, Doré et al. (1999) highlighted the significant rotation of the stress orientations over time as a characteristic

of this rifted margin. These findings are supported by findings presented by Blystad et al. (1995); that the stress orientations have changed several timed during the rifting periods (Brekke, 2022).

An increase in magmatic additions towards the outer domain of this rift was interpreted by Brekke (2022). Some of them being "smiles" - magmatic sills that are shaped as the name indicates. Those distinct features are also observed in the Vøring Basin by Planke et al. (2018).

Another incident assumed to have affected the margin is according to Zastrozhnov et al. (2018) glaciation events. These events did not affect the rifting, but they may have contributed to an expansion in depocenters across the margin, an increase in regional subsidence and tilting of the margin (Hjelstuen et al., 1999, Rise et al., 2005, Faleide et al., 2008).

Figure 6 presents a 2D seismic line interpretation performed by Brekke (2022). The line is oriented W-E and covers most of the domains in the rifted margin across the Mid-Norwegian rift. The 2D line also show the location of the Nyk High. Following the interpretation of the top basement (black line), it is interpreted at a rather shallow depth to the east, deepening towards the distal domain, then raising around Nyk High, before it again deepens further out in the outer domain, and then shallows towards the Vøring Escarpment. There are also interpreted several faults, indicating rifting and extension. The magmatic activity seems to have affected the area, and intrusions increase towards the outer domain. Additionally, Brekke (2022) located a large, wedge-shaped fault (see Figure 7), possibly indicating a syn-sedimentary depositional environment (Wang et al., 2016).

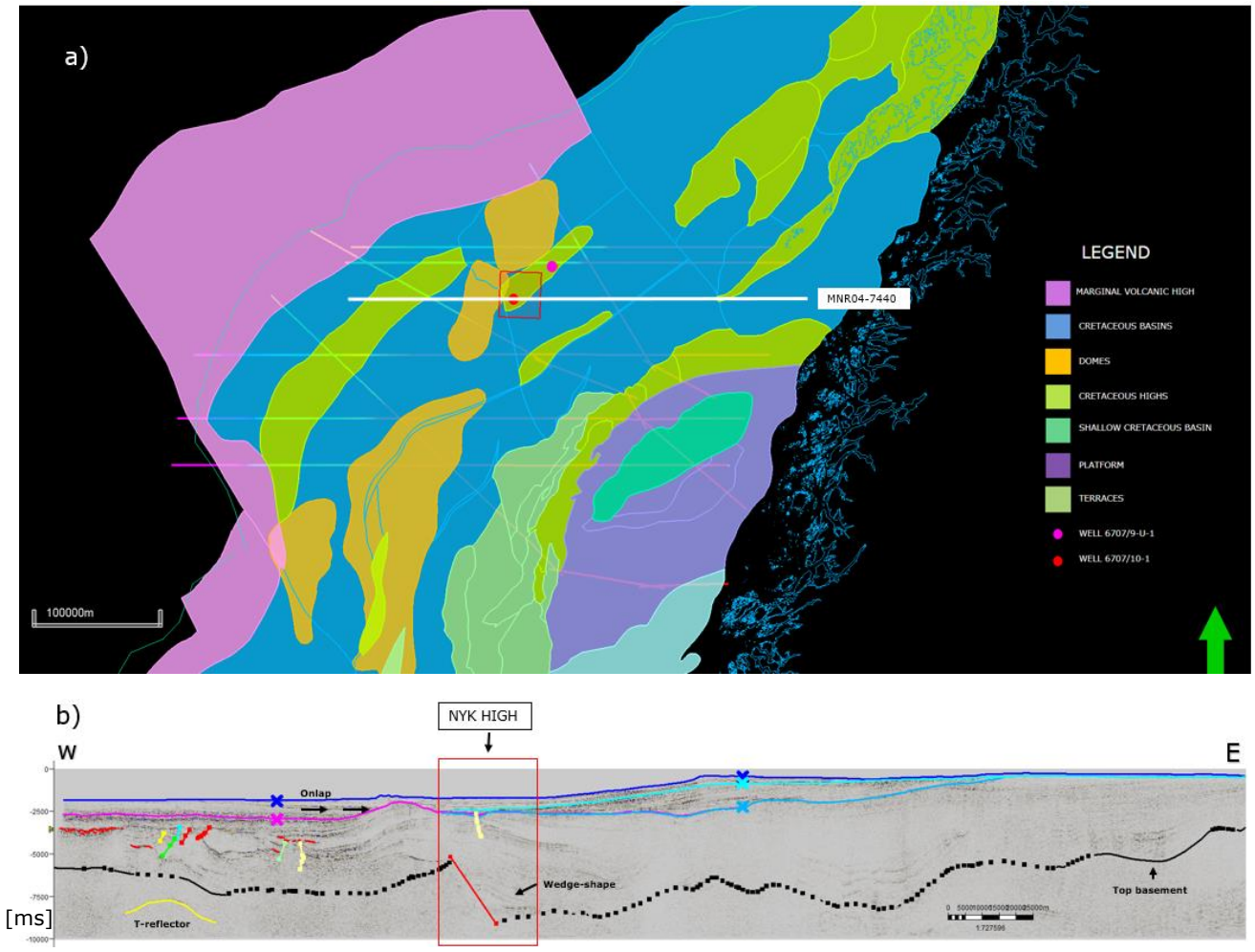

Figure 6 Figure showing the location of the seismic 2D line (a) and interpretation of the profile (b). Faults are interpreted in arbitrarily colours and are curved to semi-vertical. One large wedge-shaped fault in red is located at Nyk High. Onlap is indicated with arrows. Interpretation of the top basement is made in black (dotted line is indicating uncertainty of the mapping). Seabed is dark blue and red semi-horizontal mapping indicates magmatic intrusions. b) is slightly edited from Brekke (2022).

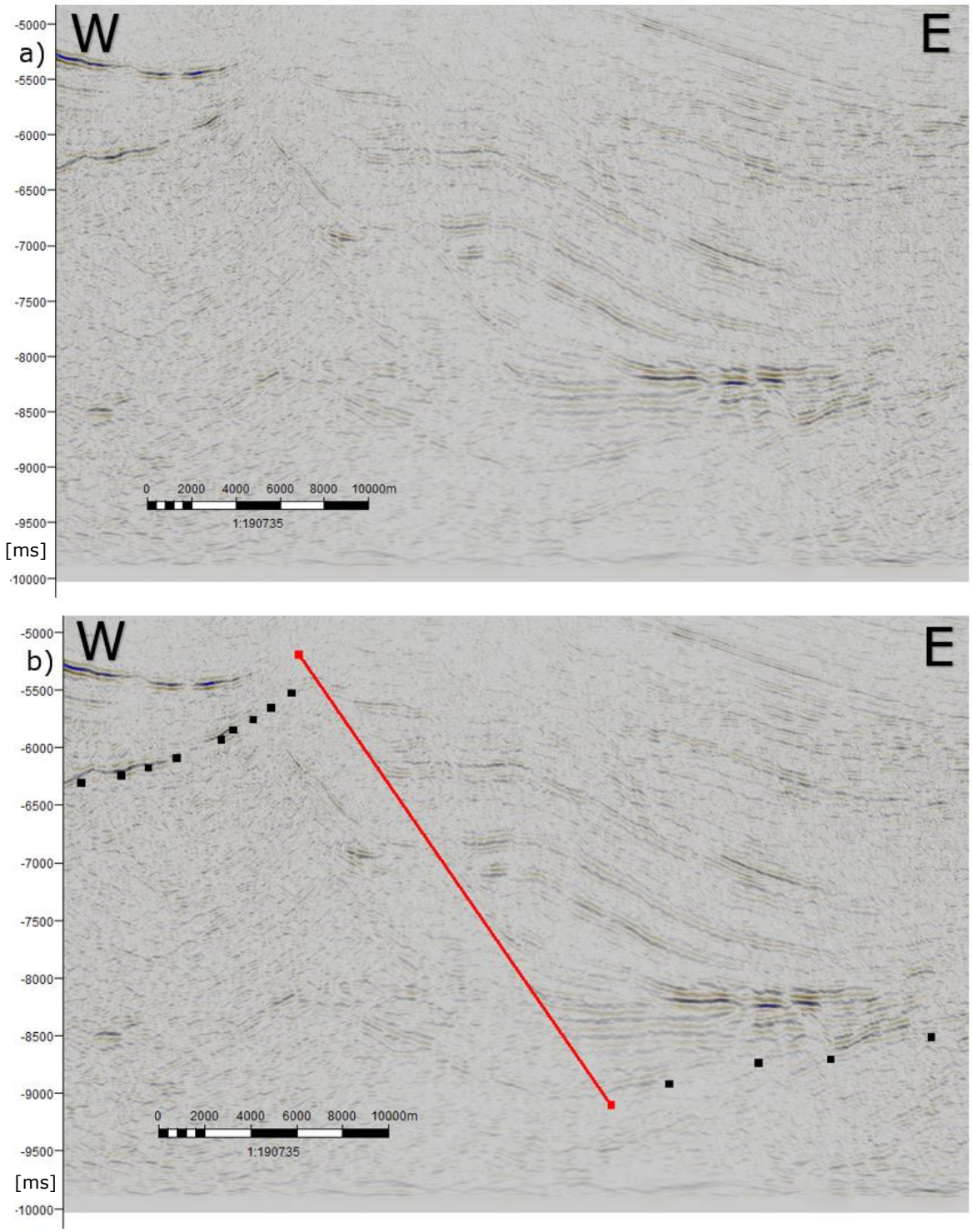

Figure 7 The large syn-sedimentary wedge interpreted by Brekke (2022). a) shows the wedge uninterpreted, while a fault and the top basement is shown in b). The wedge is increasing in thickness towards the red fault (from E to W in the profile).

2.2.4 Sedimentary setting of the Vøring Basin

The Vøring Basin is an extensional sedimentary basin located between the Trøndelag platform in the SE and the Vøring Escarpment in the NW of the Mid-Norwegian – NE Greenland rift (e.g., Blystad et al. (1995)). The geological evolution of the Vøring Basin is, according to Mørk et al. (2001), much related to the rifting and volcanism that occurred during the Early Tertiary (now termed Paleogene). The basin started to develop during the rifting period in Late Middle Jurassic, lasting to Early Cretaceous, and leading to the breakup between Scandinavia and Greenland in Early Eocene. As explained in chapter 2.2.3, duration and time for events in relation to the Mid-Norwegian – NE Greenland rift are still a hot topic for debate, and the evolution of the Vøring Basin is no exception (e.g., Ren et al. (2003)).

Zastrozhnov et al. (2018) presents a very detailed illustration of the Vøring margin, showing lithology ranging from upper Devonian to Late Quaternary (see Figure 8). The oldest rocks are found in basins at the Trøndelag Platform, and the basement is present throughout the whole profile, with different thickness. At Nyk High, the figure is showing a thick succession of Cretaceous-aged rocks, with smaller layers of Paleogene sediments, and possibly some from Quaternary. A similar interpretation of the bedrock is made by Omosanya (2020), though at a shallower level, only showing rocks from Cretaceous time and younger. Thick Cretaceous basin fills is also supported by Brekke (2000) and Færseth (2021). The core of the drilled wellbore 6707/9-U-1 was studied by Brekke (2022), and the lithology is mainly intervals of sandstone and mudstone. The location of this well is shown in Figure 6a.

The rift periods have affected the setting of the basin, and much magmatic intrusions are found, especially in the distal and outer domains of the basin, which is also illustrated in Figure 8. Brekke (2022) also argued for increasing magmatic activity towards the outer domains of the margin, this was shown in several of the interpreted 2D seismic profiles.

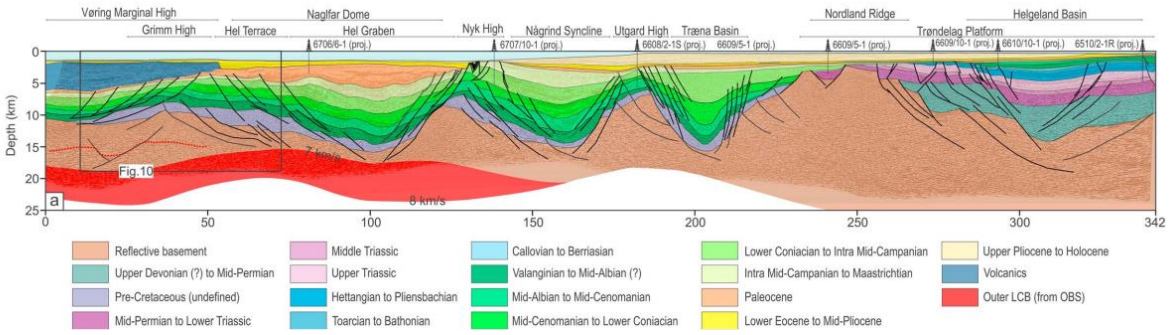

Figure 8 Illustration from Zastrozhnov et al. (2018) of the Vøring margin. Nyk High is seen between the Naglfar Dome and Någrind Syncline. Wellbore 6707/10-1 is placed at Nyk High. The profile is oriented NW-SE.

2.2.5 Wellbore 6707/10-1

The well 6707/10-1 was drilled in 1997 and was the first well to be drilled in the outer domain of the Vøring Basin (Factpages). It is located to the southwest on the Nyk High and it targeted a rotated fault block. The core consists of Late Cretaceous sandstones, in addition to a distinct flat spot, which is marked in Figure 9. Since no seismic to well tie is performed (because of limited time), well tops are not displayed.

The main reason for drilling this well was to study the quality of, and the fluid content of the of the Nise Formation from Campanian age. There was recovered 171 m of the sampled core. The drilled well pertain within the interpreted 3D-seismic block at Nyk High (see Figure 6 for location), hence giving an indication of possible lithology in the area. Figure 10 shows five meters of the sampled core, from 3040 to 3045 meters depth. It portrays mainly porous and fine to medium-grained sandstone, with occasionally features of mudstone.

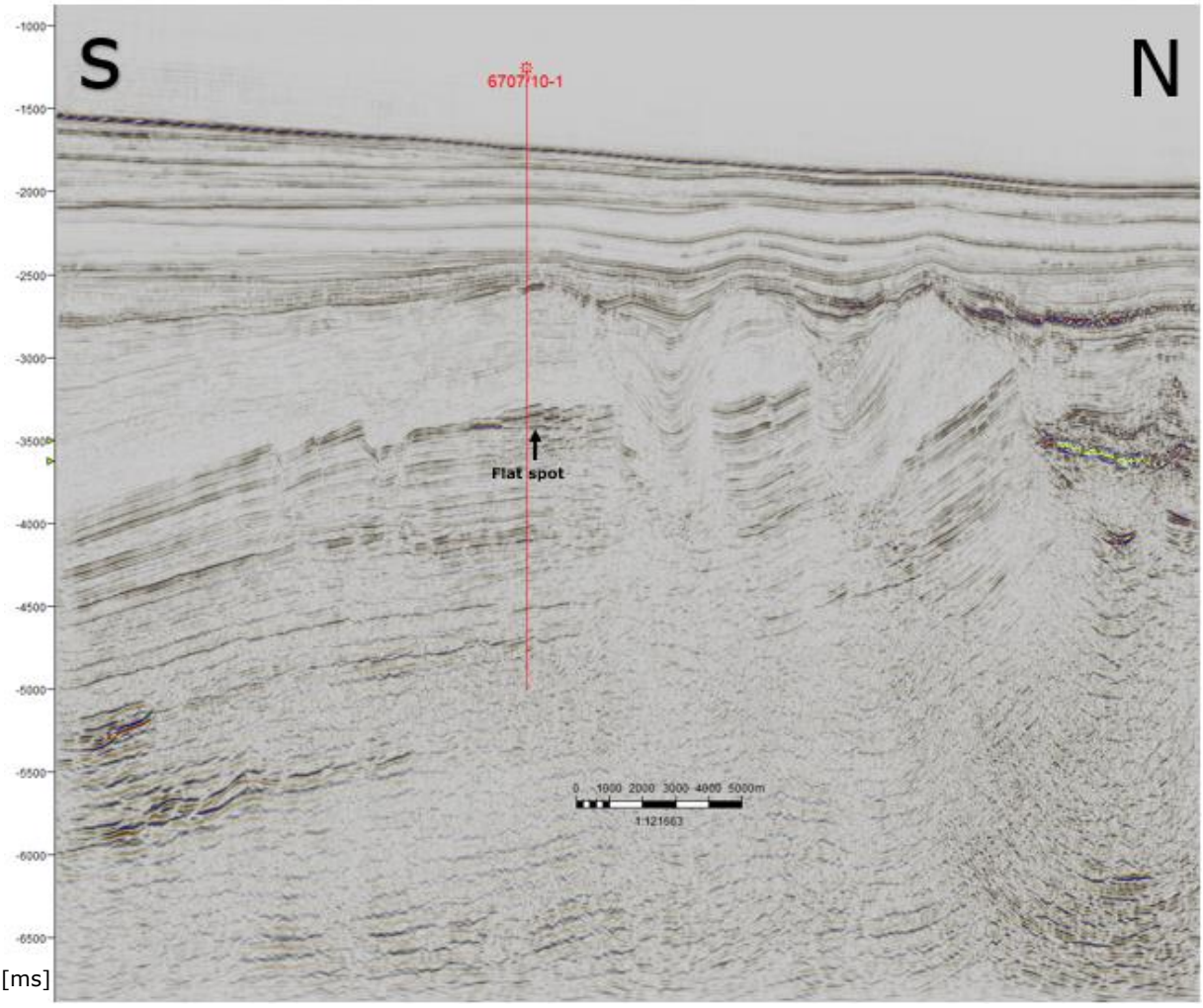

Figure 9 Seismic profile from the 3D dataset exhibiting well 6707/10-1. For location the reader is referred to Figure 6a). The flat spot is shown. NB: no seismic to well tie is performed during this study.

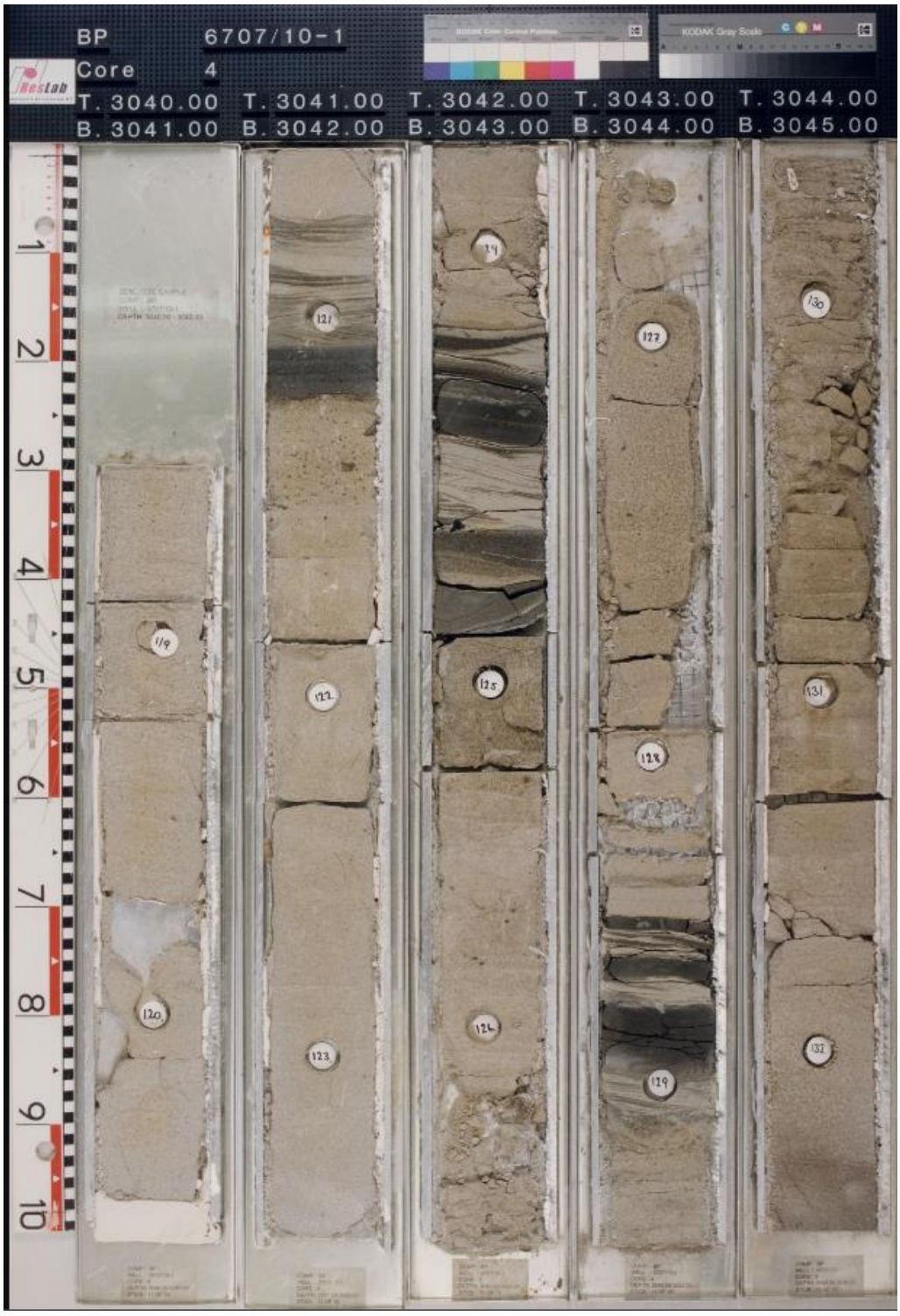

Figure 10 Five meters of the drilled core, mainly showing presence of sandstone, with smaller mudstone occurrence. The sandstone appears porous throughout and less consolidated at several places.

2.2.6 Nyk High

Nyk High is a structure located in the outer domain of the Mid-Norwegian – NE Greenland rift system in the Norwegian Sea. It is interpreted and described as a rotated fault block, and is located between the Hel Graben to its NW and the Någrind Syncline and the Utgård High to its SE (e.g., Blystad et al. (1995)). According to Blystad et al. (1995), Nyk High forms the southern part of the eastern side of the Hel Graben. The high is elongated NE-SW and is approximately 15 to 20 km wide. Further, it was created during the post-Cenomanian time, by differential subsidence across the Surt Lineament (Blystad et al., 1995). Nyk High's formation is closely related to the formation of the Hel Graben and the Någrind Syncline. To the NW of the Nyk High, the compressional structures (Lundin et al., 2013), the Naglfar Dome and the Vema Dome are found (Figure 2a)). Existence of mud diapirs are observed above the latter dome (Blystad et al., 1995).

The wellbore 6707/9-U-1 from Cretaceous time (Lundin et al., 2013) is one of few shallow cores obtained from Nyk High. The core is drilled from 98 m depth to 237.2 m. According to the interpretation made by Brekke (2022), the core consists of mainly a grey fine- to medium grained sandstone and mudstone. A significant part of the cored sample is missing, possibly indicating low-consolidated rocks in the cored area. Although this core only is representative for the area it is cored, it is reasonable to use the information presented by Brekke (2022), together with wellbore 6707/10-1 and other interpretations and observations when studying new structural and sedimentary constraints. According to Færseth (2021), a more than 800 m thick sandstone from the Lower Campanian is located at Nyk High (Fjellanger et al., 2005, Kittelsen et al., 1999).

2.2.7 Summary of the Cretaceous to Paleocene evolution in the NW Vøring Basin

Færseth (2021) published extensive research on the structural geology and basin development of the Norwegian Sea and explains the evolution from Devonian to the Cenozoic times. Since the study area of this research is mainly from Cretaceous time, this subchapter focuses on the Cretaceous to Early Paleogene evolution.

The Norwegian Sea is characterized by massive Cretaceous basins. The evolution of the Cretaceous basins in the Norwegian Sea is still ambiguous, and several authors have argued for different scenarios, including two extensional events (Doré et al., 1999), episodic phases of extensional events with cooling phases in between (Zastrozhnov et al., 2020), and how reactivation of Jurassic faults have affected the overlaying strata of Early Cretaceous time in the Vøring Basin (Zastrozhnov et al., 2018, Peron-Pinvidic and Osmundsen, 2018, Zastrozhnov et al., 2020). The constraining of Early Cretaceous extension is still poor, because of Jurassic crustal stretching (Færseth, 2021). Signs of compaction is also observed in the area (Færseth, 2021), one significant observation being compaction-induced faulting, which is created when compaction of sediments is opposed to a hanging wall, causing sediments to be dragged up towards that fault scarp. This type of compaction is observed in the Late Jurassic to Early Cretaceous, and is often related to thermal subsidence (Bertram and Milton, 1988), which is argued to have been an important mechanism, especially of the Early Cretaceous sedimentation (Færseth, 2021).

The rift phase in Campanian-Paleocene time had most impact on the north-western parts of the Vøring Basin (Skogseid and Eldholm, 1989, Roberts et al., 1999). This period is characterized by major extension and normal faulting, fault block rotation, uplift, and erosion, and it is proposed that this is the period with the main activity of normal faulting in the area (Brekke, 2000, Færseth and Lien, 2002), meaning this rift period is significant for the evolution of the Nyk High. According to Ren et al. (2003), three characteristics of the Late Cretaceous-Paleocene rifting in the NW Vøring Basin are low-angle normal faults, syn-rift sedimentation and subsidence, followed by magmatic activity and regional uplift and erosion. Despite extensive research over the past years, there is still uncertainty regarding the timing and importance of different events, including the amount of stretching (e.g., Peron-Pinvidic and Osmundsen (2018), Zastrozhnov et al. (2020), Færseth (2021)).

2.3 Fault network

Faults are types of fractures that form in different stress regimes. When stress is applied to a rock, the rock will deform and when the stress exceeds the Mohr Coulomb criterium, the rock will eventually break and create fractures (Fossen, 2010). When two fault blocks move in opposite directions relative to each other, a displacement occurs, and a fault is created. Faults are complex structures that can form in extensional, compressional, strike-slip environments, in a combination of those three, or as reactivations of older faults or fractures, and weakness zones (Fossen, 2010).

Faults usually appear in sets, which eventually create networks (Willemse, 1997, Walsh et al., 2003, Nixon et al., 2014). They are important in the understanding of how the faults have affected the research area. Fractures and faults weaken the rock, can affect the sedimentary deposition, lead to rotation, and behave as traps or as leakage paths for hydrocarbons (Fossen, 2010). Studying faults can also reveal information on different stress regimes (Fossen, 2010) that were active at the time the faults were created, and it can also give information on which faults were created when, relative to each other. When the faulting and sedimentation is active at the same time (syn-tectonic sedimentation), the sedimentary layers in the hanging wall increase in thickness towards the fault (Hongxing and Anderson, 2007) and can create an alleged wedge-shape.

As mentioned, faults are rarely created as single faults, they are part of greater segments and network. Gawthorpe and Leeder (2000) present detailed and informative figures explaining the growth of a fault in extensional basin by segment linkage. The two figures show a visualization dividing the fault growth into three stages: initiation, interaction and linkage, and through-going fault zone. Figure 11 shows the 3D evolution of the growth of a normal fault system. At initiation stage, several small faults start to develop with isolated depocenters. At the interaction and linkage stage, the isolated faults start to grow together and link. This can occur because of reactivation of faults, for instance when stress is repositioned (Gawthorpe and Leeder, 2000). The reactivation can also have impact on and create new fault sets in the stratigraphy above (Bailey et al., 2005, Frankowicz and McClay, 2010). At the final stage, the faults have grown together, and the deformation is now localized along the large fault zones. The same three stages are also illustrated in Figure 12, which shows the relation between distance and displacement. It gives a schematic presentation of how three segments over time grow together into one large segment. There is a subsidence in the major fault segment where the linkage occurred.

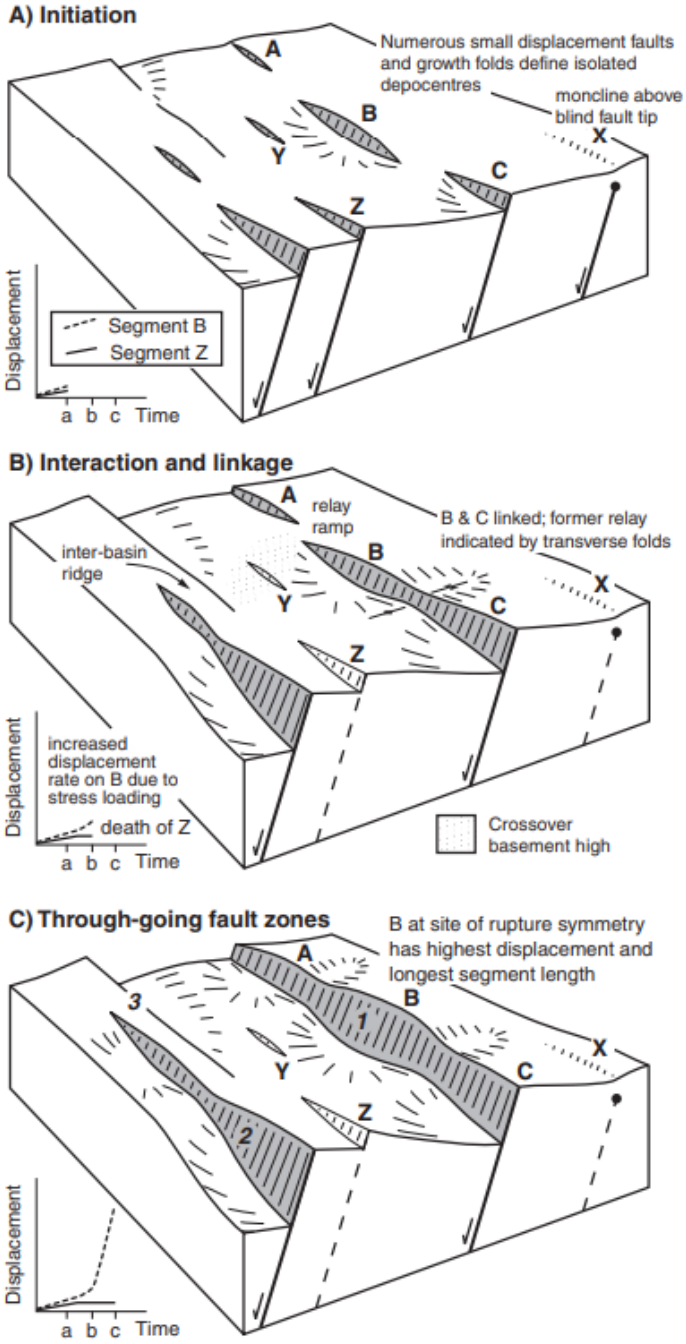

Figure 11 A 3D illustration of the evolution of fault growth divided into three stages: initiation stage, interaction and linkage stage and through-going fault zones. The evolution initiates by three isolated fault segments (A, B and C), and they start to interact and link before they are all connected into one large fault (Gawthorpe and Leeder, 2000).

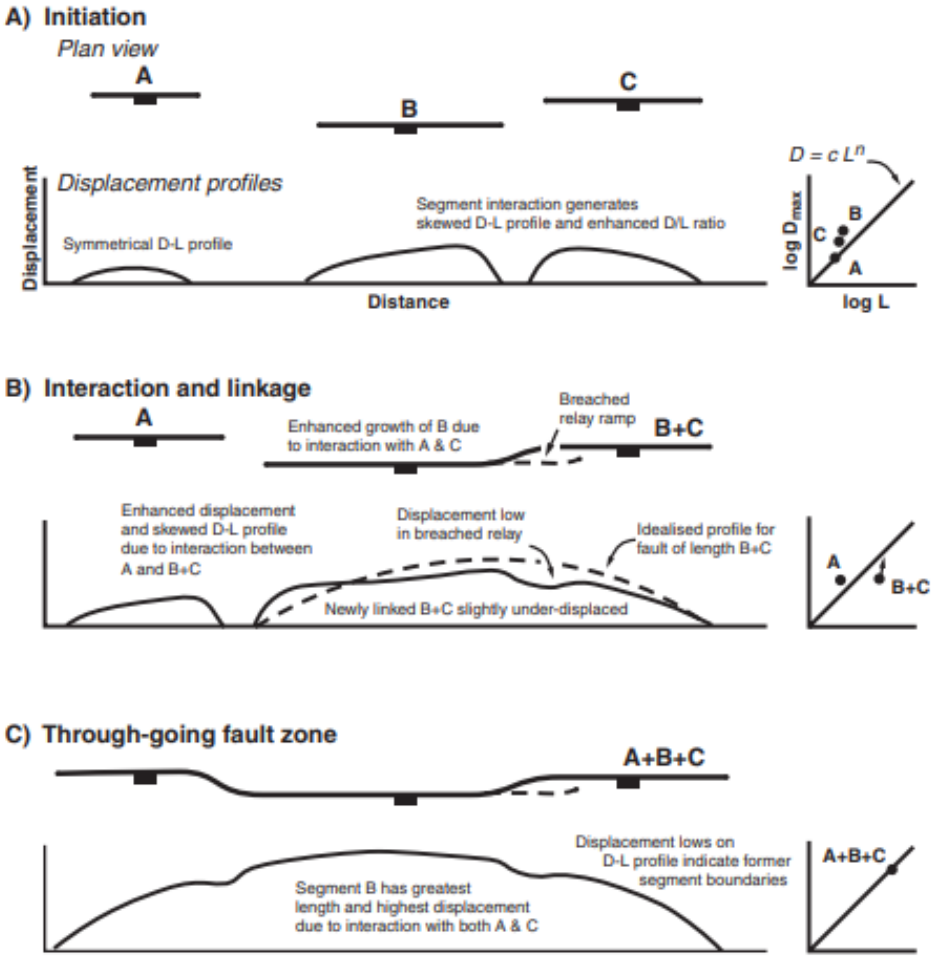

Figure 12 A schematic presentation of the evolution of fault growth divided into three stages: initiation, interaction and linkage and through-going fault zone. It starts with three isolated fault segments in A, which interact and link together in B, before they all connect to one large fault segment in C (Gawthorpe and Leeder, 2000).

Rotevatn et al. (2018) highlights the fact that textbooks within structural geology exclusively presents the propagation model, and not the constant-length model, which makes the latter model less known to those not specializing within fault growth. The propagating fault model is older and more established, while the constant-length model was introduced as an alternative model for fault growth by Walsh et al. (2002), and is therefore relative new. Results from Rotevatn et al. (2018) show that only a few of the experimental and natural faults that are studied can be described by the propagating fault model. Even though fault growth does happen accordingly to propagation, it is in the mentioned study rather described as an end-member behavior, and not as the norm. They rather suggest that faults actually grow accordingly to both fault models during their life span; at early-stage faults act accordingly to the fault propagation with linkage and lengthening (when the growth is dominated by lengthening), and later an increase in constant-length displacement follows (when the growth is dominated by an increase in displacement). The model is described as a hybrid-model of the two end-member growth methods and is illustrated in Figure 13.

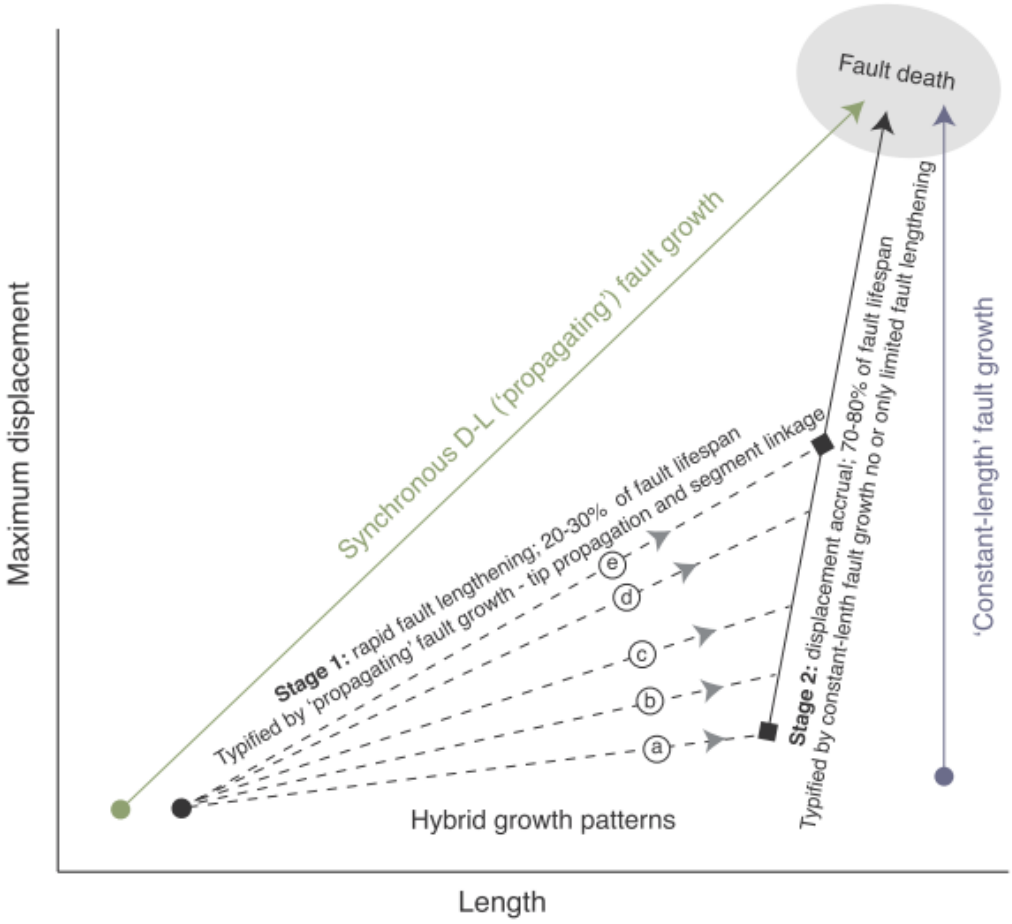

Figure 13 Illustration of how faults grow in relation to length and displacement accordingly to a hybrid growth pattern. The propagating fault growth is shown in green, and the constant-length growth is shown in blue. The growth along one of the black lines in between the two endmembers, indicate a hybrid fault growth pattern. Figure obtained from Rotevatn et al. (2018).

Throw profiles

Throw profiles are diagrams that show the vertical displacement (throw) of a fault plotted against the distance along that fault (e.g., Nixon et al. (2014)). Such diagrams can contribute to a better understanding of how the analyzed faults have grown. Consequently, a large throw indicates a large vertical displacement. Usually, each fault will have one maximum throw, thus studying throw profiles where multiple throw maximums are interpreted could indicate that multiple faults have connected and grown together (Nixon et al., 2014). The results of such diagrams can help explain how the interpreted faults have grown, and if they are one single fault, or rather a set of multiple faults that have connected.

The domino effect

Normal faults can occur in a "domino faulting" pattern. If an area is exposed to extension and the hanging wall starts to rotate, it can create fault blocks within which will create a domino-looking pattern. This type of faulting is often seen in relation to low-angle listric normal faults, and the tilting of the faults allows for greater accommodation space for syn-tectonic sedimentation (McClay and Buchanan, 1992).

2.4 Seismic interpretation

Seismic interpretation can be used to study geological and geophysical properties. This procedure allows for detailed interpretation of the subsurface, such. These data are often obtained by using seismic reflection waves that are sent from a source, through the subsurface and reflected back to a receiver. When the waves reach a boundary with different density, some of the wave will reflect back and a part will continue further down (Haldar, 2018). When the data that is collected is processed, eventually seismic images are obtained and can be interpreted. Since different formations and rock types will have different densities, the waves will travel through the media in changing velocities. Changes in seismic amplitude will appear as different reflectors, and strong reflectors often indicate a change in lithology. This can help dividing the seismic into different sedimentary sequences, in addition to detecting fluid types and structures such as faults and folds.

When performing seismic acquisition, two common surveys to collect are 2D and 3D surveys. On 2D surveys the image is provided in two dimensions, horizontal and vertical. When collecting 3D surveys, the points of collections are distributed evenly over the target area, giving an additional dimension to the acquisition compared to the 2D data (Schlumberger).

3 Methods

The following section explains the approaches and methods used for constraining the geometrical history of the Nyk High. The methods that are used are seismic interpretation of 3D-seismic in Petrel, in addition to a fault analysis by studying the relationship between the fault throw and the distance along the fault.

3.1 Seismic interpretation

For the seismic interpretations, the 3D dataset BNP9601 provided from the NTNU-NPD-SCHLUMBERGER PETREL READY Database is used. The seismic 3D data is provided down to a depth of 7 s-twtt. All seismic profiles are presented with the depth measured in milliseconds. The focus of the interpretation has been on main horizons and main faults that can be argued to have contributed to the broad structural evolution of the area. Smaller local faults were therefore not mapped.

Features that are focused on and mapped during this study are as follows:

- Horizons: mapped in different colours and labelled with numbers 1-8.
- Faults: mapped in random colours, recognized as semi-vertical lines with squares, labelled with the letter F followed by a number.
- Erosional surfaces: mapped in the same way as horizons and interpreted as erosional surfaces.
- Magmatic intrusions: mapped in red using the horizon interpretation tool in Petrel.

The seabed is interpreted with the 3D autotracking tool, while horizons 2-5 are interpreted with the 2D autotracking tool. For horizons 6-8, the manual interpretation tool was mainly used. The manual interpretation tool was used where the reflectors were either dividing or not coherent, hence challenging to interpret with the automatic options in Petrel.

This thesis is mostly based on interpretations of a 3D-seismic block, located in the Vøring Basin, covering the southwestern parts of the Nyk High. The interpretation is mainly executed by interpreting profiles in a N-S direction (inline), while the crossline-direction (E-W oriented) is used to crosscheck and improve the interpretations initially made in the inline direction.

Approach of seismic interpretation

The seismic data was approached by interpreting the main horizons and the main faults by interpreting profiles and incrementing the distance with a factor of 50 each time. This enabled the interpreter to mark the main structures relatively quickly, and it gave a wide image of different geometries. Further, the approach was to interpret profiles with a smaller distance. This process was repeated until the interpretations were detailed enough. The mapping was mostly performed with increments of 50, 25 and 10. Such an approach allowed the interpreter to locate important geometries before studying them more in detail. When interpretations made in the inline direction were inconsistent in the crossline direction, it is an indication of inconsistent mapping. When situations like that occurred, the approach was to adjust the interpretations made in the inline direction to map the actual structure as consistent as possible.

Seismic interpretation of horizons

The interpreted horizons are mapped along strong reflectors that are indicating a change in lithology. When following some of the horizons, the reflector stopped or divided in some of the profiles, making the interpretation challenging. In such cases, it was necessary to evaluate which interpretation was most correct. Although that was intended, there lies a possibility of wrong interpretations in such cases. Further, magmatic additions are interpreted using the interpretation tools intended for horizons, and they are interpreted with red colour.

Seismic interpretation of faults

Faults are interpreted with the fault interpretation tool in Petrel and are shown as lines with squares on the interpretations. Some indications of faults can be an abruptly end of reflectors, a relative movement of rocks or sediments, tilting, rotation, and subsidence. Faults are seldom entirely vertical, so the faults that are presented and discussed here are all curved. It should also be considered that there is a possibility of different fault sets, therefore explaining why the same faults are interpreted as shorter/longer/steeper/slacker in different profiles. Further, the faults that have been focused on are larger faults that have impacted the tectonic evolution of the research area.

3D grids

3D grids of important horizons have also been made in the Petrel software, including 3D visualizations of faults. Some of these grids, as well as 3D visualizations of faults, are also illustrated and discussed. 3D visualizations of faults and horizons are used to better explain and visualize the horizons, to understand how faults change laterally and vertically and how they affect the tectonic evolution of the Nyk High area.

3.2 Fault analysis

Diagrams plotting the fault throw against the distance along the fault are made and interpreted for faults F1 and F3. Such diagrams illustrate how the fault throw changes with distance. The hanging wall (Hw) and footwall (Fw) cut offs are measured from the analysed faults in Petrel by finding the depth [ms] of the used horizon on each side of the fault. The method used for obtaining the values is presented in Figure 14. The figure shows a normal fault cutting through a horizon. The footwall depth is measured by holding the cursor where the horizon is closest to the fault (blue circle) on the footwall side of the fault. The value of the hanging wall is measured similarly, just on the hanging wall side of the fault. In Petrel, the values of the depths are displayed in the lower right corner of the screen and labelled "Time". All depths have negative values; thus, the throws are calculated by using the absolute value of the hanging wall and footwall values, using this formula: |Fw-Hw| (In Figure 14 described as |Value Fw-Value Hw|).

The distance along the faults is measured by using the measuring tool (Measure Distance [D]) in a 2D window in Petrel which is displaying the fault. When measuring the distance, the measurements are made linearly, which means the measured distance is at some places shorter than the actual distance. The measured distance is rounded up/down to the nearest ten.

Calculations and diagrams are created in Excel. The collected values are plotted against each other with the distance (x-axis) and the fault throw (y-axis). The fault tips are set to zero in distance and throw, and they are marked with A and B in the created diagrams.

Because of challenging geology in the study area, several horizons were not possible to map with confidence throughout, and at some places impossible to map. Since throw profiles created from Petrel will calculate every interpretation made of the used horizon and fault, diagrams created from Petrel would not have turned out correctly. The diagrams made in Excel are based on values that are read from Petrel, which to some extent affects the credibility of the diagrams. However, the diagrams still give valuable insight in the understanding of the fault growth.

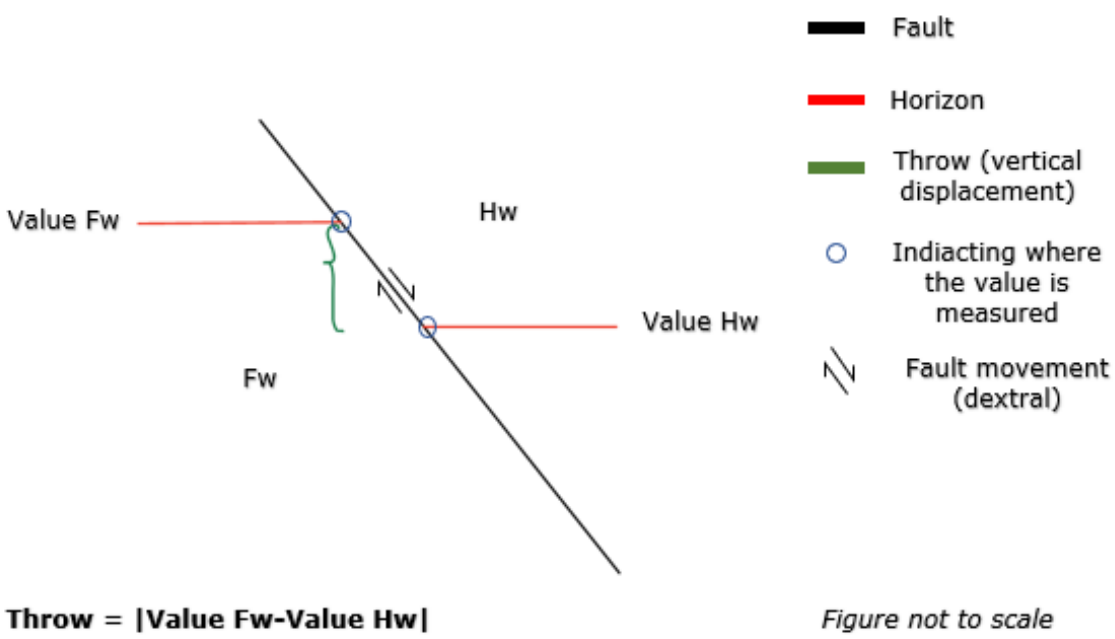

Figure 14 Simplified illustration of how the throw is calculated by obtaining the values from Petrel. Arrows indicating the movement of the footwall and hanging wall sides of the normal fault.

4 Results

In this following chapter, results from the seismic interpretation are presented. There are illustrations of interpreted structures such as horizons and faults in 3D, together with figures of interpretations and explanations. Throw profiles created for fault analysis are also presented and explained. The seismic 3D data is interpreted in a Z-scale of 5.

4.1 Seismic interpretation

In this subchapter the seismic interpretations from the 3D seismic of the Nyk High is presented. Different geological structures like faults, horizons, folds, and sills are presented with interpreted profiles and 3D-figures. Location maps of the selected profiles are also presented here.

4.1.1 Main profiles

Below are three main profiles (A, B and C) selected as key lines as they portray what is interpreted as the most important structures and features for the tectonic evolution of the Nyk High. These features will be described in the following subchapters. Figure 15 shows the locations of the three key lines: in a) an overview photo, and a zoomed-in version in b).

Figure 16 shows interpreted horizons 1-8 and faults F1-F8, together with an uninterpreted profile and its location. Figure 17 shows the second key profile, showing many of the same structures as in Figure 16, in addition to some additional faults. Profile B also points to a good example of onlap. Figure 18 shows the third key profile, showing some additional fault interpretations, including some of which are interpreted in the two other main profiles as well. The reasons for choosing these specific profiles are firstly that they portray important tectonic features, and secondly that they show how the study area changes throughout the 3D seismic cube.

Figure 19 portrays an additional profile. Here, the well 6707/10-1 is placed, and it penetrates the flat spot mentioned in chapter 2.2.5. Faults F2 and F3 are in this profile interpreted to cut through seismic horizon 6. Furthermore, several additional smaller faults are interpreted to cut through horizon 7.

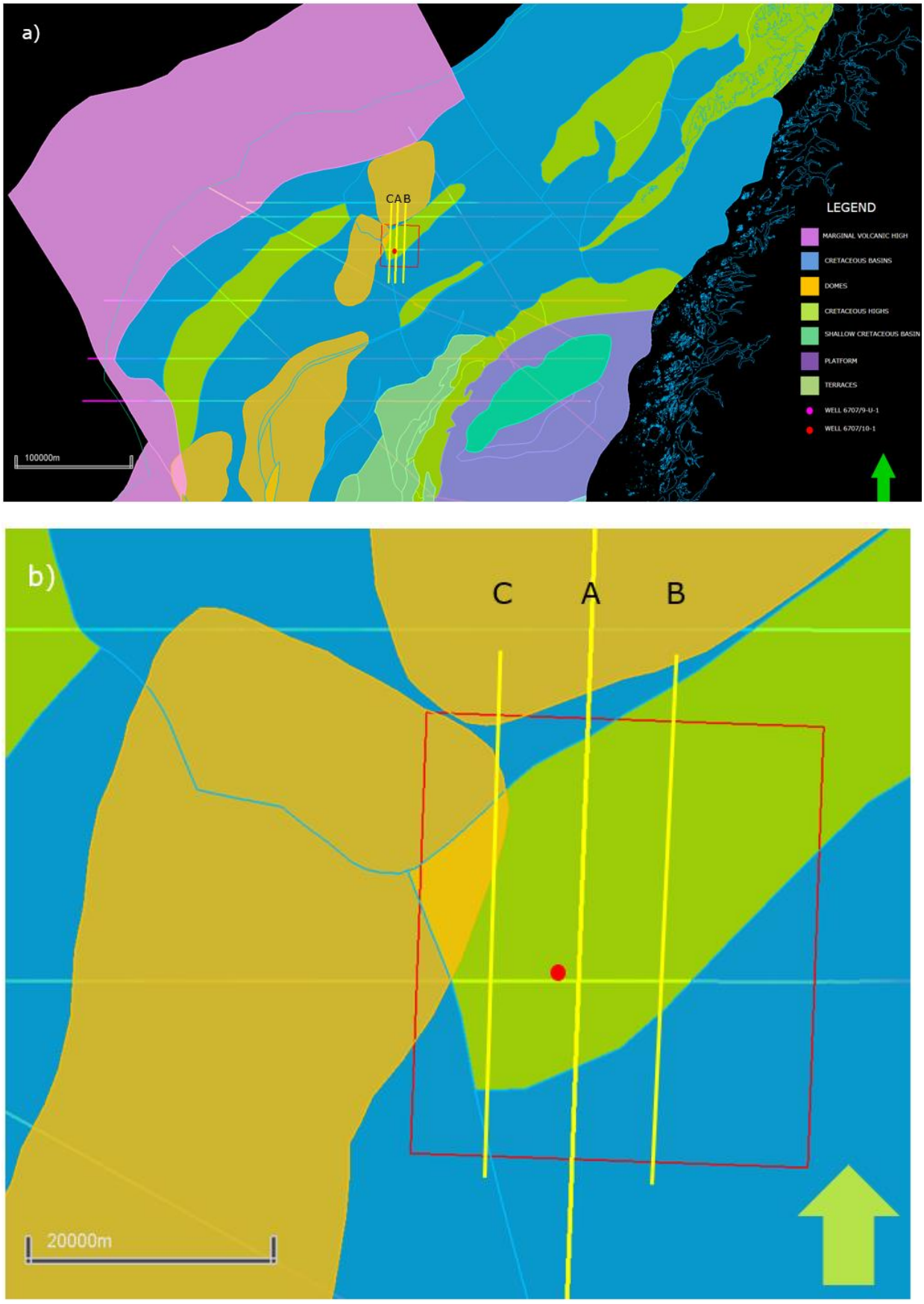

Figure 15 Map presenting the location of the three main profiles (A, B and C) at regional scale (a) and zoomed in (b). Red circle is well 6707/10-1, green arrow indicating north.

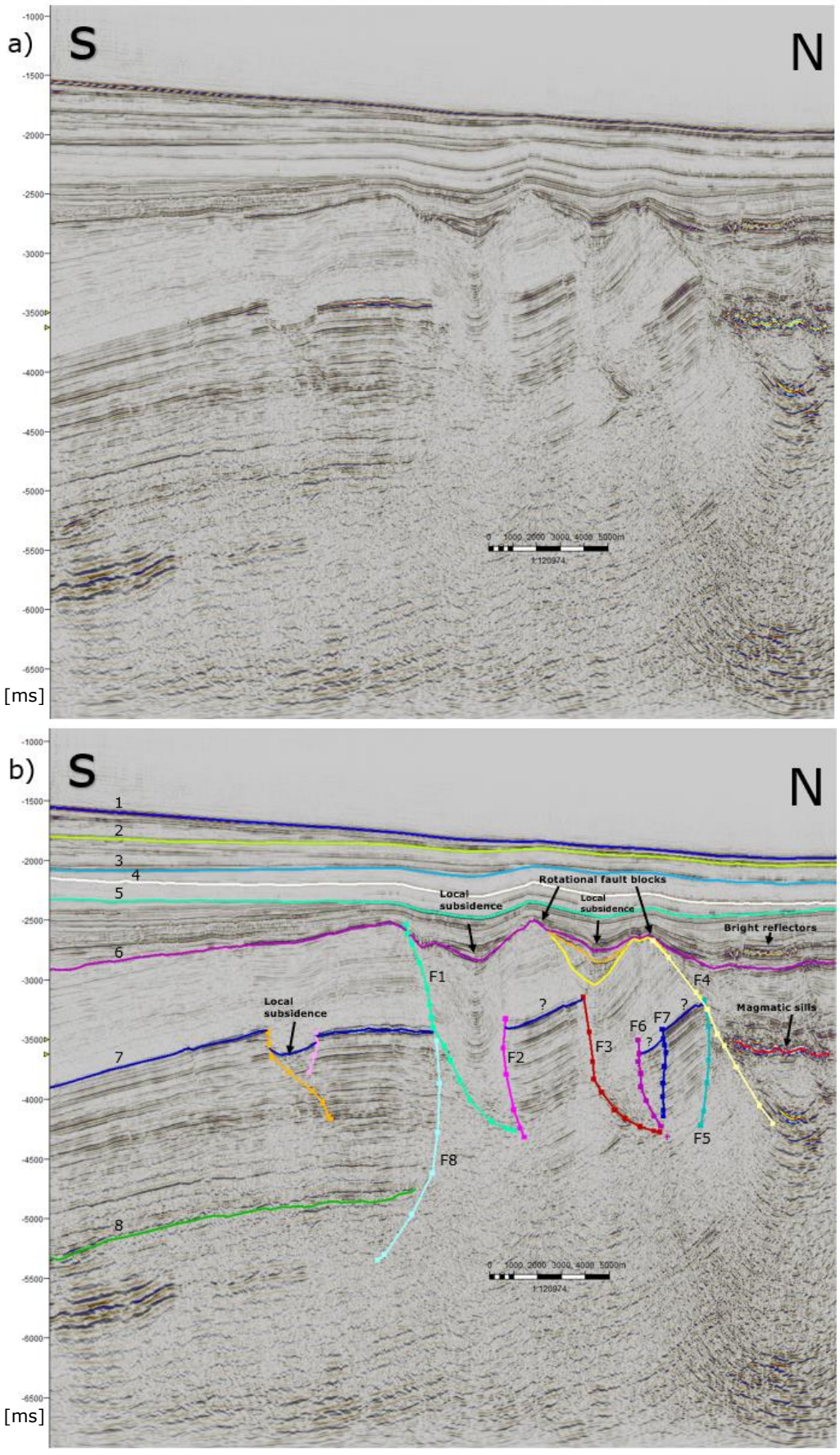

Figure 16 Seismic profile of key line A, representing some of the main horizons and faults. Uninterpreted profile in a) and interpreted profile in b). Significant features are indicated with arrows.

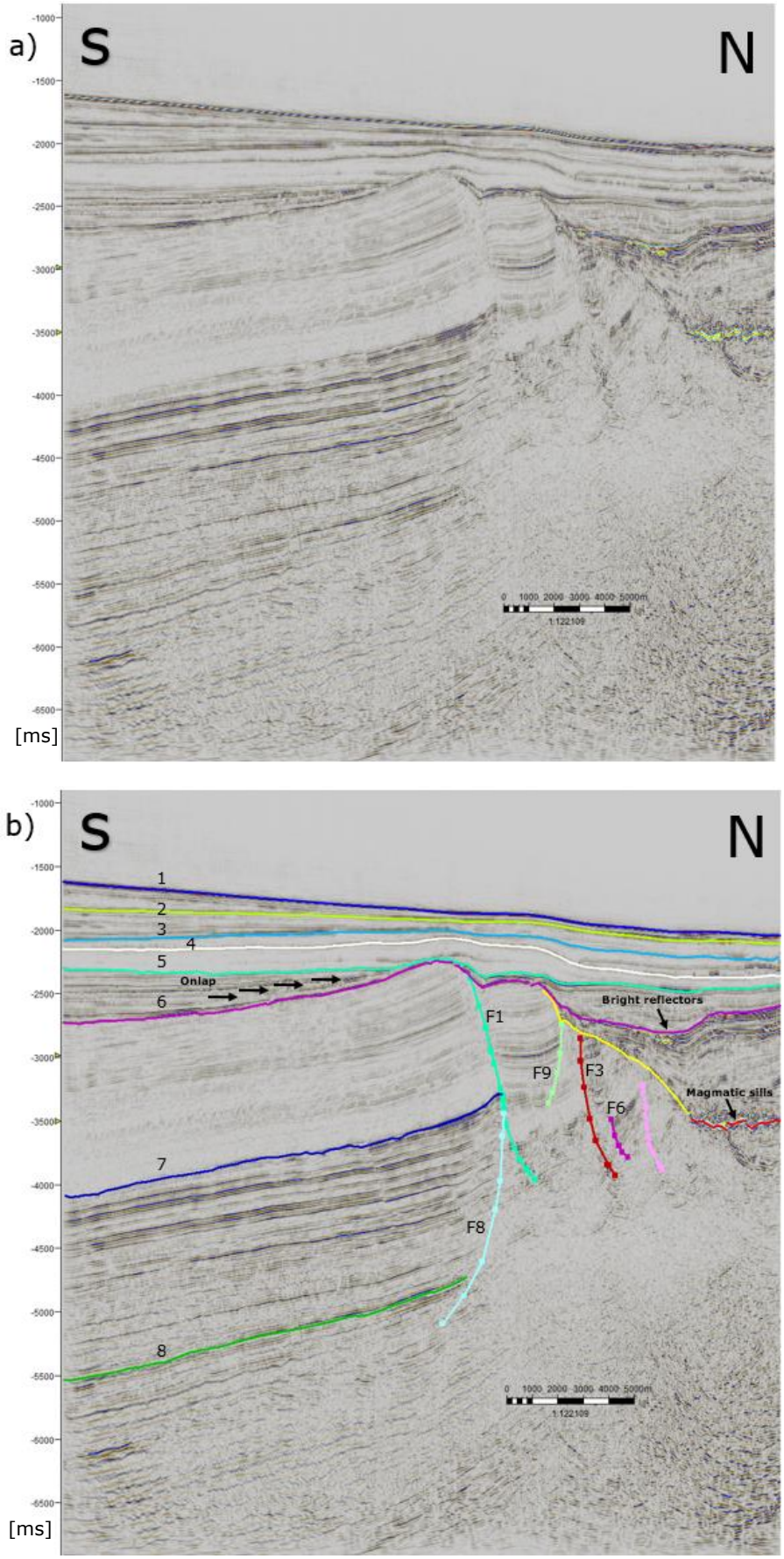

Figure 17 Seismic profile of key line B. Uninterpreted profile in a) and interpreted profile in b). Significant features are indicated with arrows.

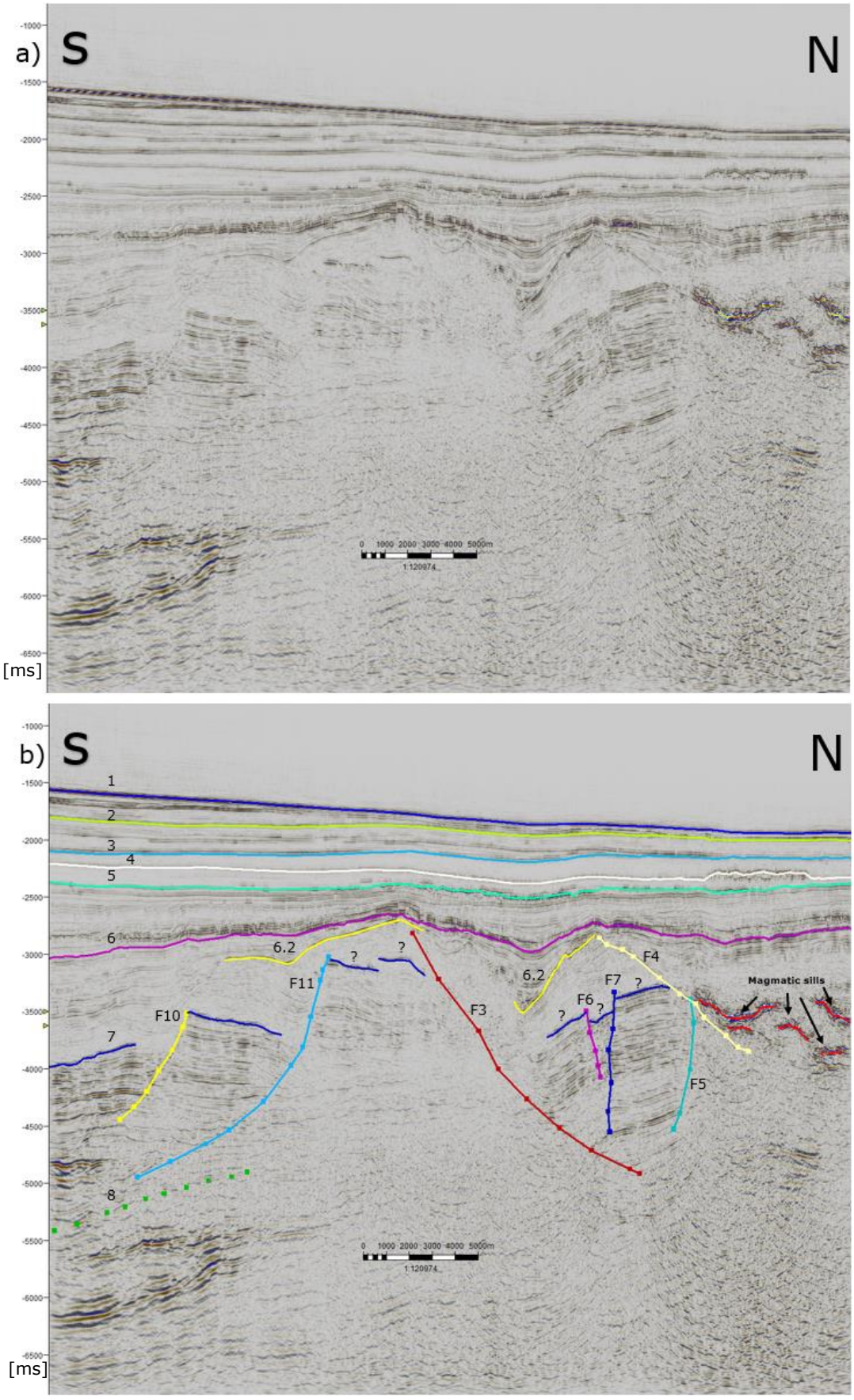

Figure 18 Seismic profile illustrating key line C. Uninterpreted profile in a) and interpreted profile in b). Numbers are indicating horizons, and F followed by a number are indicating faults.

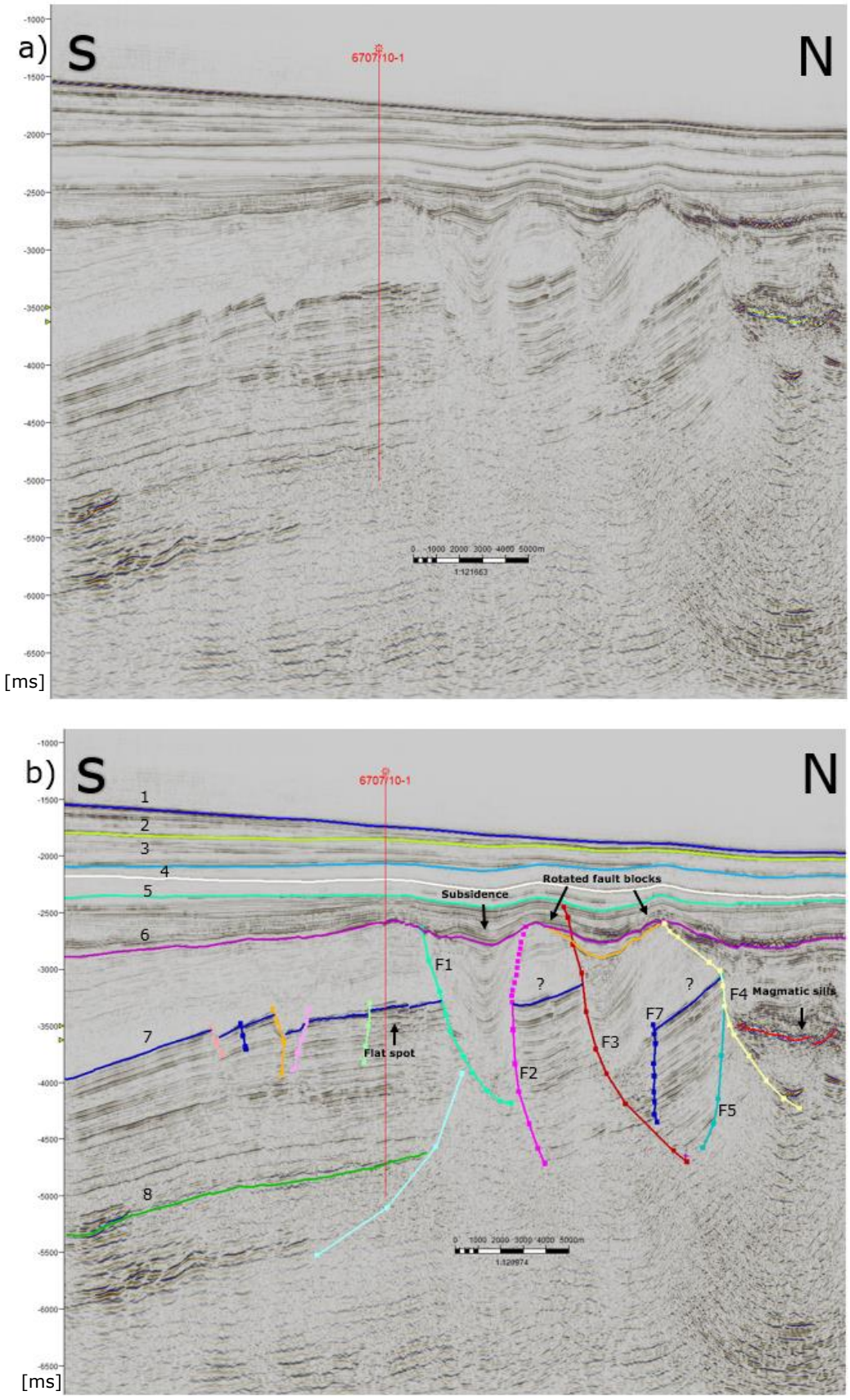

Figure 19 Uninterpreted (a) and interpreted (b) profiles of where well 6707/10-1 is drilled. As seen, both F2 and F3 cut through seismic horizon 6. F3 with more confidence than F2. A distinct flat spot is marked. For location see the placement of the well in e.g., Figure 15. The well is also presented in the illustration from Zastrozhnov et al. (2018) in Figure 8.

4.1.2 Sedimentary sequences

The horizons divide the sedimentary succession into seven possible sequences. Horizon 1 indicates the seabed. Horizon 6 is interpreted as an erosional surface. Horizons 6.1 and 6.2 are alternative interpretations of horizon 6. Horizons 7 and 8 are dividing a large sedimentary sequence into smaller divisions. The horizons are mainly interpreted where there is observed an abrupt change in seismic velocity, possibly indicating a change in lithology. Ages of the sequences are discussed in the next chapter.

4.1.2.1 Horizons 1-5

Horizon 1, the seabed, is relatively horizontal, except from two areas, one in the north and one to the WSW, where it is interpreted at a deeper level, hence the topography is dipping to those directions. This is illustrated in the created grid in Figure 20.

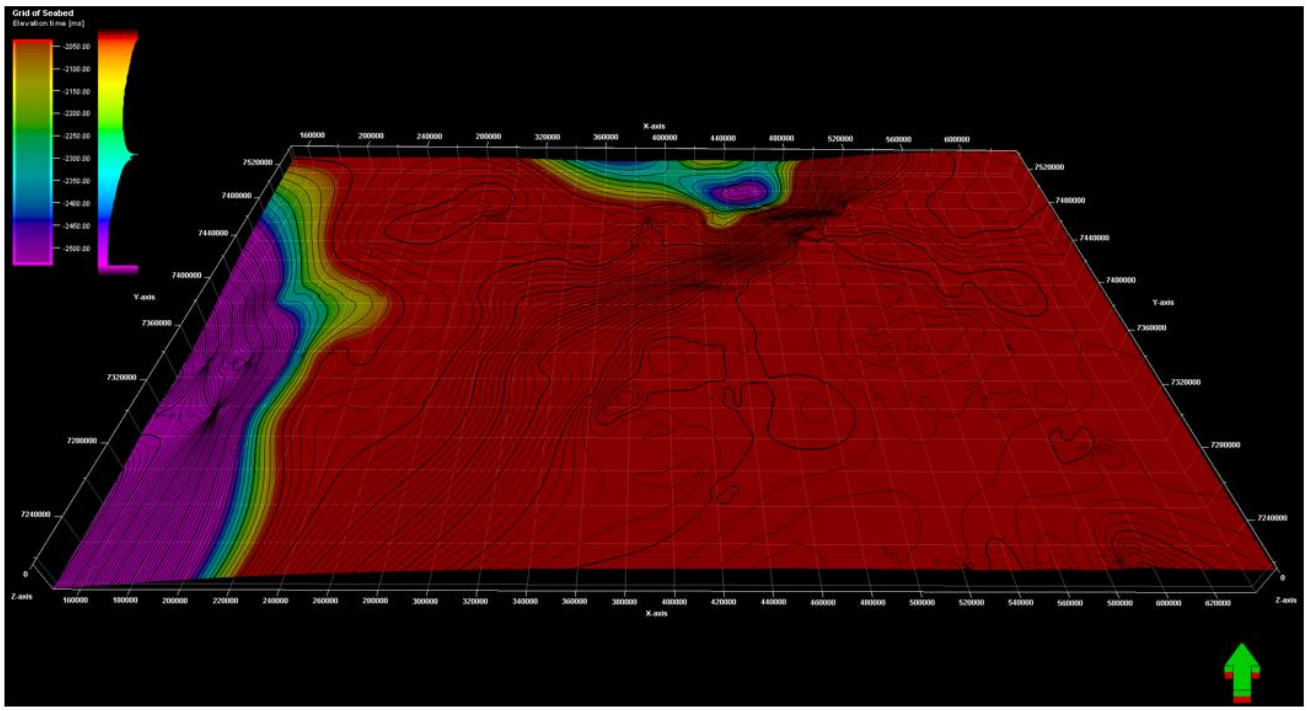

Figure 20 Grid of the seabed portraying a relatively horizonal surface with deepening towards the SE and a bit towards the N. Colour legend to the upper left. Green arrow indicating north direction.

The grid of horizon 2 shows a relatively horizontal surface, with few changes in depth. The grids made of horizons 3-5 show a similar topography, with some changes in depth, and a slight steepening towards the NW. The sediments seen in the sequence between horizons 5 and 6 are strong reflectors that are onlapping the erosional surface, which is seen in Figure 17 b). This is especially observed in the eastern part of the 3D cube. Although there are signs of onlapping, there are no obvious signs of clinoforms. Some bright reflectors are also observed in the NW of that sequence.

Neither of these sedimentary sequences appear to have been exposed to extensive rifting. There are minor faults and discontinuous reflectors in this sequence throughout the cube, but not to a great extent, and not related to faulting periods that are significant for the tectonic evolution of the Nyk High.

4.1.2.2 Horizon 6

This horizon is interpreted as an erosional surface. It has three major highs, at least two of them assumed to be related to rotated fault blocks. The surface is steepening away from the highs, especially in the SW and NW directions, but also to the SSE. The surface is at its shallowest in the NE, see Figure 21. Occasionally it was difficult interpreting the horizon because the mapped horizon at places separated into two different horizons, and because the horizon "stopped" for some profiles and then occurred again at slightly different places.

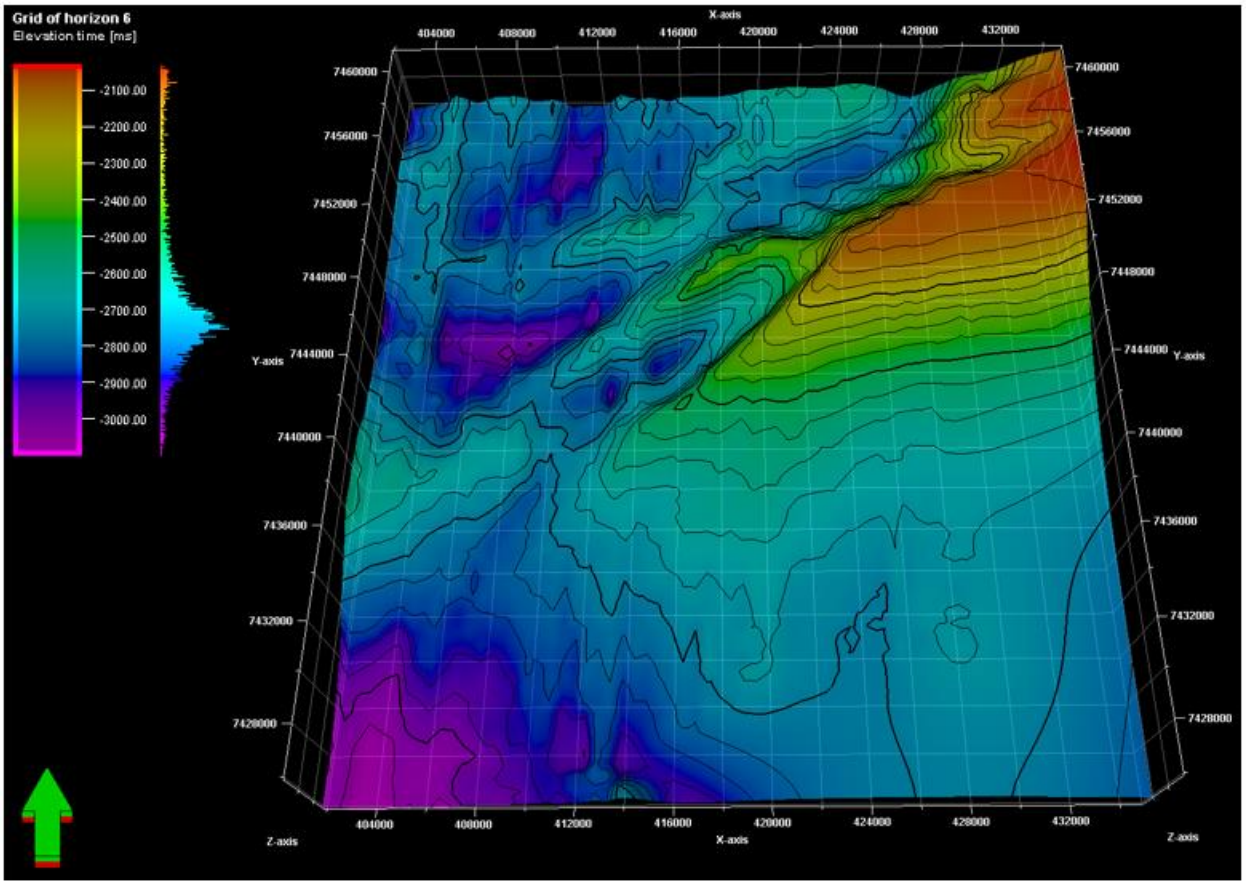

Figure 21 Grid of seismic horizon 6. The surface is steepening towards the SW and the NW. Colour legend in the upper left corner. Green arrow indicating north direction.

Seismic horizons 6.1 and 6.2 are alternative interpretations of horizon 6. These horizons appear when moving westwards in the seismic cube. The reason for these two additional horizons is that the initially followed horizon divides and is therefore difficult to map

correctly. However, 6.2 is also interpreted as part of a fault, which is explained later in this chapter.

4.1.2.3 Horizons 7 and 8

These two horizons are mainly interpreted to have been cut by faults F1 and F8. They appear to be relatively similar in shape, and they dip steeply to the SE. The strata between the two horizons portray strong reflectors (Figure 16) compared to the other sequences. Horizon 7 is cut by two relatively small faults, creating a local subsidence (Figure 16) in between those faults. Horizon 7 is not interpreted with confidence in the hanging wall off fault F1, hence the question marks (Figure 16). The horizon varies in depth, from around -3.2 s-twtt in the west to around -4.1 s-twtt in the east of the cube. Whether horizon 7 is an erosional surface or not will be discussed. The sequence between horizon 6 and horizon 7, shows indications of similar lithology both in the footwall and in the hanging wall of F1, with some semi-strong reflectors highest up, and more faded reflectors just above horizon 7. Horizon 8 is only interpreted at the hanging wall side of F8 and has a depth between -4.2 s-twtt to around -5.8 s-twtt.

4.1.3 Faults

Several faults are interpreted throughout the 3D seismic cube. At the shallowest depths, between -2.5 and -3.0 s-twtt, only minor faulting is interpreted. Multiple smaller faults are observed in this area, but since they are not decisive for the main tectonic evolution of the high, they are not studied to detail. Larger faults that are interpreted to have been pertinent for the tectonic evolution are all located below horizon 6, with faults F1, F2 and F3 possibly cutting through it.

Faults F2 and F3 and F3 and F4 create two distinct rotational fault blocks, as seen in Figure 16. Fault F6 and F7 are interpreted to have been created syn-tectonic to the fault block created by F3 and F4. A local synform folding is created between fault F1 and F2, and a large tilt is interpreted in the hanging wall of fault F8 and footwall of fault F1. The faults that are not labelled, are presumed as not crucial for the tectonic evolution, and consequently not elaborated further.

4.1.3.1 Faults F1 and F8

Faults F1 and F8 are located close to each other, F1 at shallower depths than F8 and they are dipping in opposite directions: to the NW and SE, respectively. F1 appears for the first time slightly to the east of the seismic cube, and it is present until just before the profile intersects the Vema Dome. It has a relatively similar length and dip throughout its presence. F8 is interpreted at a deeper level than F1, and it is present throughout most of the cube. These two faults are marking an abrupt change in reflectors and framing sedimentary layers in the footwall of F1 and in the hanging wall of F8. Those sequences are greatly tilted to the SE, and the tilt is steepest in the east, nearly horizontal in the

middle, and is steepening somewhat farther to the west. F1 is interpreted to possibly have cut through horizon 6. Wedge-shaped geometries are observed in some profiles in the upper hanging wall of F1, which is presented in chapter 4.1.6. A visualization of faults F1 and F8 are presented in Figure 22.

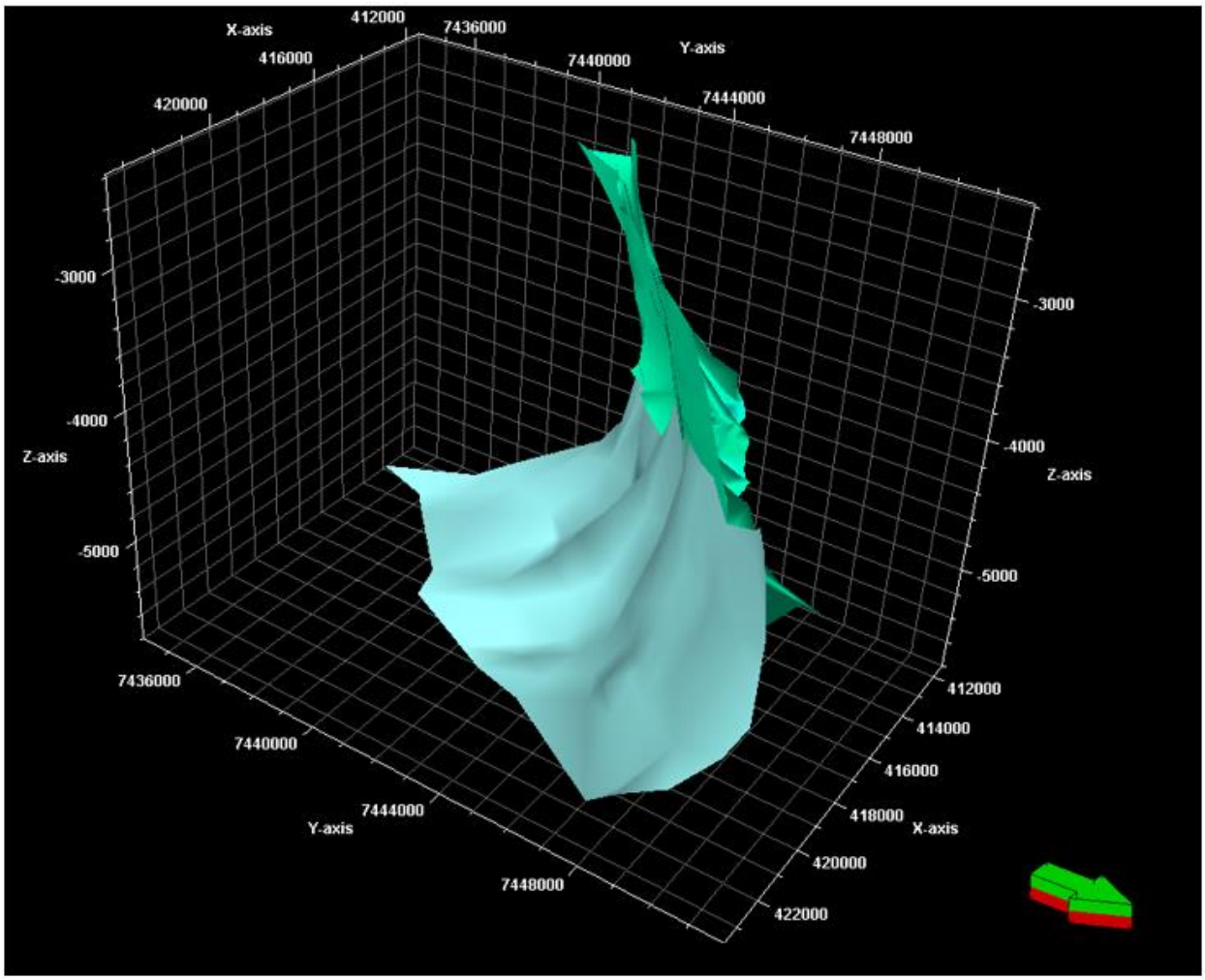

Figure 22 3D presentation of faults F1 (green) and F8 (turquoise). Green arrow indicating north direction.

4.1.3.2 Fault block 1

A rotational fault block is interpreted between fault F2 and F3 (Figure 16). The hanging wall of both faults are interpreted to have moved down, leading to the distinct rotation, with the sediment layers in the block dipping to the SE (see Figure 16). A 3D presentation of the faults is presented in Figure 23, Figure 24, and Figure 25. Fault F3 increases in length towards the west of the block. Further, the fault is also steepening towards the east. Figure 23 gives an overview of the two faults from above, with horizon 6 as surface grid. F3 is growing and flattening towards the west. In Figure 24, the two faults are viewed with a selected inline profile as a reminder of where the rotational block is located. In that

figure, the tilting appears clear. Figure 25 shows both faults in an obliquely angle from above. The change of F3 is viewed explicitly.

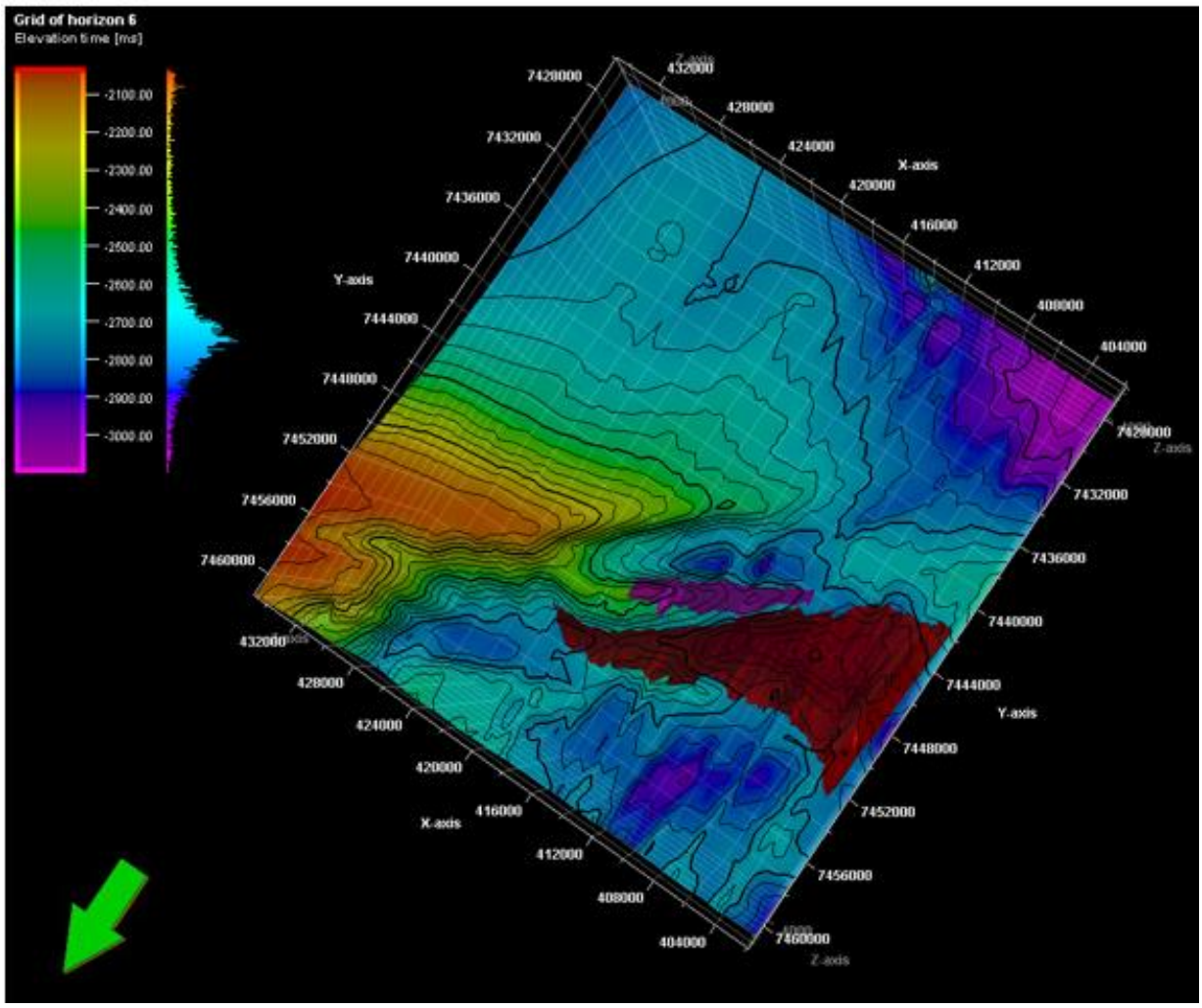

Figure 23 A *3D visualization of F2 (pink) and F3 (red) observed from above and down through horizon 6. Colour legend of horizon 6 to the upper left. Green arrow indicating north direction.*

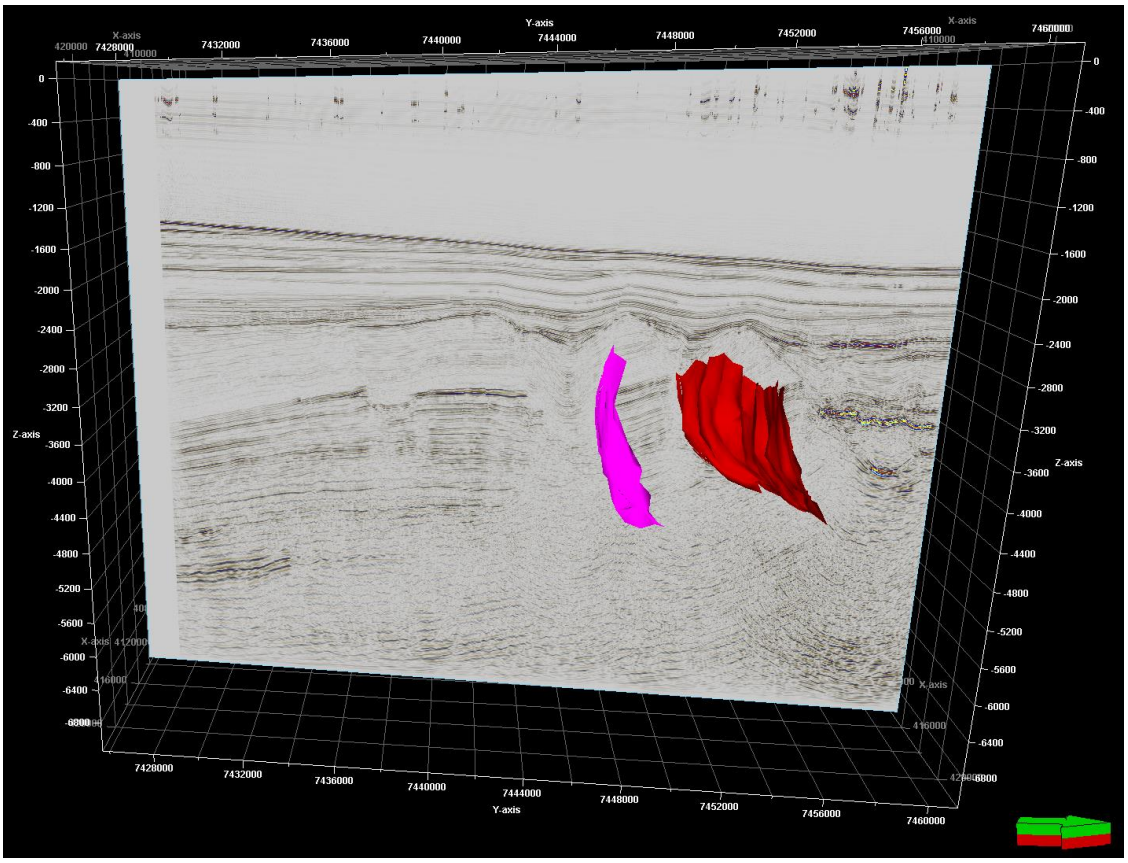

Figure 24 An illustration of faults F2 (pink) and F3 (red), with an inline for location. Green arrow indicating north direction.

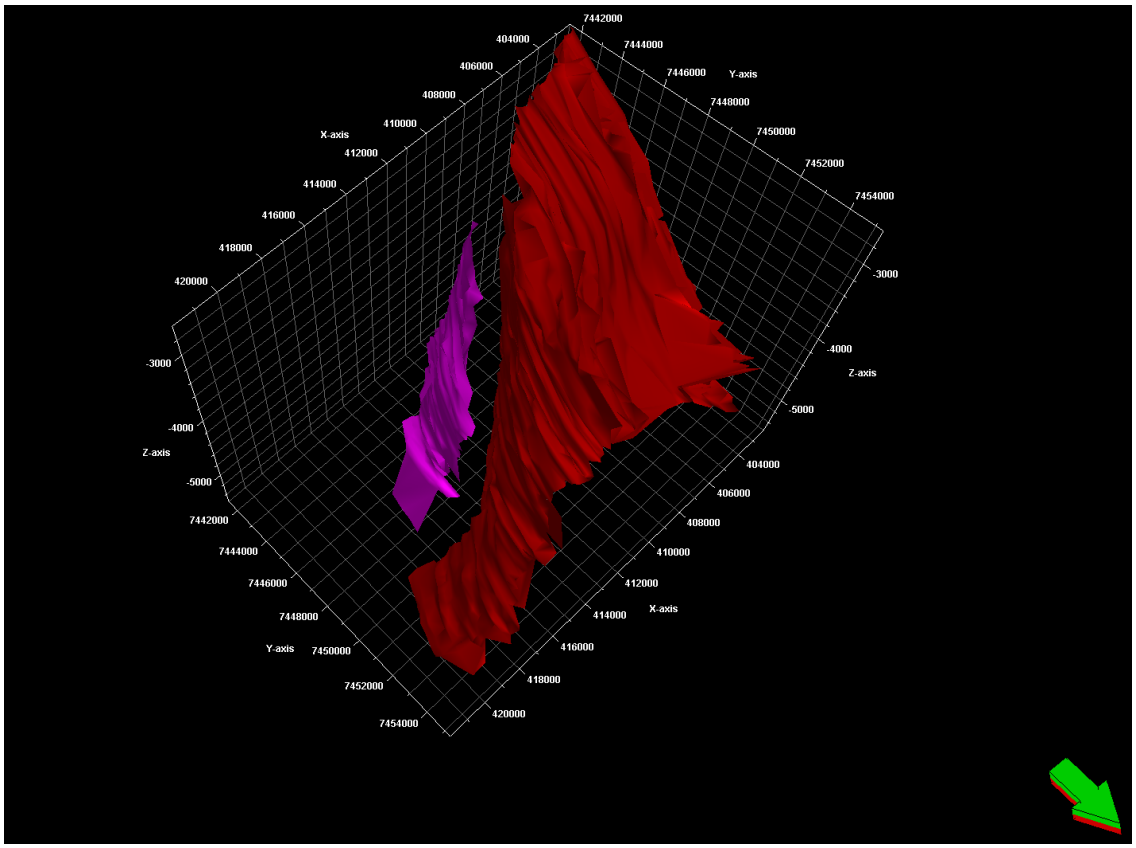

Figure 25 Visualization of F2 (pink) and F3 (red). F2 is increasing in length vertically towards the west. Green arrow indicating north direction.

Both fault F2 and F3 are interpreted higher up, possibly reaching horizon 6, as seen in Figure 19 b). This interpretation is ambiguous, please see Discussion for assessments regarding this.

4.1.3.3 Fault block 2

This fault block is located between faults F3 and F4 and is tilted to the SE. The sedimentary layers in the fault block appear to have a relatively steep dip, around 45 degrees to the SE. The hanging wall of both faults have moved down in order to create the distinct shape. The faults are presented in 3D in Figure 26. F4 is also interpreted as a possible erosional surface because of its shape, and reflectors onlapping that surface. This will be discussed later.

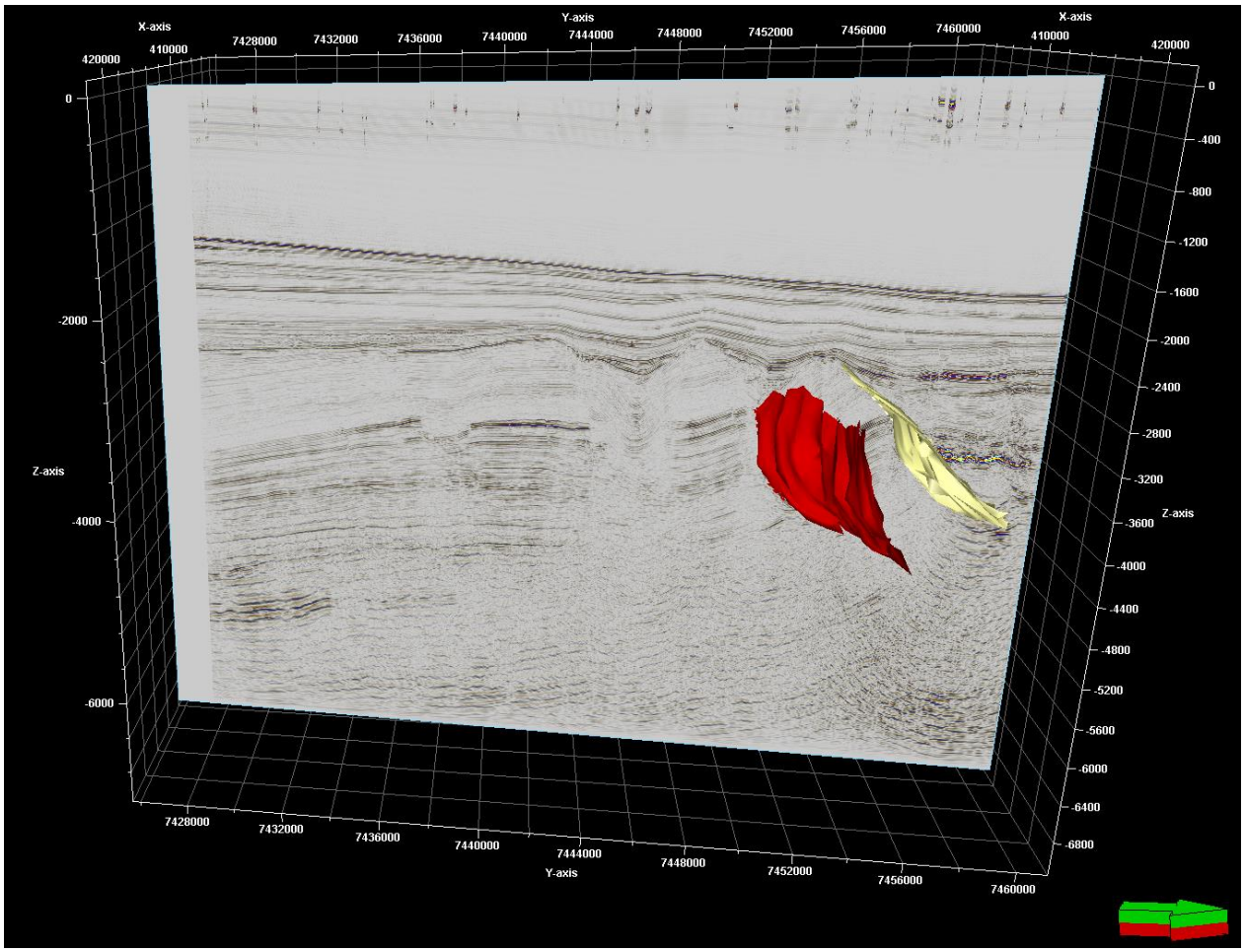

Figure 26 A 3D visualization of F3 and F4 (yellow). Green arrow indicating north direction.

4.1.3.4 Faults F9, F10 and F11

Fault F9 first appears slightly to the east of the profile in shown in Figure 17 b), and it grows vertically moving west, but fades out before reaching the profile in Figure 16. Fault F10 is present towards the west before it fades out just before reaching the end of the 3D seismic cube. Fault F11 appear somewhere between the location of profile A (Figure 16) and profile C (Figure 18) and it fades out in the area where the profile intersects the Vema Dome.

4.1.4 Local fold

As observed in Figure 16, there is a very local fold between faults F1 and F2. It first appears slightly to the east of the 3D-block and evolves more when approaching the middle of the 3D-block. It fades away further to the west. Locations of, and four seismic profiles are presented in Figure 27 and Figure 28, respectively.

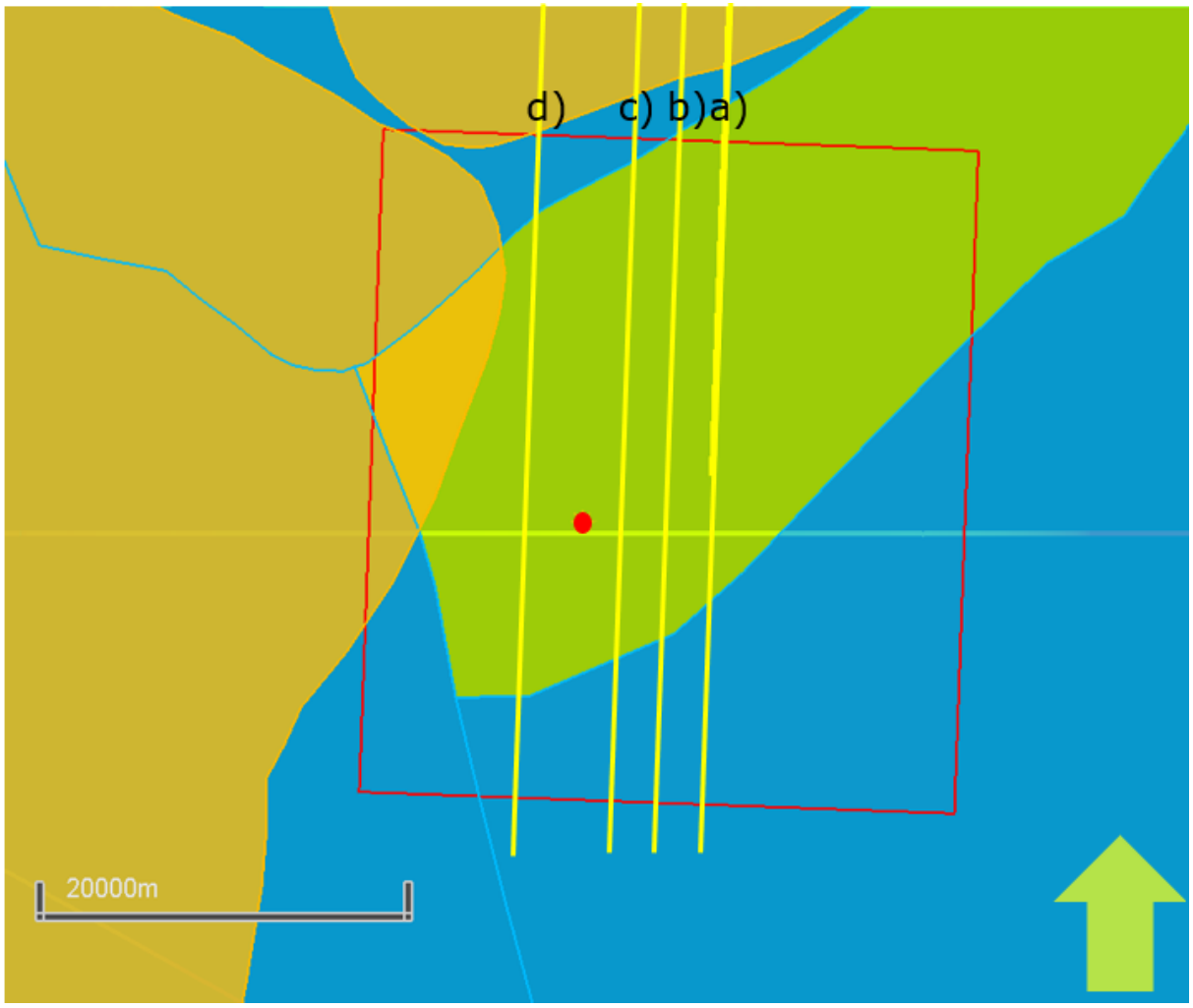

Figure 27 Figure showing the location of four selected profiles of the local folding. Green arrow indicating north direction.

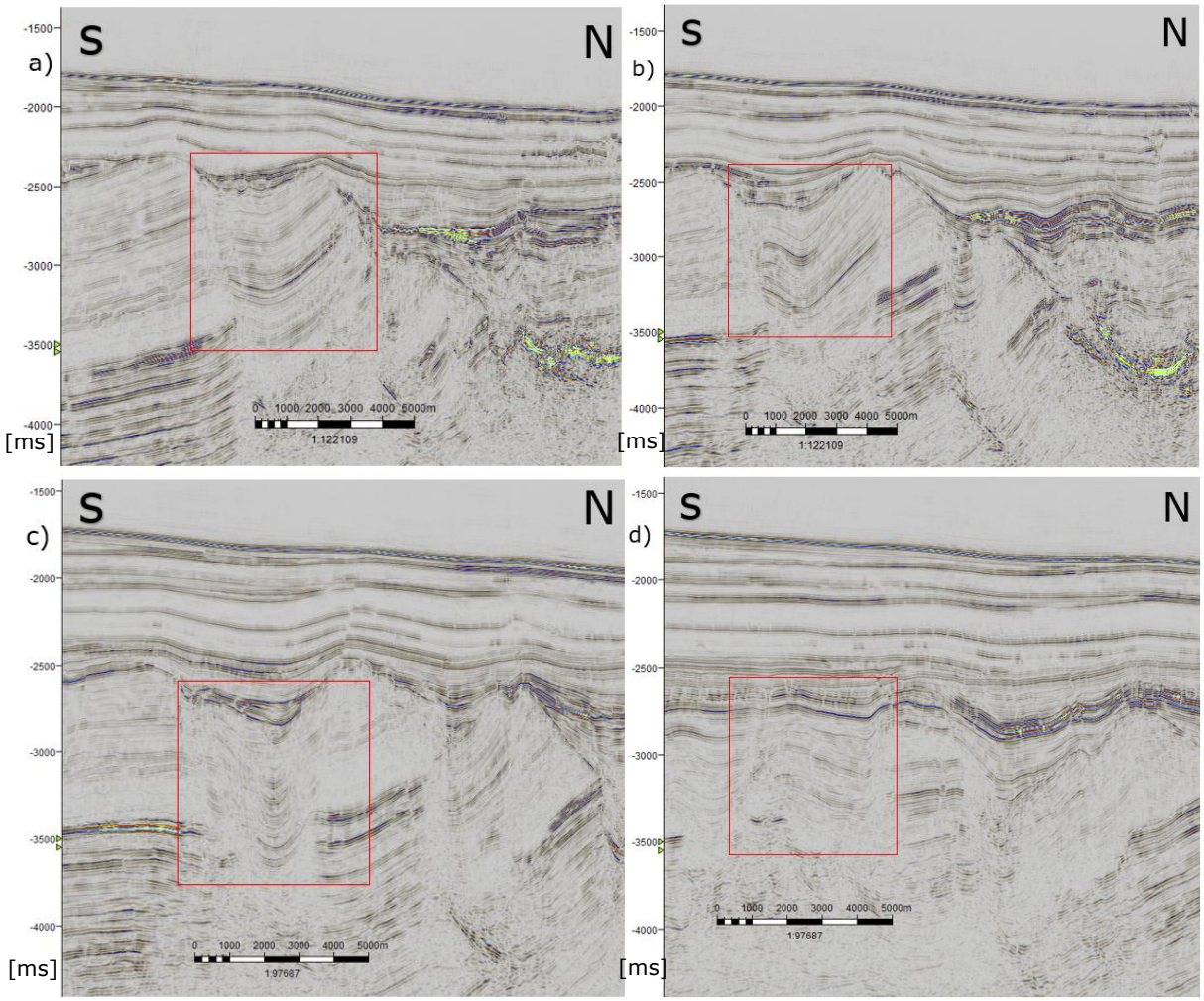

Figure 28 Evolution of the local folding. The profiles correspond to the location labelled with the same letter in Figure 27. The fold evolves from a slight synform in a) to a more distinct synform in b) and c), and it is only slightly folded in d). The red square outlines the fold.

The fold starts out as a relatively uniform synform in figure a). In b), it appears that the fold is bending towards a possible fault in the left part of the red square, creating a small antiform. In c), the fold appears as a rather symmetric synform, while it is less steep in profile d). The layers in the folding in c) appears to slightly bend in towards the southern part. Profile c) is the same profile as in Figure 16, only zoomed in. The reflectors in that profile is slightly bending in towards what is interpreted as F1 in Figure 16, somewhat in the same way as sediments behave in a brittle-ductile transition. In d), the fold is flattening.

4.1.5 Magmatic activity

Clear "textbook" examples of magmatic sills are observed to the NNW in the study area. All the main profiles show such sills, interpreted in red (e.g., Figure 16). The sills are visible in around $2/3$ of the seismic 3D-cube, and they increase in amount, size, and brightness towards the NW.

4.1.6 Features across the 3D seismic cube

Several different features are observed across the study area. The following are some important observations. Keep in mind that the figures in this subsection do not necessarily portray all the horizons or faults that would be crucial for a detailed interpretation, the focus here is to outline distinct changes that are seen across the cube.

- The sedimentary sequences above horizon 6 (location in Figure 29) are clearly disrupted to the west of the cube, as seen in Figure 30. Three profiles are shown, and the changing in disturbance is clearly interpreted to be greatest to the west.

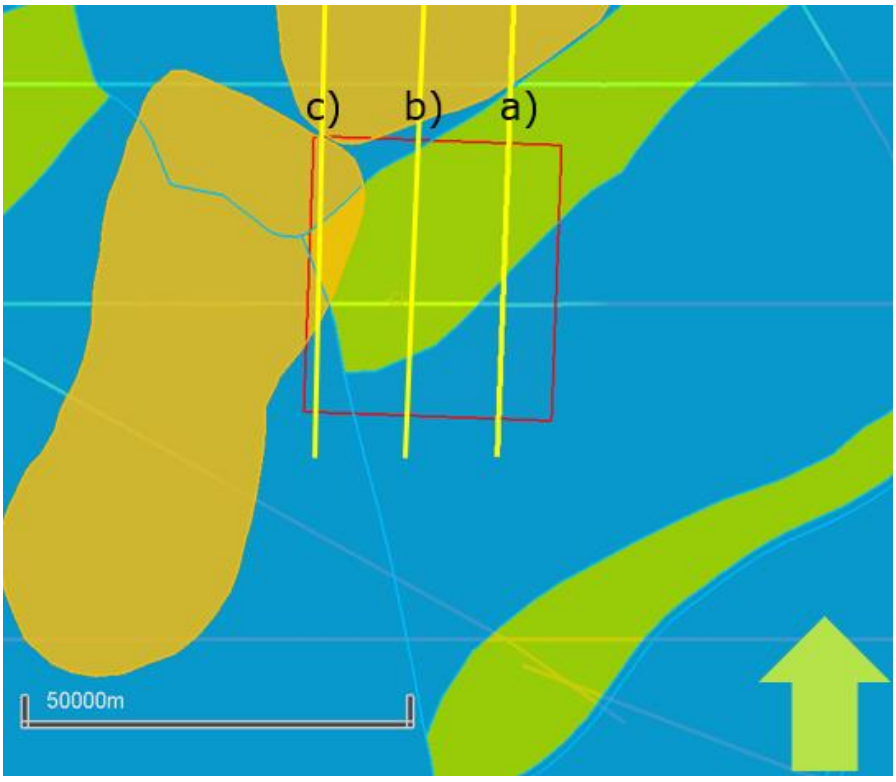

Figure 29 Figure showing the location of three selected profiles to show the change in the shallow sedimentary sequence throughout the cube. Green arrow indicating north direction.

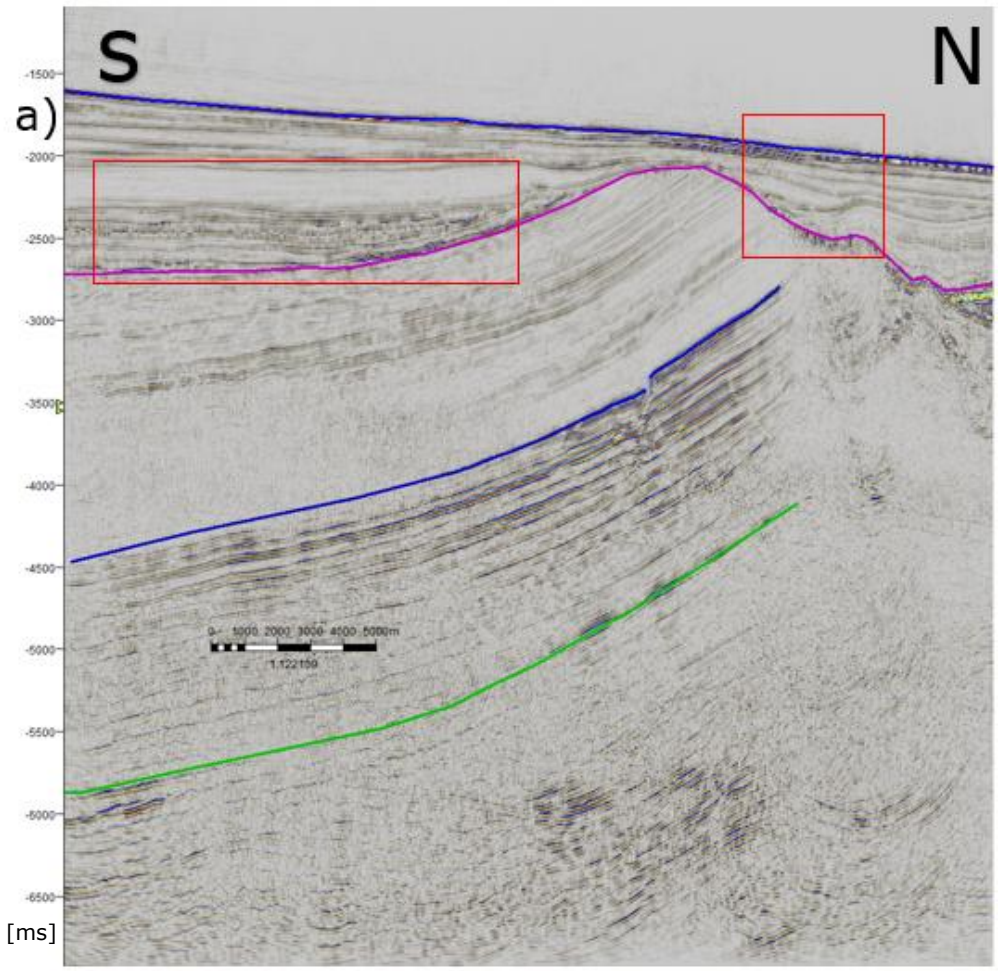
S
N
a)
-1500
-2000
-2500
-3000
-3500
-4000
-4500
-5000
-5500
-6000
-6500
[ms]
0 1000 2000 3000 4000 5000m
1:122159

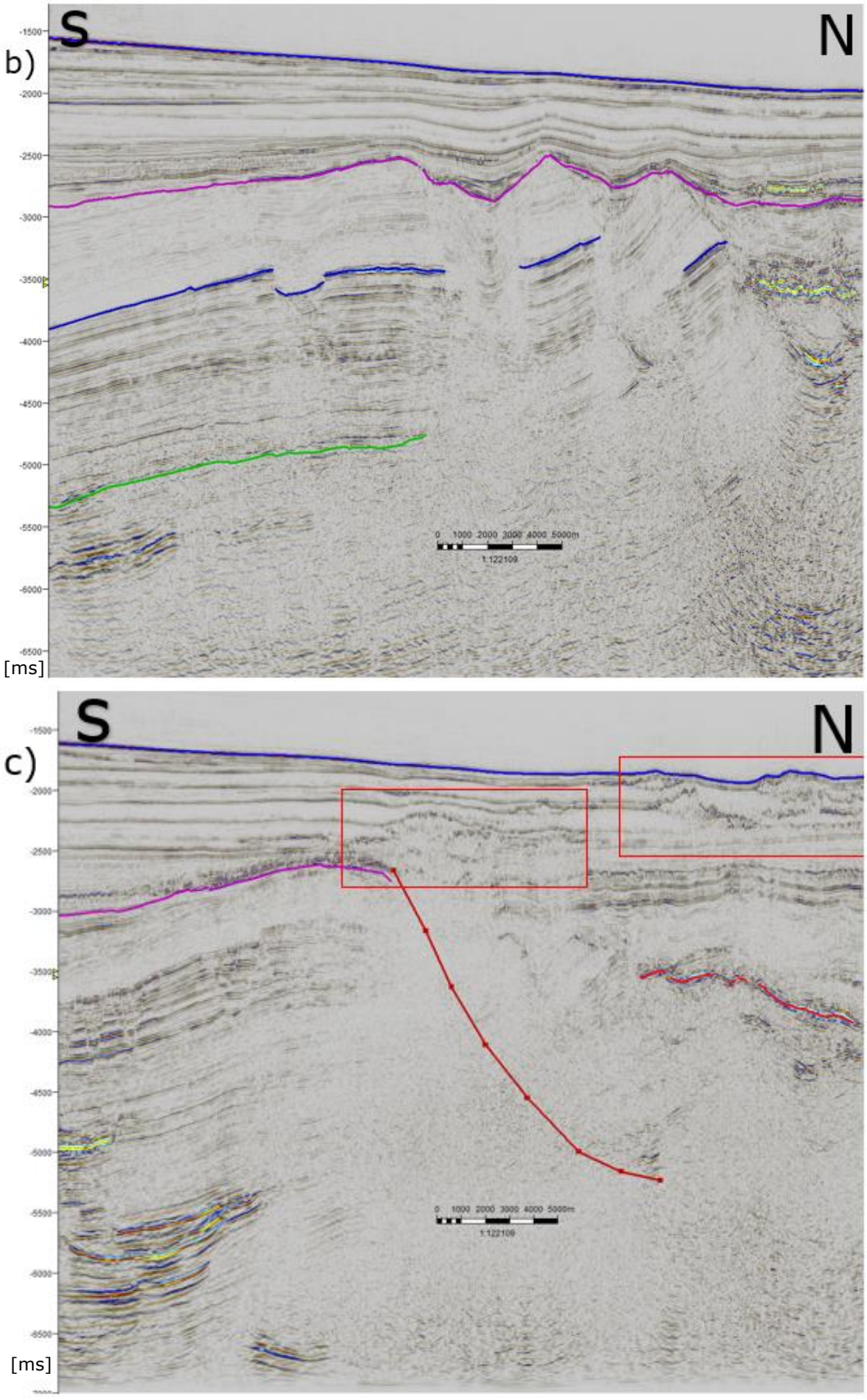

Figure 30 Seismic profiles showing how the disturbance of bedding at shallow depths changes throughout the cube, portrayed at three different locations (a, b, and c).

- A possible wedge-shaped sedimentary structure. This is observed along the upper parts of fault F1, at a few places. This structure is interpreted as a syn-rift structure and is presented in Figure 31.

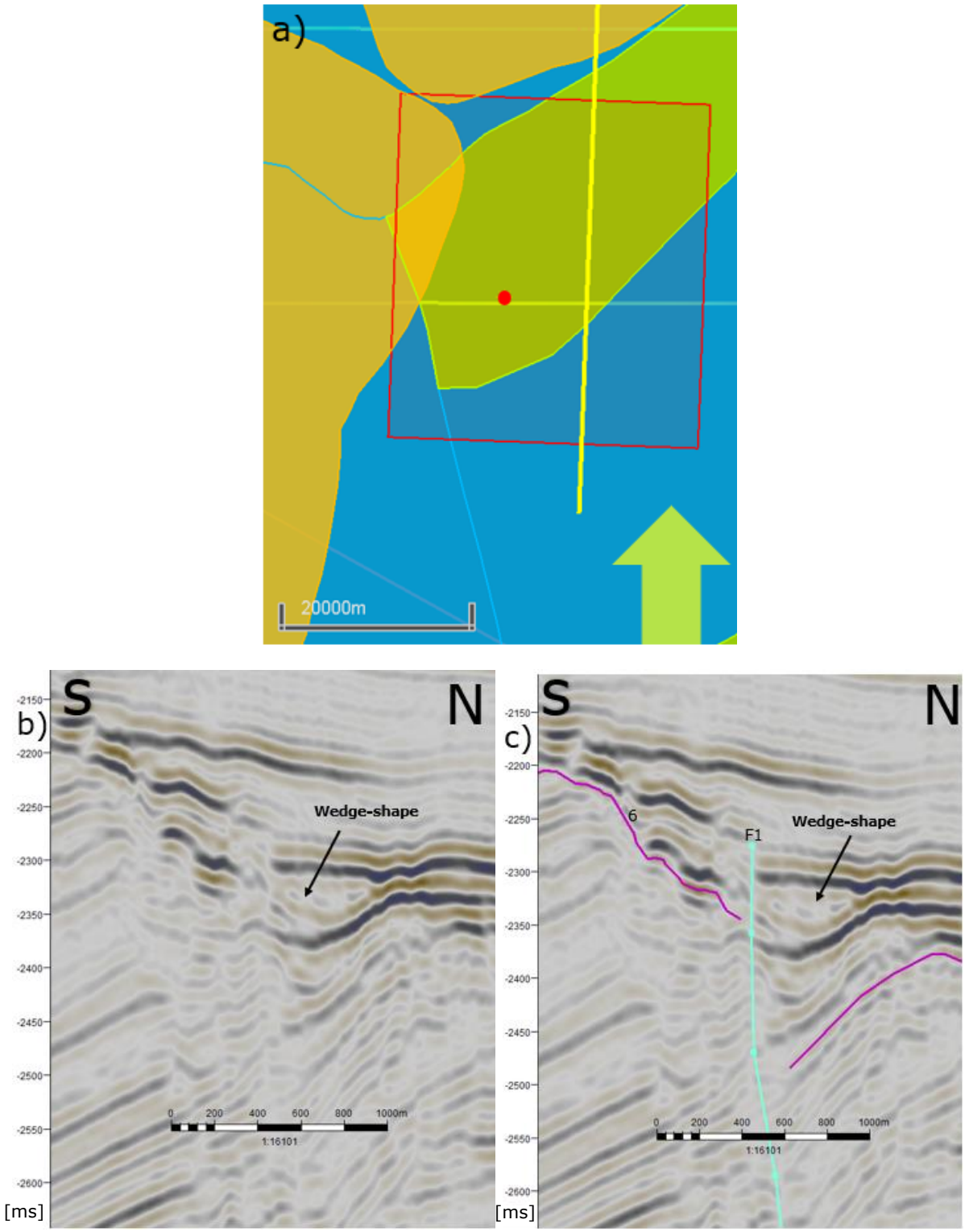

Figure 31 Profiles of a wedge-shaped sedimentary structure, with the location in a), a visualization of the wedge without any interpretation in b), and c) showing how the sedimentary layers somewhat increase in thickness towards the fault. Green arrow indicating north direction.

4.2 Fault analysis, throw profiles

Diagrams plotting the fault throw against the distance along the chosen fault are created. Such diagrams were made for faults F1 and F3. For F1, horizon 6 is used, and for F3, horizon 7 is used. Figure 32 shows a 2D image of F1 and F3. The values used for calculations of the throw profiles are enclosed in the Appendix.

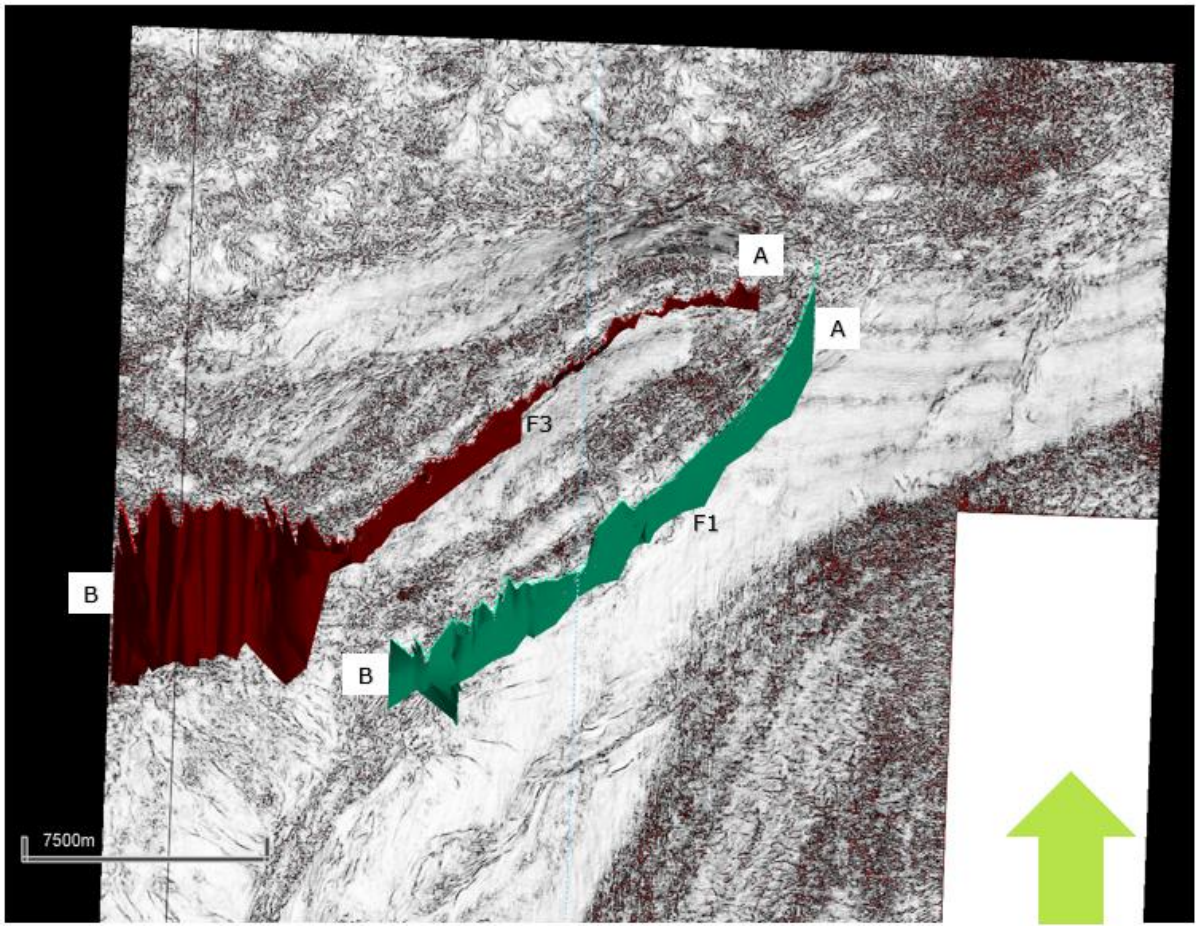

Figure 32 Map illustration of faults F1 and F3 in a 2D window in Petrel. The throw and the length of the faults were measured from A to B with an increment of mostly 50. Green arrow indicating north direction.

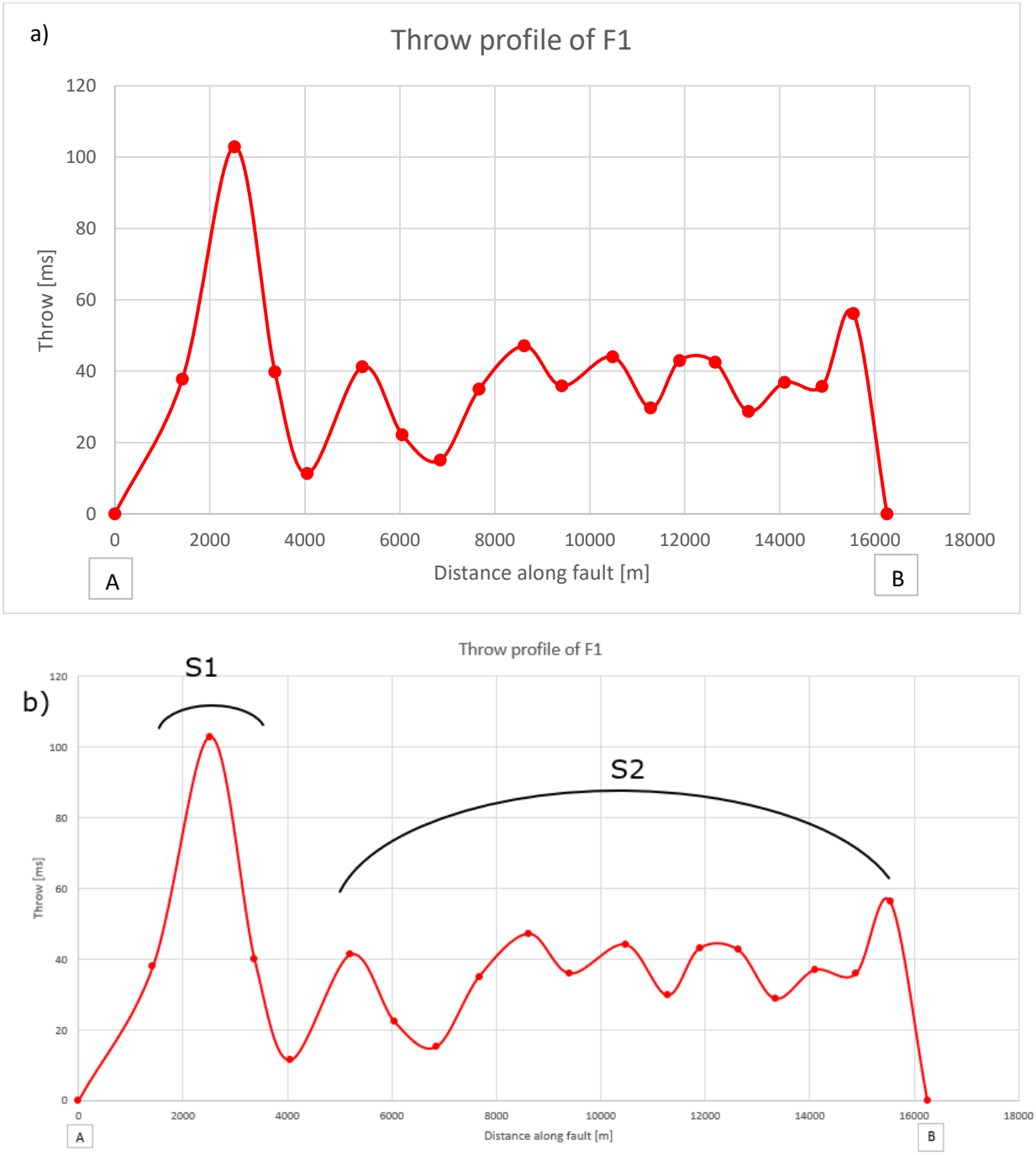

Figure 33 a) *showing the throw profile of fault F1 plotting the distance along the fault (x-axis) against the throw (y-axis). A and B corresponds to the locations in Figure 32. b) propose a possible division of the fault into two fault segments: S1 and S2.*

The throw profile for F1 is presented in Figure 33 a). The fault has a peak at around a throw of 100 ms, whilst the rest of the measurements show a relatively similar throw, except from the interval between 4000 m and 7000 m, and the peak closest to B. Figure 33 b) portray the same diagram as presented in a), including a dividing of the graph into two possible fault segments (named S1 and S2). The throw profile shows that F1 is growing most in displacement closest to A, and more in lengthening when approaching B.

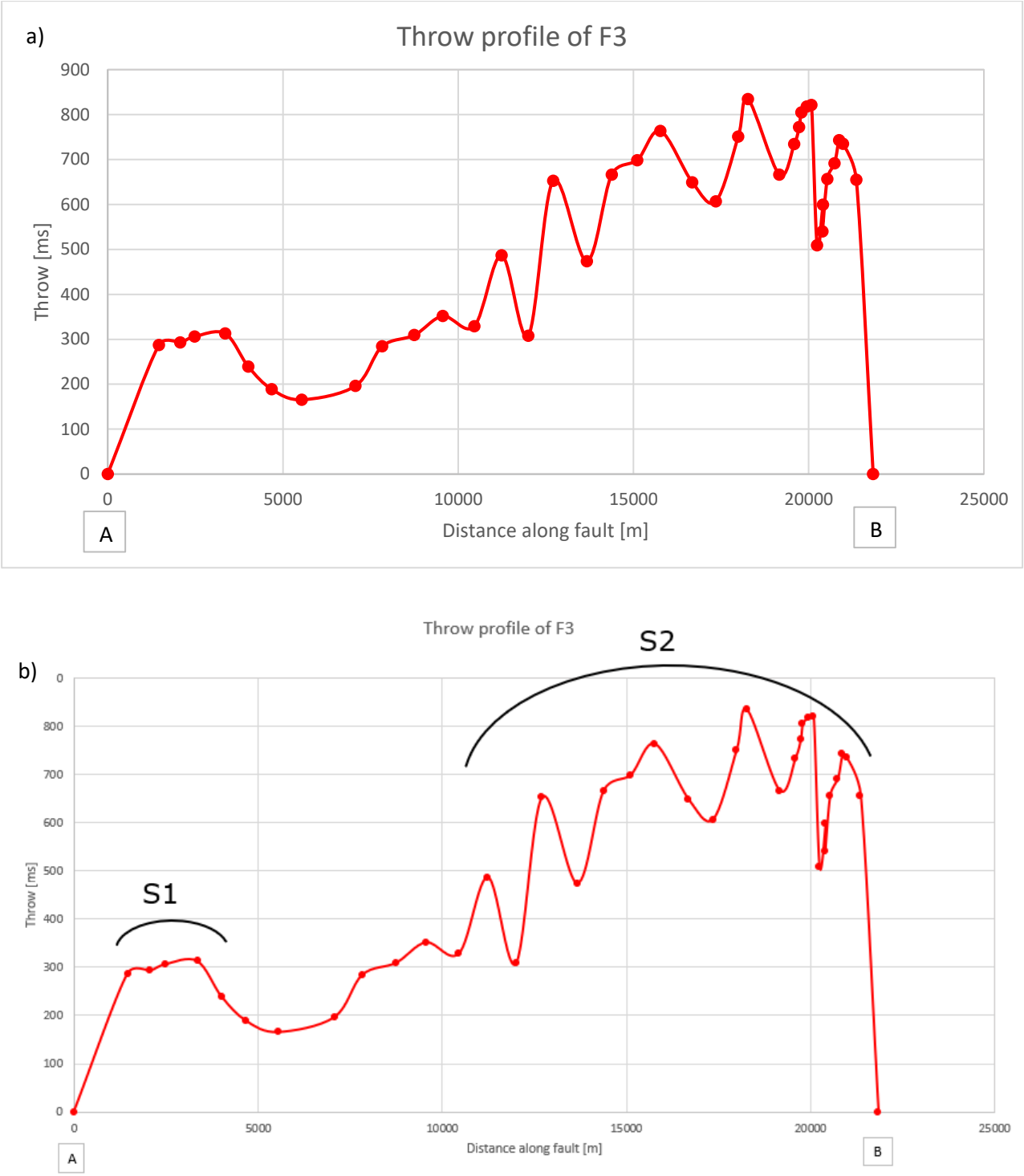

Figure 34 Diagrams showing the throw profile of fault F3. The distance is plotted along the x-axis and throw along the y-axis. b) suggests two fault segments: S1 and S2.

The created throw profile of fault F3 is presented in Figure 34. As seen in a), the graph is peaking at around 2500 meters distance, then the slope decreases before it again starts to increase. The graph increases globally (with locally fluctuations) approaching B. In Figure 34 b), an attempt of dividing the graph into two segments is presented. The second segment being larger and containing larger throws than the first segment. The displacement appears more dominant closer to B, while lengthening appears more significant closer to A. Approaching B, the increment was immersed to 10. This was in an

attempt of getting more reliable results than what was obtained with an increment of 50. The Appendix shows where the increment was changed to 10.

Evolution of Nyk High

When comparing the three main profiles presented in this chapter, there are clearly changes of structures across the seismic cube. Moving westwards, the sedimentary sequences below horizon 6 are dipping steeply towards the SE, and they flatten progressively westwards, before they again steepen close to the Vema Dome. The same sequences have also clearly been affected by more and larger faulting in the western parts of the cube, which is seen by comparing Figure 16, Figure 17 and Figure 18 to each other. What can be interpreted as a folding, increase in the same direction. Generally, the western parts of the study area show more indications of structural impact such as the increase in faulting, folding and the disturbance of shallow sedimentary sequences. The interpreted sills are present from somewhat east of the middle of the 3D cube and increases in size and amount towards the west.

The two described rotational fault blocks appear around the middle of the 3D cube, and they are present almost up until the intersection of the Vema Dome. Fault block 1 disappears just before fault block 2.

All the interpreted faults also change throughout the cube. No fault is interpreted to be present throughout the whole area, and they seem to have impacted the study area to a different degree. For instance, F3 appears somewhat east of the middle of the cube, interpreted relatively steep and short, and it increases in length and shallows in steepness towards the west. Fault F8 appears to be present through most of the cube, at least until the profile intersects the Vema Dome.

Horizon 6 is interpreted at its shallowest in the east of the cube, at around -2.10 s-twtt, and it gradually deepens towards the west, with its deepest point at around -2.99 s-twtt. The shape of the surface appears to be affected by the rotational fault blocks, folding, tilting, subsidence, and other faults.

5 Discussion

In this chapter important and significant findings are discussed and elaborated further. To understand the tectonic evolution, some fault interpretations, rotational fault blocks and folds are discussed to more detail. Further, two figures are added to make it easier to follow the discussion.

5.1 Horizons

The same formations usually vary in depth (and thickness), as illustrated in some of the figures in chapter 4, Results. This means that comparing the depth of different horizons in this study to horizons' interpreted depth in other publications can lead to some misinterpretations since the locations of the horizons can vary.

Since no seismic to well-tie is performed during this study, and no well tops are displayed, a confident interpretation of different sedimentary surfaces is challenging. However, both horizons 6 and 7 are clearly marking two different sequences, possibly erosional surfaces.

The 3D seismic shows several strong reflectors, some of which are possible erosional surfaces. Seismic horizon 6 and 7 are such. Horizon 6 is interpreted continuously throughout the whole cube (disregarded the fact that the interpretation is ambiguous at certain places). This horizon is also where the highs of the rotated faults blocks are best observed, and layers are onlapping this surface in the east of the seismic cube. Both its shape and the strong reflector indicate an erosional surface.

Several authors have interpreted the erosional surface top Cretaceous (or base Tertiary) on both a regional and a smaller scale. As presented in Figure 8, Zastrozhnov et al. (2018) present a detailed interpretation of the sectioning of the Mid-Norwegian rift. In their publication they also present sectioning of structures at a more zoomed-in scale. At Nyk High, top Cretaceous is interpreted at around a depth of -3.0 s-twtt, and top Paleocene at -2.6 s-twtt. From this study, horizon 6 is interpreted at around roughly -2.6 to -2.8 s-twtt depth, corresponding well with interpretations from both Zastrozhnov et al. (2018) and Fjellanger et al. (2005). Compared to Omosanya (2020), the top Cretaceous is interpreted deeper, at around -3.5 to -4.0 s-twtt. However, the published figures have a larger scale than the data used during this study, thus a comparison to interpretations made on larger scales are to a certain degree ambiguous, but they are good indicators. The placement of top Cretaceous at horizon 6 is therefore probable (Figure 35). Ren et al. (2003) found that Paleocene sediments are onlapping the regional top Cretaceous unconformity, which corresponds well with the findings of onlapping layers onto horizon 6 in this study (see Figure 17 b)), and therefore strengthens the theory of horizon 6 as top Cretaceous.

Horizon 7 is also indicating a change in seismic velocity. However, that horizon was not possible to map with confidence throughout the 3D seismic cube. This horizon is where the flat spot from Cretaceous time in well 6707/10-1 is interpreted (Factpages), thereby confirming the horizon is from Cretaceous time. The horizon is affected by rifting and uplift. If the interpreted flat spot occurs in the Nise Formation, which formed between Santonian and Campanian age (Factpages), the layer between horizon 7 and the top Cretaceous would be of Maastrichtian age, which could indicate that horizon 7 corresponds to the intra mid-Campanian horizon (Zastrozhnov et al., 2018). Although the interpretations of top Cretaceous and intra mid-Campanian can be supported by other publications, the depth of the interpreted horizons varies throughout the seismic cube, thus adding uncertainty to the liability of comparing the horizons.

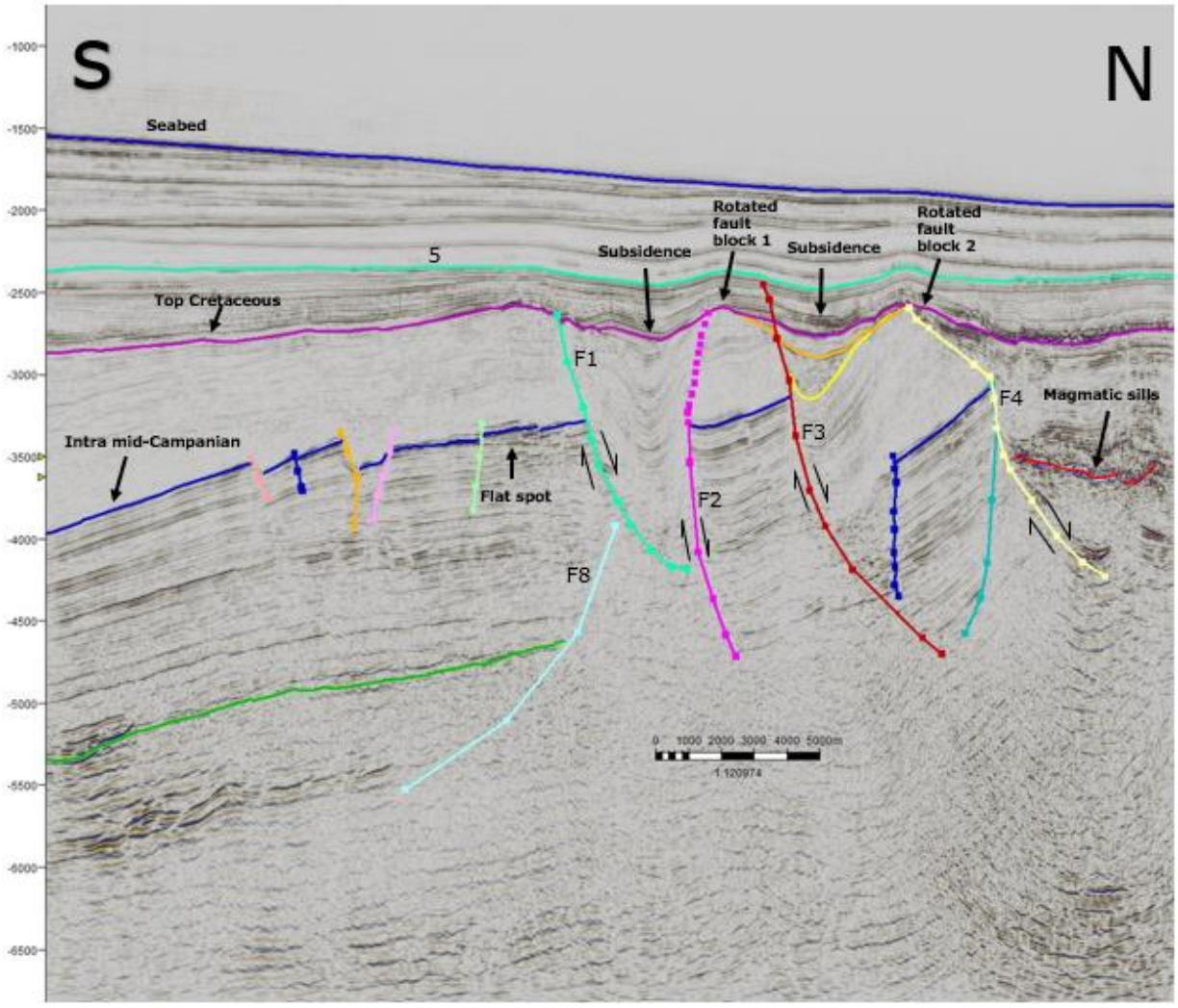

Figure 35 Seismic profile of several of the discussed structures. The profile is located in the same place as Figure 19 a). A proposal of the placements of top Cretaceous and intra mid-Campanian is presented. Faults F1-F4 and F8 are labelled. So is the seabed, horizon 5, subsidence, rotational fault blocks and magmatic sills. Arrows indicating the interpreted direction of fault movement.

5.2 Faults

Throughout the 3D seismic cube, faults are interpreted to be dipping to either the NW or the SE. Since all the faults show indications of normal faulting, it is reasonable to argue that the faults were formed during at least two different rift periods. Some of the faults are also changing in steepness through the 3D cube.

Fault blocks

As illustrated in Figure 35, fault block 1 is constrained by the main faults F2 and F3. The rotation is towards the SE and relatively similar throughout its presence in the seismic cube. The rotational block is distinct, however, there are some uncertainties related to the lengths of F2 and F3. As seen in Figure 35, F2 and F3 are interpreted higher up than in the main profiles. F3 appears to have cut through the top Cretaceous erosional surface and farther up, close to horizon 5. F2 could also possibly have been interpreted higher up. Such indications are visible in several profiles, but in other profiles those observations are ambiguous. However, since both faults seemingly cut the top Cretaceous in several profiles, it is probable that both faults, thus the rotational fault block, was created during a rifting period that must be younger than the top Cretaceous horizon. Further, sedimentary layers that are cut abruptly above the initial interpretation of the two faults strengthens the alleged theory of extended faults. F2 and F3 are initially interpreted as faults because of the observed rotation, which demand faulting, in addition to an abruptly cutting of the sedimentary sequences. Derived from that, the abrupt cut off of the sedimentary layers above, although somewhat ambiguous, could indicate faulting at shallower depths as well.

The results show that fault block 2 is bounded by fault F3 and F4 and tilted to the SE. F3 is part of both this fault block, but also fault block 1, indicating that they developed during the same rift period. The upper part of F4 is however also interpreted as a horizon (horizon 6.2). Moving through the cube from east to west, the first occurrence of the structure appears more as a horizon than a fault. That is because of its relatively strong reflector, no obvious displacement nor abruptly cutting of sediments. Towards the west, the feature steepens exceedingly, and sedimentary layers are somewhat onlapping the feature. However, to obtain this distinct, sort of domino rotation that is interpreted in this fault block, a fault where F4 is interpreted must exist.

F4 is interpreted to not penetrate the top Cretaceous erosional surface. This also cause some uncertainty regarding the time of the faulting. Since the two fault blocks are created simultaneously, the main faults that have caused the faulting and rotation must have been active during the same time. F2 and F3 clearly cut through the top Cretaceous in some profiles. This is not the case for F4, which throughout the cube shows no indications of cutting through the top Cretaceous. One possibility is that the fault blocks were created during two rift periods. F2, F3 and F4 could have been active during a first rift period, before the area was uplifted and eroded, then creating the intra mid-Campanian horizon. Further, new sediment deposits occurred and a new uplift and erosion then created the top Cretaceous, before a second rift period started. Bailey et al. (2005) and Frankowicz and McClay (2010) argued for the influence reactivation can have on the stratigraphy above ancient faults. This understanding could support active faults during one rift period, then a later reactivation. An explanation to why F4 is not cutting through the top Cretaceous, can be that this fault was not reactivated.

F3 grows significantly towards the west and the Vema Dome, where it appears as if one large fault was created during only one rift period. This interpretation contradicts the theory of reactivation. However, the area where F3 is at its largest is where the Nyk High intersects the Vema Dome, which was created under compressional regimes (Blystad et al., 1995), and that portrays shale diapirs, structures that may disturb the quality of seismic data. In addition, disturbed strata in the upper parts of the western area (Figure 30) also support the impact the formation of the Vema Doma had on the Nyk High and structures there. The exact evolution of the fault blocks therefore still remains difficult to explain.

Faults F8-F11 are dipping to the SE, and F1-F4 are dipping to the NW. If assuming that F1-F4 are reactivated, the faults could have been created during two rift periods. During the first period, after the intra mid-Campanian, all the mentioned faults were active. This assumed faulting period must have occurred sometime after intra mid-Campanian and before the Paleocene. After the top Cretaceous was created and Paleocene sediments were deposited, a new period of rifting occurred and reactivated at least F1-F3. The extensional period could be related to the Campanian-Paleocene rift period. Færseth (2021) asserts that the major fault events occurred in that period (Brekke, 2000, Færseth and Lien, 2002), which correspond with the results and interpretations from this study: F2-F4 are crucial for the creation of the rotated fault blocks, and if the blocks were created because of reactivation, the reactivation occurred during the proposed rift period.

In the presented key profiles, subsidence is marked on several occasions. Færseth and Lien (2002) argued for thermal subsidence in relation with the Cretaceous sedimentation in the Norwegian Sea. However, I would argue that the subsidence at the Nyk High is mostly related to tectonic subsidence because of their bounding by faults. The key profiles presented in chapter 4.1.1 mark subsidence at several places, all of which are related to faults. With that being said, it can be challenging to distinguish between thermal and tectonic subsidence from seismic profiles, and especially with the Nyk High being exposed to several rifting periods and other tectonic regimes, an exact explanation of the subsidence is difficult.

Folding

Apart from some minor folding where the Nyk High intersects the Vema Dome, one of few other signs of folding in the research area is the local folding explained and illustrated in chapter 4, Results. Folds formed because of a compressional regime in the Vøring Basin are discussed by multiple authors e.g., Blystad et al. (1995), Larsen and Skarpnes (1984), Omosanya (2020). Moreover, the folding is also argued to have formed by normal faulting with components of strike-slip faulting and flexuring (Gowers and Lunde, 1984). Considering that there is only one fold throughout the studied 3D seismic, it is likely that the folding has been very local and minimal. It is reasonable to assume that a larger part of the area would have been folded if the compression was greater. Further, near horizontal reflectors on both flanks of the synform fold (see Figure 35), substantiates that the compressional regime did not (not to a great extent at least) lead to this folding.

Another approach to understand the mechanisms behind the folding is to view how the faulting may have affected the folding process. One possibility is an oblique faulting: a normal fault with strike-slip components (a transtensional regime), together with syn-sedimentary strata creating the folds. An interpreted syn-tectonic wedge is found in the upper hanging wall of F1 in this study, and together with the large wedge-shaped geometry

found in Brekke (2022), syn-tectonic events have affected the Nyk High. Such structures are also found in the Vøring Basin by e.g., Færseth (2021). Anyhow, the suggestion of a syn-tectonic folding contradicts the interpretation of F1 cutting through the top Cretaceous. The subsidence just above the fold is similar in shape to the fold, which could indicate that the subsidence and the folding was created together. Since the layers of the fold in the hanging wall of F1 is bending towards the fault, it could indicate that the sediments in the folding act somewhat ductile, even though the location is too shallow to be near the brittle-ductile transition zone (Condie, 2005).

5.3 Fault analysis, throw profiles

The observed variation in throw indicates that the accommodation of displacement changes along both faults (see Figure 36). To my knowledge, no throw profiles of the Nyk High are created by other authors, excluding the opportunity of comparing the results found in this study to other studies. However, studies on general normal fault growth can be used.

According to the throw profiles, F3 shows throws up to above 800 ms, while F1 has throws just above 100 ms. Since the vertical displacement is significantly larger in F3, it indicates that the stress accumulation was much greater for F3 than for F1. F3 also display a significant increase in throw from about where F1 is not present anymore.

Using the hybrid-model of fault growth presented by Rotevatn et al. (2018), a fault often grows according to a combination of the two endmember growth models: the propagating fault growth model and the constant-length model. Since lengthening by tip propagation is seen in the first state of fault growth and increase in displacement is presented as dominant in the later process of the growth, it appears from the diagrams that F1 and F3 could have grown in the opposite directions of each other. F1 has its largest throw at a distance of around 2000 m, which is to the east of the interpreted block, while F3 has its largest throw values way to the west, where Nyk High intersects the Vema Dome. Both profiles also show a little increase in throw in the opposite directions as well. This could indicate that the lengthening stage of both faults occurred at similar places, but that the vertical displacement increased in opposite directions. Why this has happened is difficult to determine only with the data used for this study, often the direction a fault dips and grows is randomly determined. Larger faults often experience larger amount of stress, which can impact the formation and growth of faults.

Although the hybrid-model seemingly explains the fault growth, the model of fault propagation and linkage, nicely illustrated and described by Gawthorpe and Leeder (2000), can also be used. As presented in chapter 4.2, both profiles can be divided into two possible segments based on the peaks. S1 and S2 may have developed as two separate faults with maximum vertical displacement in the centre of each segment. Followingly, the segments grew and linked because of fault propagation. At least for F1, I would argue that the hybrid-model from Rotevatn et al. (2018) fits better, because the area where S2 is proposed is seemingly more affected by an increase in length and not in displacement. As for F3, the graph is more varying, but the displacement is greater where S2 is proposed, and lengthening is larger at S1.

The profiles are created with manual interpretation of the cut offs and measuring of the length can have impacted the liability of the throw profiles to some extent, but besides

from that, they do represent the growth of the faults. To get more reliable data, it could be possible to calculate the throw of several horizons cutting through the same fault. That suggestion is, however, very challenging with the dataset available, because of the nearly impossible task of interpreting the same horizons in both the hanging wall and the footwall of the faults.

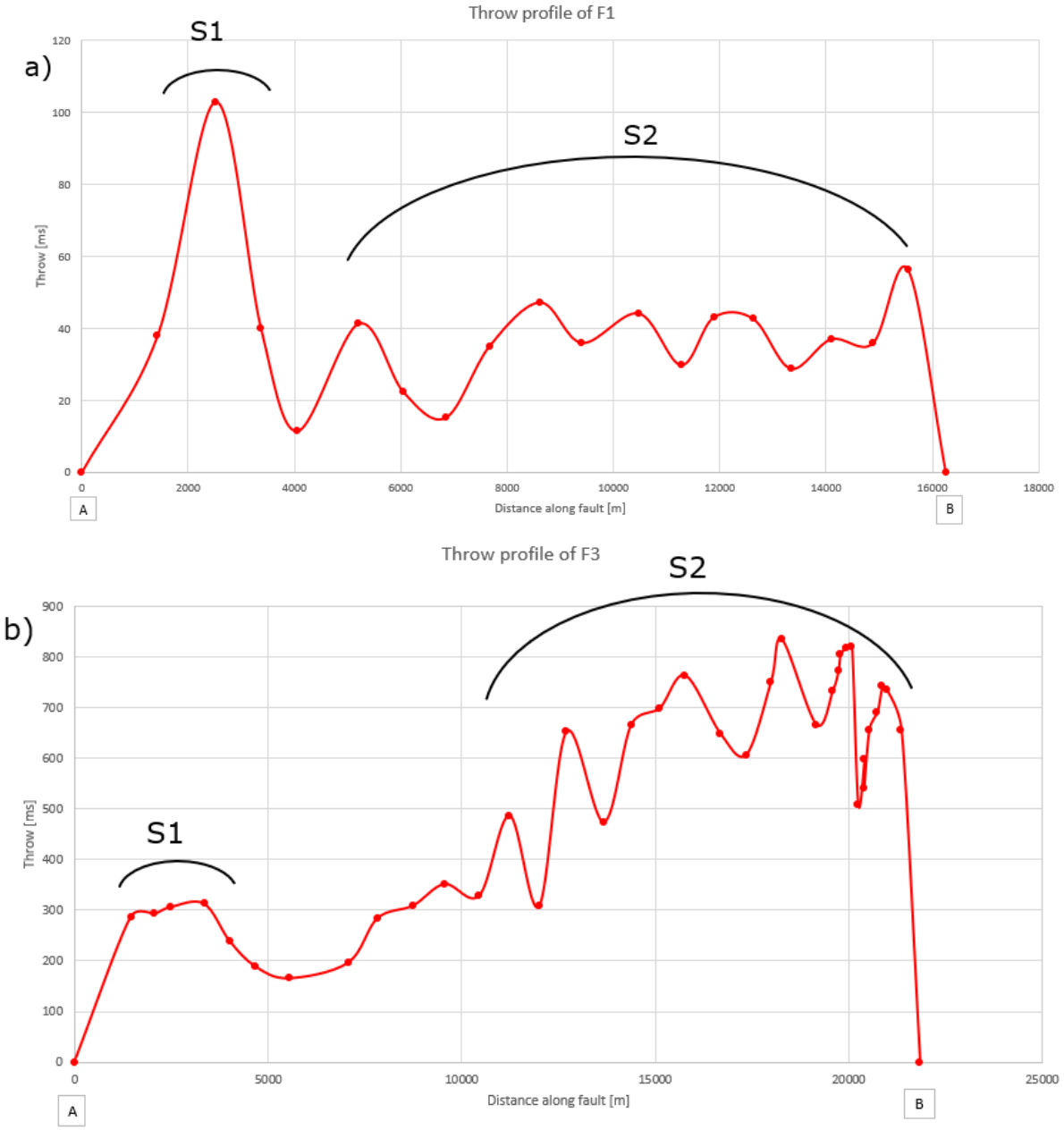

Figure 36 Repetition of the throw profiles for faults F1 and F3, with a suggestion of segment division of both faults. Subsidence between the possible segment linkages. For locations, please see Figure 32.

5.4 Tectonic regimes at the Nyk High and surrounding areas

Faults, tilting, uplift, and folding are structures that formed because of different tectonic regimes. According to different authors e.g., Blystad et al. (1995), Larsen and Skarpnes (1984) and Omosanya (2020), the stress regime in the Vøring complex has changed from extensional to compressional over time. Since this study area is part of a rift system, it is reasonable to assume that most of the structures and tectonics are created and affected because of an extensional regime, an assumption that is supported by much research, some of which are referred to in chapter 2, Theory, in addition to findings discussed above. Anyhow, structures created in other tectonic settings are also observed.

Most of the interpreted faults are high-angle normal faults. This finding contradicts the claim by Ren et al. (2003), that a characteristic in the NW Vøring Basin is low-angled normal faults (created in the Late Cretaceous-Paleocene rifting). It is possible that this characteristic is representative for other parts of the NW Vøring Basin, but based on the results from this study, the architecture of Nyk is not described by low-angled normal faults. The high-angle normal faults correspond to an extensional regime. The subsidence observed appears to be related to the normal faulting, relating these features to an extensional regime.

The main tectonic phase regarding the formation of the Nyk High is an extensional regime, because the study area is part of the outer domain of the large Mid-Norwegian – NE Greenland rift system. High-angle normal faults especially support that tectonic phase, in addition to the syn-tectonic wedge that is interpreted. The minor folding that occurs is challenging to relate to one specific tectonic regime. Good arguments for a compressional regime, an extensional regime and features of some strike-slip environments are discussed. As presented earlier, compressional structures are interpreted in the study area by several authors (e.g., Gowers and Lunde (1984), Blystad et al. (1995), Omosanya (2020)), and the folding interpreted in this study could be compressional. All the interpreted tectonic phases approach the outer domain of the rifted margin. This area is nearing the breakup phase, an area with complex geology, including different tectonic regimes, an increase in magmatic activity and changes in the local stress orientations, which possibly could have led to a compressional regime, disregarding that the area is affected by regional extension of the rift.

Several authors and publications refer to Nyk High as "a rotated fault block" (e.g., Blystad et al. (1995)), and to my knowledge, they do not discuss whether it consists of one or multiple rotational blocks. According to the results from this study, I would argue that Nyk High is a structure created by at least two main rotational blocks.

6 Conclusion

In this master's thesis I have presented important structural and sedimentary features interpreted from a 3D seismic cube located at Nyk High in the distal Vøring complex. The results from this interpretation are discussed together with comparisons to published literature and findings from my specialisation project Brekke (2022). The focus of this study and discussion has been on important structural and sedimentary constraints that can help to better the understanding of and constraining the Nyk High and the outer ridges of the Mid-Norwegian rift system further. Main conclusions retrieved from this thesis are listed as follows:

- Based on findings from this study compared to other publications, a proposal constraining the top Cretaceous and the intra mid-Campanian is illustrated.
- Interpretations show that the Nyk High is created by two distinct rotational fault blocks, constrained by the normal faults F2 and F3, and by F3 and F4, respectively.
- Nyk High is located in the distal margin domain, a specific area of the rift that is approaching the breakup phase. Complex stress setting and potential reorganization may have led to a local compressional regime or a transtensional setting that can be advocated as the driving force of the observed folding.
- Distinct magmatic sills are present in the NNW of the 3D seismic cube, and they are increasing in size and quantity towards the NW, supporting that magmatic activity increases towards the outer domain, and that the area is approaching the breakup phase.
- Faults' vertical displacement is significantly larger to the NW of the cube, close to the Vema Dome, where Nyk High is approaching breakup.

7 Further work

During this research period I see potential for further work in some areas. Suggestions are listed below:

- If possible, create more throw profiles to investigate other faults as well as improving the throw-profiles created in this study (ideally under Petrel, in conjugation with well-tie information). This is crucial in the further constraining of especially timing of events, and a greater understanding of the faults is also important for the petroleum industry.
- Perform well-to-seismic-tie with well 6707/10-1 and import well tops to constrain the sedimentary horizons correctly. This will simplify the process of deciding which horizons to focus on when mapping.
- Another suggestion is to create thickness maps in Petrel to further investigate the thickness between two chosen horizons. This approach requires consistently mapped horizons throughout the 3D seismic cube for a most correct outcome. Such maps can be used to evaluate how different interpreted sedimentary sequences change throughout the area, and where the accumulation of sediments is largest.
- To further investigate the amount of extension in the study area, strain analysis can be performed to understand how strain accommodation is distributed in the study area.

References

ALLEN, P. A. & ALLEN, J. R. 2013. Basins due to lithospheric stretching. *Basin Analysis: Principles and Application to Petroleum Play Assessment, third edition.* UK: John Wiley & Sons, Ltd.

BAILEY, W. R., WALSH, J. J. & MANZOCCHI, T. 2005. Fault populations, strain distribution and basement fault reactivation in the East Pennines Coalfield, UK. *Journal of Structural Geology,* 27**,** 913-928.

BERTRAM, G. T. & MILTON, N. J. 1988. Reconstructing basin evolution from sedimentary thickness; the importance of palaeobathymetric control, with reference to the North Sea. *Basin Research,* 1**,** 247-257.

BLYSTAD, P., BREKKE, H., FÆRSETH, R. B., LARSEN, B. T., SKOGSEID, J. & TØRUDBAKKEN, B. 1995. Structural elements of the Norwegian continental shelf.

BREKKE, H. 2000. The tectonic evolution of the Norwegian Sea Continental Margin with emphasis on the Vøring and Møre Basins. *Geological Society, London, Special Publications,* 167**,** 327-378.

BREKKE, H. M. 2022. *The northern Vøring outer riges complex: new structural and sedimentary constraints.* Specialization project, Norwegian University of Science and Technology (NTNU).

BRONNER, A., SAUTER, D., MANATSCHAL, G., PÉRON-PINVIDIC, G. & MUNSCHY, M. 2011. Magmatic breakup as an explanation for magnetic anomalies at magma-poor rifted margins. *Nature Geoscience,* 4**,** 549-553.

CANNAT, M., MANATSCHAL, G., SAUTER, D. & PÉRON-PINVIDIC, G. 2009. Assessing the conditions of continental breakup at magma-poor rifted margins: What can we learn from slow spreading mid-ocean ridges? *Comptes Rendus Geoscience,* 341**,** 406-427.

CONDIE, K. C. 2005. 2 - The Crust. *In:* CONDIE, K. C. (ed.) *Earth as an Evolving Planetary System.* Burlington: Academic Press.

DORÉ, A. G., LUNDIN, E. R., JENSEN, L. N., BIRKELAND, Ø., ELIASSEN, P. E. & FICHLER, C. 1999. Principal tectonic events in the evolution of the northwest European Atlantic margin. *Geological Society, London, Petroleum Geology Conference Series,* 5**,** 41-61.

DORÉ, A. G., LUNDIN, E. R., KUSZNIR, N. J. & PASCAL, C. 2008. Potential mechanisms for the genesis of Cenozoic domal structures on the NE Atlantic margin: pros, cons and some new ideas. *Geological Society, London, Special Publications,* 306**,** 1-26.

FACTPAGES, N. *6707/10-1* [Online]. NPD Facktpages. Available: https://factpages.npd.no/nb-no/wellbore/pageview/exploration/all/3075 [Accessed 1st of February 2023].

FACTPAGES, N. *NISE FM* [Online]. NPD Facktpages. Available: https://factpages.npd.no/nb-no/strat/pageview/litho/formations/112 [Accessed 12th of May 2023].

FALEIDE, J. I., TSIKALAS, F., BREIVIK, A., MJELDE, R., RITZMANN, O., ENGEN, O., WILSON, J. & ELDHOLM, O. 2008. Structure and evolution of the continental margin off Norway and the Barents Sea. *Episodes,* 31**,** 82-91.

FJELLANGER, E., SURLYK, F., WAMSTEEKER, L. C. & MIDTUN, T. 2005. Upper cretaceous basin-floor fans in the Vøring Basin, Mid Norway shelf. *In:* WANDÅS, B. T. G., NYSTUEN, J. P., EIDE, E. & GRADSTEIN, F. (eds.) *Norwegian Petroleum Society Special Publications.* Elsevier.

FOSSEN, H. 2010. *Structural Geology,* Cambridge, Cambridge University Press.

FRANKE, D. 2013. Rifting, lithosphere breakup and volcanism: Comparison of magma-poor and volcanic rifted margins. *Marine and Petroleum Geology,* 43**,** 63-87.

FRANKOWICZ, E. & MCCLAY, K. R. 2010. Extensional fault segmentation and linkages, Bonaparte Basin, outer North West Shelf, Australia. *AAPG Bulletin,* 94**,** 977-1010.

FÆRSETH, R. 2021. Structural geology and basin development of the Norwegian Sea. *Norwegian Journal of Geology*.
FÆRSETH, R. & LIEN, T. 2002. Cretaceous evolution in the Norwegian Sea—A period characterized by tectonic quiescence. *Marine and Petroleum Geology,* 19**,** 1005-1027.
GAWTHORPE, R. L. & LEEDER, M. R. 2000. Tectono-sedimentary evolution of active extensional basins. *Basin Research,* 12**,** 195-218.
GOWERS, M. B. & LUNDE, G. The geological history of Trænabanken. 1984.
HALDAR, S. K. 2018. Chapter 6 - Exploration Geophysics. *In:* HALDAR, S. K. (ed.) *Mineral Exploration (Second Edition).* Elsevier.
HJELSTUEN, B. O., ELDHOLM, O. & SKOGSEID, J. 1999. Cenozoic evolution of the northern Vøring margin. *GSA Bulletin,* 111**,** 1792-1807.
HONGXING, G. & ANDERSON, J. K. 2007. Fault Throw Profile and Kinematics of Normal Fault: Conceptual Models and Geologic Examples. *Geological Journal of China Universities,* 13**,** 75-88.
KITTELSEN, J. E., OLSEN, R. R., MARTEN, R. F., HANSEN, E. K. & HOLLINGSWORTH, R. R. 1999. The first deepwater well in Norway and its implications for the Upper Cretaceous Play, Vøring Basin. *Geological Society, London, Petroleum Geology Conference Series,* 5**,** 275-280.
LARSEN, R. M. & SKARPNES, O. Regional interpretation and hydrocarbon potential of the Trænabanken area. *In:* SPENCER, A. M., ed. Petroleum Geology of the North European Margin, 1984// 1984 Dordrecht. Springer Netherlands, 217-236.
LUNDIN, E., DORE, A., RONNING, K. & KYRKJEBO, R. 2013. Repeated inversion and collapse in the Late Cretaceous-Cenozoic northern Vøring Basin, offshore Norway. *Petroleum Geoscience,* 19.
MCCLAY, K. R. & BUCHANAN, P. G. 1992. Thrust faults in inverted extensional basins. *In:* MCCLAY, K. R. (ed.) *Thrust Tectonics.* Dordrecht: Springer Netherlands.
MCKENZIE, D. 1978. Some remarks on the development of sedimentary basins. *Earth and Planetary Science Letters,* 40**,** 25-32.
MOSAR, J., LEWIS, G. & TORSVIK, T. 2002. North Atlantic sea-floor spreading rates: implications for the Tertiary development of inversion structures of the Norwegian–Greenland Sea. *Journal of the Geological Society,* 159**,** 503-515.
MÜNTENER, O., MANATSCHAL, G., DESMURS, L. & PETTKE, T. 2010. Plagioclase Peridotites in Ocean–Continent Transitions: Refertilized Mantle Domains Generated by Melt Stagnation in the Shallow Mantle Lithosphere. *Journal of Petrology,* 51**,** 255-294.
MØRK, M. B. E., LEITH, D. A. & FANAVOLL, S. 2001. Origin of carbonate-cemented beds on the Naglfar Dome, Vøring Basin, Norwegian Sea.
NEWMAN, R., WHITE, N., BUCK, W. R., GALLAGHER, K., WATTS, A. B., MCKENZIE, D., KUSZNIR, N., GELI, L. & WHITE, R. S. 1999. The Dynamics of Extensional Sedimentary Basins: Constraints from Subsidence Inversion [and Discussion]. *Philosophical Transactions: Mathematical, Physical and Engineering Sciences,* 357**,** 805-834.
NIXON, C., SANDERSON, D., DEE, S., BULL, J., HUMPHREYS, R. & SWANSON, M. 2014. Fault interactions and reactivation within a normal-fault network at Milne Point, Alaska. *AAPG Bulletin,* 98**,** 2081-2107.
OMOSANYA, K. O. 2020. Cenozoic tectonic inversion in the Naglfar Dome, Norwegian North Sea. *Marine and Petroleum Geology,* 118**,** 104461.
OSMUNDSEN, P. T. 2022. Extensional basins. The β-factor and the McKenzie model. Normal faults. *TGB4135 Basin Analysis*. Available: https://ntnu.blackboard.com/ultra/courses/_32453_1/cl/outline [Accessed 9th of February 2023].
PERON-PINVIDIC, G., MANATSCHAL, G. & , T. I. R. W. P. 2019. Rifted Margins: State of the Art and Future Challenges. *Frontiers in Earth Science,* 7.
PERON-PINVIDIC, G., MANATSCHAL, G. & OSMUNDSEN, P. T. 2013. Structural comparison of archetypal Atlantic rifted margins: A review of observations and concepts. *Marine and Petroleum Geology,* 43**,** 21-47.

PERON-PINVIDIC, G. & OSMUNDSEN, P. T. 2016. Architecture of the distal and outer domains of the Mid-Norwegian rifted margin: Insights from the Rån-Gjallar ridges system. *Marine and Petroleum Geology,* 77**,** 280-299.
PERON-PINVIDIC, G. & OSMUNDSEN, P. T. 2018. The Mid Norwegian - NE Greenland conjugate margins: Rifting evolution, margin segmentation, and breakup. *Marine and Petroleum Geology,* 98**,** 162-184.
PERON-PINVIDIC, G., ÅKERMOEN, T. & LEIVESTAD, L. I. 2022. The North-East Atlantic Mid-Norwegian rifted margin: Insights from the deep imaging Geoex MCG RDI19 dataset. *Tectonophysics,* 824**,** 229225.
PLANKE, S., RABBEL, O., GALLAND, O., MILLETT, J., MANTON, B., JERRAM, D., PALMA, O. & SPACAPAN, J. 2018. *SEISMIC IMAGING AND PETROLEUM IMPLICATIONS OF IGNEOUS INTRUSIONS IN SEDIMENTARY BASINS CONSTRAINED BY OUTCROP ANALOGUES AND SEISMIC DATA FROM THE NEUQUÉN BASIN AND THE NE ATLANTIC*.
REN, S., FALEIDE, J. I., ELDHOLM, O., SKOGSEID, J. & GRADSTEIN, F. 2003. Late Cretaceous–Paleocene tectonic development of the NW Vøring Basin. *Marine and Petroleum Geology,* 20**,** 177-206.
RISE, L., OTTESEN, D., BERG, K. & LUNDIN, E. 2005. Large-scale development of the mid-Norwegian margin during the last 3 million years. *Marine and Petroleum Geology,* 22**,** 33-44.
ROBERTS, D. G., THOMPSON, M., MITCHENER, B., HOSSACK, J., CARMICHAEL, S. & BJØRNSETH, H. M. 1999. Palaeozoic to Tertiary rift and basin dynamics: mid-Norway to the Bay of Biscay – a new context for hydrocarbon prospectivity in the deep water frontier. *Geological Society, London, Petroleum Geology Conference Series,* 5**,** 7-40.
ROTEVATN, A., JACKSON, C. A. L., TVEDT, A. B. M., BELL, R. E. & BLÆKKAN, I. 2018. How do normal faults grow? *Journal of Structural Geology,* 125**,** 174-184.
SAUNDERS, A., FITTON, J., KERR, A. & KENT 1997. The North Atlantic Igneous Province.
SCHLUMBERGER, E. G. *three-dimensional (3D) seismic data* [Online]. Available: https://glossary.slb.com/Terms/t/three-dimensional_seismic_data.aspx [Accessed 6th of June 2023].
SCLATER, J. G. & CÉLÉRIER, B. 1987. Extensional models for the formation of sedimentary basins and continental margins. *Norsk Geologisk Tidsskrift,* 67**,** 253-267.
SKOGSEID, J. & ELDHOLM, O. 1987. Early Cenozoic crust at the Norwegian continental margin and the conjugate Jan Mayen Ridge. *Journal of Geophysical Research,* 92**,** 11471-11491.
SKOGSEID, J. & ELDHOLM, O. 1989. Vøring Plateau Continental Margin: Seismic Interpretation, Stratigraphy, and Vertical Movements. *Proc., scientific results, ODP, Leg 104, Norwegian Sea,* 104**,** 993-1030.
TALWANI, M. & ELDHOLM, O. 1977. Evolution of the Norwegian-Greenland Sea. *GSA Bulletin,* 88**,** 969-999.
VÅGNES, E., GABRIELSEN, R. H. & HAREMO, P. 1998. Late Cretaceous–Cenozoic intraplate contractional deformation at the Norwegian continental shelf: timing, magnitude and regional implications. *Tectonophysics,* 300**,** 29-46.
WALSH, J. J., BAILEY, W., BONSON, C., CHILDS, C., NICOL, A. & SCHOEPFER, M. 2003. How Significant is Segment Linkage in Fault Growth? *AGU Fall Meeting Abstracts,* -1**,** 06.
WALSH, J. J., NICOL, A. & CHILDS, C. 2002. An alternative model for the growth of faults. *Journal of Structural Geology,* 24**,** 1669-1675.
WANG, P.-J., MATTERN, F., DIDENKO, N. A., ZHU, D.-F., SINGER, B. & SUN, X.-M. 2016. Tectonics and cycle system of the Cretaceous Songliao Basin: An inverted active continental margin basin. *Earth-Science Reviews,* 159**,** 82-102.
WERNICKE, B. 1985. Uniform-sense normal simple shear of the continental lithosphere. *Canadian Journal of Earth Sciences,* 22**,** 108-125.

WILLEMSE, E. J. M. 1997. Segmented normal faults: Correspondence between three-dimensional mechanical models and field data. *Journal of Geophysical Research: Solid Earth,* 102**,** 675-692.
WILSON, J. T. 1966. Did the Atlantic Close and then Re-Open? *Nature,* 211**,** 676-681.
WILSON, R. W., HOUSEMAN, G. A., BUITER, S. J. H., MCCAFFREY, K. J. W. & DORÉ, A. G. 2019. Fifty years of the Wilson Cycle concept in plate tectonics: an overview. *Geological Society, London, Special Publications,* 470**,** 1-17.
ZASTROZHNOV, D., GERNIGON, L., GOGIN, I., ABDELMALAK, M. M., PLANKE, S., FALEIDE, J. I., EIDE, S. & MYKLEBUST, R. 2018. Cretaceous-Paleocene Evolution and Crustal Structure of the Northern Vøring Margin (Offshore Mid-Norway): Results from Integrated Geological and Geophysical Study. *Tectonics,* 37.
ZASTROZHNOV, D., GERNIGON, L., GOGIN, I., PLANKE, S., ABDELMALAK, M. M., POLTEAU, S., FALEIDE, J. I., MANTON, B. & MYKLEBUST, R. 2020. Regional structure and polyphased Cretaceous-Paleocene rift and basin development of the mid-Norwegian volcanic passive margin. *Marine and Petroleum Geology,* 115**,** 104269.

Appendix

Fault F1 (E-W movement)				
Hanging wall cutoff [ms]	**Footwall cutoff [ms]**	**Throw |(Fw-Hw)| [ms]**	**Distance [m]**	**Distance rounded [m]**
0	0	0	0	0
-2247,88	-2210,1	37,78	1416,69	1420
-2440,8	-2337,92	102,88	2522,26	2520
-2378,26	-2338,46	39,8	3373,09	3370
-2334,98	-2323,67	11,31	4050,46	4050
-2391,53	-2350,32	41,21	5209,4	5210
-2499,43	-2477,24	22,19	6050,17	6050
-2532,07	-2516,99	15,08	6852,76	6850
-2631,26	-2596,32	34,94	7668,66	7670
-2513,02	-2465,92	47,1	8616,54	8620
-2603,17	-2567,32	35,85	9409,05	9410
-2557,56	-2513,51	44,05	10481,2	10480
-2639,76	-2610,07	29,69	11276,5	11280
-2625,96	-2583,03	42,93	11890,4	11890
-2636,6	-2594,11	42,49	12636,1	12640
-2669,29	-2640,58	28,71	13335,4	13340
-2693,15	-2656,28	36,87	14095,7	14100
-2756,18	-2720,43	35,75	14888,5	14890
-2784,23	-2728,08	56,15	15549,6	15550
0	0	0	16264,3	16260

Values used for creating throw profile for F1. The values in columns 1, 2 and 4 are obtained from Petrel. Values in yellow(y-axis) and green (x-axis) are used for creating the throw profile.

Fault F3(E-W movement)				
Hanging wall cutoff [ms]	**Footwall cutoff [ms]**	**Throw |(Fw-Hw)| [ms]**	**Distance [m]**	**Distance rounded [m]**
0	0	0	0	0
-3289,33	-3002,11	287,22	1456,22	1460
-3316,31	-3023,23	293,08	2066,55	2070
-3363,43	-3057,53	305,9	2474,85	2480
-3365,69	-3052,83	312,86	3354,43	3350
-3299,08	-3059,79	239,29	4013,13	4010
-3271,43	-3082,74	188,69	4677,38	4680
-3285,17	-3119,61	165,56	5540,57	5540
-3381,44	-3185,18	196,26	7073,71	7070
-3425,56	-3141,33	284,23	7825,16	7830
-3451,43	-3142,22	309,21	8745,99	8750
-3473,67	-3122,09	351,58	9562,77	9560
-3479,51	-3150,41	329,1	10460,2	10460
-3596,76	-3109,93	486,83	11238,8	11240
-3381,24	-3073,43	307,81	12001,5	12000
-3733,58	-3081	652,58	12713,5	12710
-3471,1	-2997,3	473,8	13672,8	13670
-3885,72	-3219,44	666,28	14383,7	14380
-3808,09	-3109,72	698,37	15105,4	15110
-3794,9	-3031,46	763,44	15771	15770
-3857,38	-3208,24	649,14	16682,9	16680
-3748,25	-3141,29	606,96	17348,8	17350
-3758,06	-3007,22	750,84	17986,3	17990
-3821,62	-2987,19	834,43	18266,6	18270
-3735,83	-3069,53	666,3	19164,7	19160
-3813,51	-3079,32	734,19	19586,2	19590
-3806,16	-3034,24	771,92	19730,4	19730
-3896,79	-3092,09	804,7	19786	19790
-3861,68	-3043,98	817,7	19944,9	19950
-3906,16	-3084,68	821,48	20076,1	20080
-3778,85	-3269,61	509,24	20236,7	20240
-3802,38	-3203,04	599,34	20413	20410
-3741,75	-3201,59	540,16	20388,1	20390
-3850,84	-3194,24	656,6	20530,8	20530
-3922,4	-3230,77	691,63	20743,3	20740
-3932,05	-3189,17	742,88	20867	20870
-3898,83	-3163,99	734,84	20978	20980
-3842,96	-3188,04	654,92	21359,3	21360
0	0	0	21838,8	21840

Values used for creating throw profile for F3. The values in columns 1, 2 and 4 are obtained from Petrel. Values in yellow (y-axis) and green (x-axis) are used for creating the throw profile. Blue coloured row indicates where the increment is changed from 50 to 10.

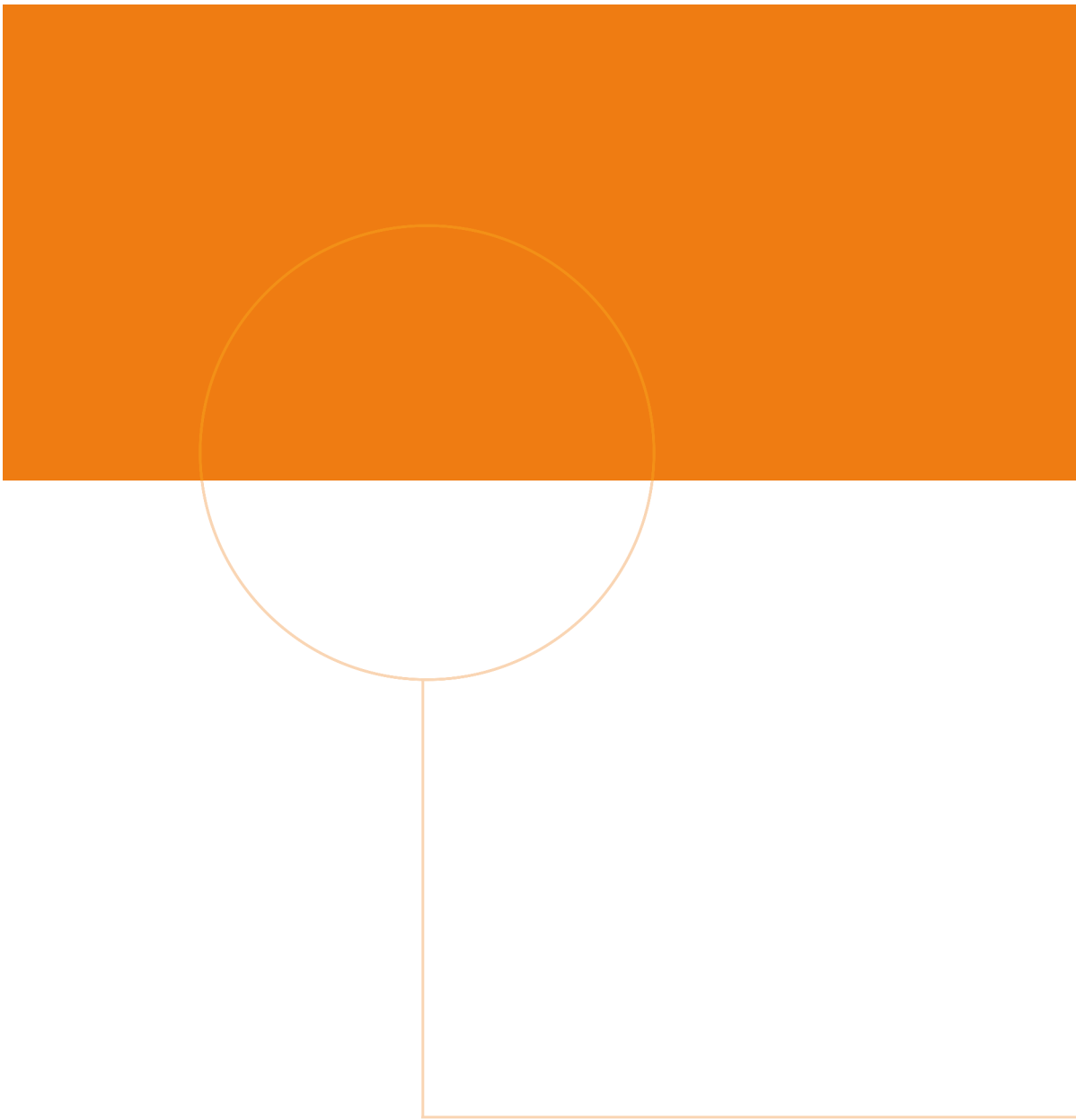

NTNU

Norwegian University of
Science and Technology